Macrophage-Dependent Trafficking and Remodeling of Extracellular Matrix Barriers

By

Julian Carlos Bahr

A dissertation submitted in partial fulfillment
of the requirements for the degree of
Doctor of Philosophy
(Cancer Biology)
in the University of Michigan
2018

Doctoral Committee:

Professor Stephen J. Weiss, Chair
Associate Professor Elizabeth R. Lawlor
Professor Benjamin L. Margolis
Professor Marc Peters-Golden

Julian Carlos Bahr

Jcbahr@umich.edu

ORCID iD: 0000-0001-5949-6504

This dissertation is dedicated to the loving memory of my mother, Carolina Rojas Bahr, whose unpublished dissertation was titled "A History of Langley Park McCormick Elementary School Through Its Students' Recollections"

Acknowledgements

I thank my mentor, Stephen J. Weiss, for developing me as a scientist. His critical deconstruction and presentation of scientific concepts are skills I will forever try to emulate. Thank you to my committee members: Beth Lawlor, Ben Margolis, and Marc Peters-Golden for their scientific and professional guidance.

Thank you to the many lab members who have helped train me and to Stephanie King (Life Sciences Institute) for assistance with illustrations, Craig Johnson (University of Michigan) for assistance with microarray analysis, and Pedro Lowenstein for assistance with glioblastoma models. This work was supported in part by the Cancer Biology Training Grant at the University of Michigan.

Table of Contents

List of Figures

List of Videos

List of Abbreviations

ECM: Extracellular matrix

MMP: Matrix metalloproteinase

MT-MMP: Membrane-tethered matrix metalloproteinase

TIMP: Tissue inhibitor of matrix metalloproteinase

BMDM: Bone marrow-derived macrophage

TAM: Tumor associated macrophage

LPS: Lipopolysaccharide

HSC: hematopoietic stem cell

3-D: 3-dimensional

Abstract

Macrophages are evolutionarily-conserved immune cells distributed throughout all tissues in the body, which rapidly mobilize to defend against a range of insults. In executing events ranging from wound healing and host defense functions to regulating the tumor microenvironment, macrophages traverse and remodel extracellular matrix (ECM) barriers, i.e. the basement membrane and interstitial matrix. To date, the molecular mechanisms operative during macrophage migration and remodeling of ECM barriers have relied on non-physiologic *in vitro* constructs whose relevance to the *in vivo* environment remains unclear. As such, we have adopted an *ex vivo* native tissue model as well as a 3-dimensionsal type I collagen hydrogel model that retain structural crosslinks integral to the barrier characteristics of the *in vivo* ECM. Using primary mouse and human macrophages in conjunction with high-resolution confocal microscopy, we characterize a program wherein macrophages degrade the basement membrane and infiltrate the interstitial matrix. We find that of the dozens of proteases that macrophages express in response to immune stimuli, only the membrane-anchored metalloprotease, MT1-MMP, is absolutely required for basement membrane degradation. Furthermore, we discover a unique hybrid ability of macrophages to either degrade the basement membrane in an MT1-MMP-dependent fashion or alternatively, mobilize actomyosin-mediated mechanical forces to non-proteolytically traverse preformed portals that exist in the basement membrane. Though macrophages can transmigrate the basement membrane via either mechanism, the transcriptional program of tissue-invasive macrophages is alternatively regulated during proteinase-dependent versus independent invasion. Following basement membrane transmigration, macrophages then confront a high-density

interstitial matrix that is dominated by type I collagen. Under these conditions, macrophages must again mobilize MT1-MMP to create passageways through the interstitial matrix that permit the transit of the rigid macrophage nucleus. Strikingly, in the absence of MT1-MMP activity, the macrophage is incapable of creating matrix tunnels that support efficient invasion. Instead, the macrophage traverses the matrix while the rigid nucleus remains trapped and distorted above the surface of the collagen matrix. These studies, together with preliminary data from mouse models of cancer, establish new paradigms for MT1-MMP-dependent macrophage trafficking and remodeling of physiologically-relevant ECM barriers.

Chapter 1: Introduction

The importance of diverse macrophage subtypes

Since the evolution of multicellular animals, phagocytic immune cells have emerged as sentinels essential to tissue maintenance and host defense functions (Buchmann, 2014; Wynn et al., 2013). In humans, this role is fulfilled, in part, by macrophages, which reside in all tissues in the body as well as in the bloodstream as circulating or patrolling precursors, i.e. monocytes (Buchmann, 2014; Wynn et al., 2013). Resident tissue macrophages have essential tissue maintenance functions specific to their organ of residence, i.e. erythrocyte clearance in the spleen, metabolic regulation in the liver, or antigen presentation in the lymph node (Gray and Cyster, 2012; Kohyama et al., 2009; Mebius and Kraal, 2005; Wynn et al., 2013). However, when tissue damage occurs, such as during an infection or as a consequence of carcinogenic processes, additional macrophages are recruited, which necessitates their rapid trafficking across extracellular matrix (ECM) barriers as they infiltrate affected sites (Fidler et al., 2017; Noy and Pollard, 2014; Rowe and Weiss, 2009; Wynn and Vannella, 2016). Upon reaching the affected tissue, macrophages can mediate pleiotropic effects that range from defending the host from infection and the repair of damaged tissue, to mediating pathological remodeling of the ECM in non-resolving, inflammatory environments (Duffield et al., 2005; Franklin and Li, 2016; Vannella and Wynn, 2017; Wynn and

Vannella, 2016). The potential consequences of dysregulated tissue remodeling are dire: fibrosis can grow unchecked to the point of organ failure, compromised tissue barriers can allow pathogen invasion, and degraded ECM can free carcinomas to metastasize (Noy and Pollard, 2014; Rockey et al., 2015; Wynn and Vannella, 2016). Therefore, it is essential to define how macrophages traverse and remodel diverse ECM environments to better understand, and perhaps one day modulate, these critical tissue remodeling functions.

The diversity of macrophage functions can be partially explained by their distinct origins (Gautier et al., 2012; Gosselin et al., 2014; Lavin et al., 2014). While it has long been assumed that all adult macrophages derive from hematopoietic stem cells (HSC) in the bone marrow, recent lineage tracing experiments in mice have demonstrated at least three distinct origins for adult macrophages that arise early during embryonic development (Ginhoux and Guilliams, 2016; Samokhvalov et al., 2007; van Furth et al., 1972; Yona et al., 2013; Yona and Gordon, 2015). By mouse embryonic day 7.5, yolk-sac derived macrophages are generated and infiltrate the fetal brain before blood flow has been established (Ginhoux et al., 2010; Hoeffel et al., 2015; Palis et al., 1999). Upon the formation of the circulatory system, a second wave of macrophages is established in the fetal liver, and together with yolk sac macrophages, persist and replicate as the resident tissue macrophages that populate most adult tissues, including the brain, liver, and lung (Figure 1.1) (Ginhoux and Guilliams, 2016; Hoeffel et al., 2015; Schulz et al., 2012). Interestingly, some exceptions have been found, e.g., embryonic-derived resident tissue macrophages of the heart and dermis are progressively replaced by monocytes arising in the adult bone marrow that then differentiate into macrophages after infiltrating

the target tissue (Figure 1.1) (Epelman et al., 2014; Ginhoux and Guilliams, 2016; Molawi et al., 2014; Tamoutounour et al., 2013). Finally, the "primitive" yolk-sac and fetal liver progenitor cells are replaced by a third wave of "definitive" hematopoiesis when fetal liver HSCs colonize the bone marrow before birth (Ginhoux and Guilliams, 2016; Orkin and Zon, 2008). Bone marrow HSCs continue to renew the circulating monocyte population found in blood throughout adulthood and in turn, circulating monocytes infiltrate tissue and differentiate into the immune-responding macrophages that remodel ECM during infection, wound repair, and carcinogenesis (Figure 1.2) (Murray and Wynn, 2011; Nathan and Ding, 2010; Wynn and Vannella, 2016). Independent of origin, affected tissue or inflammatory stimuli, macrophages are confronted by two distinct ECM barriers, i.e. a dense sheet-like (50-400 nm thick) basement membrane and an expansive 3-dimensional (3D) fibrillar interstitial matrix (Candiello et al., 2007; Halfter et al., 2015; Rowe and Weiss, 2008, 2009). However, how these macrophages interact with these barriers, and the mechanism by which they effect remodeling, is not well understood. Herein, we review the composition of the ECM barriers that macrophages traverse and remodel, as well as the model systems used to study macrophage-ECM interactions. Finally, we examine the potential mechanisms of ECM remodeling with a special focus on the *in vivo* tumor contexts in which they may be operative.

Basement membrane barriers

Basement membranes arose ~500 million years ago in conjunction with the genesis of multicellular organisms (Fidler et al., 2014, 2017). Organized as a thin, dense matrix, the basement membrane subtends all epithelial and endothelial cell layers, as well as ensheathes muscle, fat, and Schwann cells (Figure 1.3A) (Fidler et al., 2017; Rowe and

Weiss, 2008). Originally thought of as a passive structure simply demarcating dynamic groups of cells, it is now appreciated as an essential regulator of diverse cellular processes (Yurchenco, 2011). In addition to acting as an anchor for cell adhesion, the basement membrane transduces mechanical signals that modulate differentiation, organizes and polarizes epithelial cells into functional units (Vracko, 1972; Vracko and Benditt, 1972), and mediates epithelial-mesenchymal crosstalk (McClugage et al., 1986; Toner et al., 1970). While there is some variability in its morphology, the fundamental components of the basement membrane are encoded by an evolutionarily conserved group of macromolecules that include type IV collagen, laminin, nidogen and perlecan (Fidler et al., 2017; Rowe and Weiss, 2008; Yurchenco, 2011).

Basement membrane assembly and structure

Construction of the nascent basement membrane begins with the organization of large (~400-800 kDa) laminin heterotrimers formed into a cruciform shape of three long arms and one short arm that are reinforced with intramolecular disulfide bonds (Rowe and Weiss, 2009; Yurchenco, 2011). Upon recruitment by integrin and α-dystroglycan adhesion receptors on the cell surface, laminin self-associates to form a polymerized network (Li et al., 2005; McKee et al., 2007). In turn, three intracellular type IV collagen α-chains assemble into a triple-helical protomer and are secreted (Figure 1.3B) (Khoshnoodi et al., 2008). In the extracellular space, the carboxy terminus of two protomers associate as a hexameric NC1 domain while the amino terminus of four protomers associate as a dodecameric 7S domain (Figure 1.3B) (Cummings et al., 2016). In contrast to the disulfide reinforcements between laminin trimers, the intermolecular NC1 and 7S domain connections of type IV collagen are covalently crosslinked, and thus,

imbue type IV collagen networks with remarkable stability (Figure 1.3B) (Añazco et al., 2016; Vanacore et al., 2009). Once the polymerized sheets of laminin and type IV collagen are formed, they are then non-covalently linked together by nidogens and the heparan sulfate proteoglycan, perlecan (Yurchenco, 2011). Deletion or mutation of these or other accessory basement membrane macromolecules can cause embryonic lethality, terminal skin blistering diseases, and other severe tissue disorganization phenotypes in humans (Rozario and DeSimone, 2010).

Interstitial matrix barriers

Juxtaposed to the basement membrane, the interstitial matrix is organized into a thick 3D meshwork dominated by type I collagen fibers and elastin fibrils that are intermixed with dozens, if not hundreds, of additional bioactive macromolecules (Figure 1.4A) (Hynes and Naba, 2012; Perumal et al., 2008; Sabeh et al., 2009a). Lying parallel to the basement membrane, the interstitial matrix is almost ubiquitously distributed between cell layers, making type I collagen the most abundant extracellular protein in mammals (Kadler et al., 1996; Ricard-Blum, 2011). Embedded within the interstitial matrix are fibroblasts, smooth muscle cells and pericytes, as well as macrophages, and other related cell types. Beyond physically supporting cells, the interstitial matrix also acts as a reservoir of growth factors and chemoattractants whose release during tissue remodeling events have wide-ranging growth- and migration- promoting effects on cell behavior (Hynes, 2009; Overall and Blobel, 2007; Page-McCaw et al., 2007; Schenk and Quaranta, 2003).

Interstitial matrix assembly and structure

Type I collagen is formed from the organization of narrow fibrils (10-300nm diameter) into thick cords and “tapes” 1-20um wide (Figure 1.4B) (Kadler et al., 1996; Ushiki, 2002). Resident stromal fibroblasts synthesize and assemble two type I collagen α-1 chains and one α-2 chain into a triple-helical fiber terminating at each end with nonhelical telopeptide domains (Kadler et al., 1996; Sabeh et al., 2009a). Upon deposition into the extracellular space, lysyl oxidase-driven crosslinking of spontaneously associated N-terminal and C-terminal telopeptide domains stabilize type I collagen molecules into a 3D polymeric network (Orgel et al., 2000). The arrangement of the collagen network can imbue tissues with distinct properties e.g. thick parallel bundles of type I collagen lending enormous tensile strength to the Achilles tendon, while the distinct orthogonal arrangement of type I collagen fibers in the cornea allow for its optical clarity. (Benedek, 1971; Kadler et al., 1996; Meek and Knupp, 2015; Mouw et al., 2014; Roeder et al., 2002; Ushiki, 2002).

Interwoven with the collagen network, elastin is responsible for providing the elastic recoil that distinguishes tissues undergoing repeated expansion-retraction cycles (Mansfield et al., 2009; Sherratt, 2009). As such, elastin is found at the highest concentrations in arteries, heart, skin and lung tissue, but also at sites where elasticity is required for sheathing internal organs, e.g., the peritoneum (Kelleher et al., 2004; Shifren and Mecham, 2006; Wagenseil et al., 2009; Wagenseil and Mecham, 2007). Elastin is organized as a web or sheet of thin (0.1-0.2 um diameter) fibrils assembled in the extracellular space by fibroblasts (Figure 1.4C) (Ushiki, 2002). Before the mature elastin fiber can be formed, a pericellular microfibril scaffold, composed mainly of fibrillins, is secreted and assembled (Wagenseil and Mecham, 2007). Elastin precursors are then

secreted and aggregate with the cell surface-associated fibrillin scaffold where they can be processed into macromolecular elastin structures (Wagenseil and Mecham, 2007). In a similar fashion to type I collagen assembly, elastin is heavily crosslinked by lysyl oxidase family members (i.e. LOX, LOXL1, LOXL2, etc.) to form an elastic web of interlocking fibrils (Mouw et al., 2014; Rowe and Weiss, 2009; Wagenseil and Mecham, 2007). The coalescence of type I collagen, elastin, and hundreds of additional attendant macromolecules forms a complex 3D matrix barrier with diverse *in vivo* functionality (Hynes, 2009; Hynes and Naba, 2012).

Macrophage migration across ECM barriers *in vivo*

While the relative density and composition of the ECM in the body is diverse, the core group of proteins, and the inter-molecular crosslinks that reinforce them, are conserved across tissues and evolutionary timescales (Fidler et al., 2014, 2017; Zbek et al., 2010). Macrophages perform critical homeostatic functions organism-wide, and thus are constantly interacting with these core ECM proteins, including associating with basement membrane structures in lymph node, intestine, lung, and mammary gland (Figure 1.5) (Vannella and Wynn, 2017; Wynn and Vannella, 2016). Macrophages also interact with the ECM during migration to sites of tissue damage and inflammation *in vivo* (Duffield et al., 2005; Eming et al., 2017; Vannella and Wynn, 2017). Indeed, large numbers of infiltrating bone marrow-derived macrophages (BMDM) are found in a range of microenvironments, such as those arising in aortic aneurysms, obesity-affected adipose tissue, and bacterial infections (Vannella and Wynn, 2017; Wynn and Vannella, 2016; Xiong et al., 2009). In an inflammatory model wherein one lobe of the liver is cauterized and the opposite lobe left untouched, macrophages from the uninjured lobe

are found crossing the intervening basement membrane into the damaged lobe (Suzuki et al., 2015). Furthermore, in a mouse model of obesity, macrophage numbers positively correlate with growing adipocyte size and total body mass (Weisberg et al., 2003). Interestingly, adipose tissue macrophages also tightly associated with the higher density of elastin fibrils found in the interstitial matrix of obese mice (Martinez-Santibanez et al., 2015). Therefore, macrophages appear to readily associate with and traverse both basement membrane and interstitial matrix barriers during inflammatory events.

Macrophage-mediated ECM remodeling and repair

In addition to increased macrophage infiltration correlating with migration across ECM barriers, the advent of powerful tools to effect macrophage depletion has allowed for a more definitive examination of the impact of accumulating macrophages on tissue remodeling *in vivo* (Naglich et al., 1992; Saito et al., 2001; van Rooijen and Hendrikx, 2010). In a seminal study, Duffield and colleagues utilized a reversible model of carbon tetrachloride (CCL_4)-induced liver fibrosis to evaluate macrophage functions during distinct stages of injury and repair (Duffield et al., 2005). Selective macrophage depletion was achieved with a CD11b-DTR mouse, wherein the injection of diphtheria toxin selectively ablates diphtheria toxin receptor-expressing macrophages (Duffield et al., 2005; Naglich et al., 1992; Saito et al., 2001). In control mice, CCL_4 administration for 12 weeks induces a fibrotic response marked by increased ECM deposition that is then lost over a 7-day recovery period (Iredale et al., 1998; Issa et al., 2004). Selective macrophage depletion during peak fibrosis caused a marked reduction in total collagen and elastin accumulation (Duffield et al., 2005). Thus, during injury and subsequent inflammation, macrophages directly or indirectly promote the deposition of ECM. In

contrast to early macrophage depletion, when macrophages were depleted during recovery i.e. the week after CCL_4 administration was ended, the fibrotic scar remained (Duffield et al., 2005). Therefore, during wound healing, macrophages promote the degradation and resorption of ECM. Indeed, macrophages infiltrating into a range of inflammatory environments mediate similar fibrosis-promoting and wound resolving phenotypes (Barreiro et al., 2016; Wynn and Vannella, 2016). Although a recognized oversimplification, the opposing pro-inflammatory (I.e., M1) and pro-repair macrophage (I.e., M2) phenotypes are a convenient shorthand for describing a continuous spectrum of macrophage activity (Figure 1.6) (Murray et al., 2014). However, as an additional layer of complexity, depending on the tissue and the disease model, the contribution of resident tissue macrophages and BMDM to tissue damage and repair varies significantly (Ghosn et al., 2010; Gundra et al., 2014; Lavine et al., 2014; Noy and Pollard, 2014; Wynn and Vannella, 2016).

Macrophage-ECM interactions in the tumor microenvironment

To progress from carcinoma *in situ* to a metastatic lesion, invading carcinoma cells degrade and transmigrate intervening ECM barriers (Hanahan and Weinberg, 2011; Rowe and Weiss, 2008, 2009). While some carcinoma cells eventually acquire the ability to degrade the ECM in an autonomous fashion, recent studies have suggested that carcinomas are able to recruit a complex mix of stromal cells to aid pre-malignant tumor dissemination (Banys et al., 2012; Hüsemann et al., 2008; Linde et al., 2018; Sänger et al., 2011; Turajlic and Swanton, 2016). Within the tumor microenvironment, tumor-associated macrophages (TAMs) are one of the earliest and most numerous tumor-promoting stromal cell types recruited to neoplastic sites (Franklin et al., 2014; Lin et al.,

2001; Linde et al., 2018). Indeed, recent clinical studies correlate increasing macrophage numbers with poor patient survival in lung, breast, and prostate carcinomas, as well as malignant brain tumors (Noy and Pollard, 2014; Ries et al., 2014). Furthermore, in a mouse model of breast cancer (*MMTV-PyVT*), real-time intravital imaging captures carcinoma cells migrating towards, and invading into, basement membrane-ensheathed tumor vasculature in close association with macrophage ”chaperones” (Harney et al., 2015; Lewis et al., 2016; Wyckoff et al., 2007). As such, tumor and macrophage migration presumably necessitate traversing both interstitial matrix and vascular basement membrane barriers.

The differentiation and chemotaxis of macrophages to tumor sites is mediated by secreted growth factors and chemokines i.e. CSF-1 and CCL-2, that are produced by carcinoma cells (Figure 1.7) (Qian et al., 2011; Ries et al., 2014). Consistent with macrophages acting as pivotal remodelers of ECM barriers in the tumor microenvironment, targeted inhibition of CSF-1 or CCL-2, as well as chemical or genetic depletion of macrophages, significantly abrogates carcinoma cell dissemination and metastasis (Linde et al., 2018; Noy and Pollard, 2014; Ries et al., 2014). Interestingly, primary tumor growth is largely unaffected by macrophage depletion, suggesting a specific effect on the dissemination of carcinoma cells. Thus, macrophages are hypothesized to play a critical role in promoting tumor progression (Franklin and Li, 2016; Noy and Pollard, 2014; Ries et al., 2014). However, the question remains: what are the mechanisms that support macrophage-mediated ECM remodeling?

Mechanisms of ECM remodeling

The ability of a cell to traverse the ECM is dependent on the properties of both the ECM barrier, and the cell itself (Rowe and Weiss, 2009; Sabeh et al., 2009a; Wolf et al., 2013). The pore size of a matrix, and thus the function of that matrix as a barrier, are dictated by the density and crosslinking of its constituents. For example, the pore size of a dense (~2 mg/ml) crosslinked type I collagen matrix are less than 2 μm in diameter (Sabeh et al., 2009a; Wolf et al., 2013). In turn, the ability of a cell to traverse the pores in the ECM depends on the pore size of the matrix relative to the size and rigidity of the nucleus (~10 μm diameter), the least deformable organelle in the cell (Dahl, 2004; Davidson et al., 2014; Gerlitz and Bustin, 2011; Wolf et al., 2013). Therefore, cells traversing dense, crosslinked ECM with pores that are significantly smaller than the nucleus are thought to remodel intervening fibers, either by proteolytic degradation or non-proteolytic displacement (Rowe and Weiss, 2009; Sabeh et al., 2009a; Wolf et al., 2013). Similar, if not identical, mechanisms are thought to be mobilized to remodel ECM at sites of tissue damage or inflammation (Rowe and Weiss, 2009; Sabeh et al., 2009a).

Over 600 distinct proteinases belonging to 5 distinct families (aspartate, cysteine, metallo, serine, and threonine) are expressed in mouse and human cells alike (Page-McCaw et al., 2007; Rowe and Weiss, 2008). *In vivo* transcript arrays suggest macrophages basally express dozens, if not hundreds of proteinases, that following exposure to immune stimuli, growth factors, or cytokines, are up- or down-regulated (Afik et al., 2016; Murray et al., 2013; Ojalvo et al., 2009, 2010; Wynn and Vannella, 2016). By extension, *in vitro* studies have defined a spectrum of macrophage responses to immune stimuli by characterizing the distinct patterns of gene and protein expression, including proteinases (Beyer et al., 2012; Martinez et al., 2006; Murray et al., 2013). At one end of

this spectrum, “classically” activated macrophages, polarized with lipopolysaccharide (LPS), model the initial response to injury and inflammation (Murray et al., 2014). At the other extreme of macrophage activation states, “alternatively” activated macrophages, polarized with the interleukin-4 (IL-4), model a wound healing response (Murray et al., 2014). Interestingly, dozens of extracellular proteinases, including members of the cysteine, serine, and metalloprotease families, correlate with macrophage migration and distinct activation states associated with tissue remodeling and repair (Murray et al., 2013; Ojalvo et al., 2009, 2010). For example, a recent study demonstrated macrophages mobilize cysteine proteinases, i.e., CtsB, CtsX, and CtsS, in order to migrate across an *in vitro* 3D matrix (Jevnikar et al., 2012). In addition, gene expression analysis of mouse macrophages reveals at least 7 matrix metalloproteinases (MMPs) are induced by LPS-stimulation, including MMP-2, MMP-9, and MMP-14, in order to degrade an *in vitro* 3D matrix (Murray et al., 2013). While a remarkable number of proteinases correlate with macrophage migration and ECM remodeling, arguably, the most well-established ECM remodeling proteases are MMPs (Rowe and Weiss, 2009; Sabeh et al., 2009; Page-McCaw et al., 2007).

Macrophage MT1-MMP as an effector of ECM remodeling

The matrix metalloproteinase family has been repeatedly implicated in ECM remodeling programs of fibroblasts, carcinoma cells, and macrophages (Page-McCaw et al., 2007; Rowe et al., 2011; Rowe and Weiss, 2009). The 25-member MMP family is an evolutionarily-conserved class of zinc-dependent endopeptidases that can be further divided into two subclasses: 18 secreted MMPs and 6 membrane-tethered MMPs (MT-MMPs) (Page-McCaw et al., 2007). MT-MMPs are associated with the cell membrane

either by a hydrophobic transmembrane domain (i.e., MT1-MMP, MT2-MMP, MT3-MMP, and MT5-MMP) or a glycosylphosphatidyl inositol (GPI)-anchor (i.e., MT4-MMP and MT6-MMP) (Page-McCaw et al., 2007). MT-MMPs are synthesized as latent zymogens with an auto-inhibitory prodomain that is proteolytically removed by the proprotein convertase, furin, as the zymogen traverses the trans-golgi network (Pei and Weiss, 1995). Upon the intracellular removal of the inhibitory prodomain, MT-MMPs traffic to the cell surface where they are displayed as active enzymes (Pei and Weiss, 1996; Wiesner et al., 2013; Yana and Weiss, 2000). While MMP family members are capable of degrading a wide array of substrates, e.g. ranging from surface proteins, to growth factors and cytokines as well as almost every ECM component, global knockouts of MMPs in transgenic mice unexpectedly display only subtle defects, with a single exception (Page-McCaw et al., 2007). Following knockout, MT1-MMP-deficient mice display progressive cranio-facial abnormalities and dwarfism, uniformly expiring by 3-12 weeks after birth, depending on the strain (Holmbeck et al., 1999; Zhou et al., 2000). In large part, this phenotype is due to a failure of MT1-MMP knockout mice to remodel the ECM, particularly type I collagen (Itoh, 2015; Rowe and Weiss, 2009).

ECM models

Evidence from patient data and *in vivo* animal studies support a model wherein macrophages respond to diverse physiologic and pathologic microenvironments by mobilizing proteases to degrade or repair the ECM (Eming et al., 2017; Murray et al., 2014). However, the complex milieu of cells *in vivo* hinder efforts to define the mechanisms of macrophage-mediated ECM remodeling. By necessity, investigations of the underlying mechanisms of ECM migration and remodeling have adopted a range of

in vitro matrix constructs (Murray et al., 2013; Van Goethem et al., 2010; Vérollet et al., 2011). Not only do *in vitro* models permit the study of macrophage autonomous functions in the presence of distinct immune modulators, but in addition, degradation of these constructs can readily be imaged in real-time and at high resolution. Therefore, mechanistic studies using *in vitro* models have significant advantages over *in vivo* models in terms of mechanistic analysis, but often, if not always, these models oversimplify the structural and mechanical properties of the native ECM.

Given the complex structure and relative insolubility of the covalently crosslinked basement membrane *in vivo*, the harvesting of soluble basement membrane extracts from mouse Engelbreth-Holm-Swarm sarcoma cells in the 1970's as a basement membrane "mimetic" was a boon to early investigators (Kleinman and Martin, 2005; Orkin et al., 1977). Commercially sold as Matrigel, this composite contains laminin, type IV collagen, nidogen, and perlecan, in short, nearly all the components of *in vivo* basement membrane (Kleinman and Martin, 2005). Extensively used as a 3D scaffold in migration and degradation studies even today, an often-overlooked shortcoming of Matrigel is that it is mainly comprised of an isoform of laminin rarely found in adult animals and lacks the type IV collagen covalent crosslinks that define the basement membrane as a mechanical barrier (Halfter et al., 2015; Rowe and Weiss, 2008, 2009; Willis et al., 2013). Given that the non-covalently crosslinked components of Matrigel may be traversed by non-proteolytic displacement of ECM fibers alone, it is unclear whether it should be used as a basement membrane surrogate for transmigration studies (Rowe and Weiss, 2009; Sodek et al., 2008). Yet, due to its ubiquitous availability as a simple 3D matrix scaffold, a bevy of publications have used Matrigel to study the mechanisms of macrophage-

mediated ECM remodeling (Akkari et al., 2014; Fleetwood et al., 2014; Gui et al., 2014; Jevnikar et al., 2012; Murray et al., 2013; Vérollet et al., 2011; Wiesner et al., 2014).

In contrast to the basement membrane, interstitial matrix mimics are typically assembled using purified extracts of relatively homogenous type I collagen instead of a complex mix of interstitial matrix proteins (Rowe and Weiss, 2009; Sabeh et al., 2009a). However, similar to Matrigel, type I collagen extracts are readily gelled into 3D scaffolds in concentrations meant to reflect *in vivo* ECM (Sabeh et al., 2009a; Wiesner et al., 2014; Wolf et al., 2013). Typically isolated from rat tail or bovine skin, the extraction process is a critical determinant of the model's physiologic relevance (Sabeh et al., 2009a). Specifically, a commonly used pepsin-extraction process removes the N- and C-terminal type I collagen telopeptides, and with them, the site of lysyl oxidase-mediated crosslinking that dictates the mechanical integrity of type I collagen hydrogels (Demou et al., 2005; Sabeh et al., 2009a). As a consequence of the loss of crosslinking, pepsin-extracted type I collagen gels readily permit non-proteolytic invasion, as migrating cells can physically displace the non-covalently crosslinked collagen fibrils during transmigration (Demou et al., 2005; Sabeh et al., 2009a). In contrast to the pepsin extraction process, acid-extracted type I collagen retains the telopeptide domains and allows for the reversible assembly and disassembly of lysyl oxidase-mediated aldamine crosslinks (Demou et al., 2005; Sabeh et al., 2009a). Consequently, highly crosslinked hydrogels can only be traversed coincident with mobilization of a proteolytic remodeling program.

Given the complexity of protease expression in macrophages and the relative dearth of studies utilizing ECM models that recapitulate the critical mechanical properties that define the ECM *in vivo*, the mechanisms macrophages employ to traverse and

degrade native basement membrane and interstitial matrix barriers has remained undefined.

Thesis Summary

Herein, using an *ex vivo* mesenteric tissue model and an *in vitro* high-density matrix hydrogel, we define the molecular mechanisms of macrophage remodeling and trafficking of basement membrane and interstitial matrix barriers. Upon adhering to the mesenteric ECM, primary human and mouse macrophages rapidly mobilize a microenvironmentally-tunable basement membrane degradation program that is dependent on MT1-MMP activity (Chapter 2). While, in turn, macrophages traverse the basement membrane-interstitial matrix interface, unexpectedly, neither MT1-MMP, nor cysteine or serine proteases, are required (Chapter 2). However, we find that macrophages actively traversing high-density interstitial matrix barriers require MT1-MMP to degrade passageways through the matrix permissible for cellular trafficking (Chapter 3). Finally, we consider the *in vivo* implications of macrophage-mediated ECM degradation illustrated by preliminary data from a mouse model of brain cancer (Chapter 4). Together, these studies define MT1-MMP-dependent and independent mechanisms by which macrophages traffic and remodel the extracellular matrix barrier.

Figure 1.1

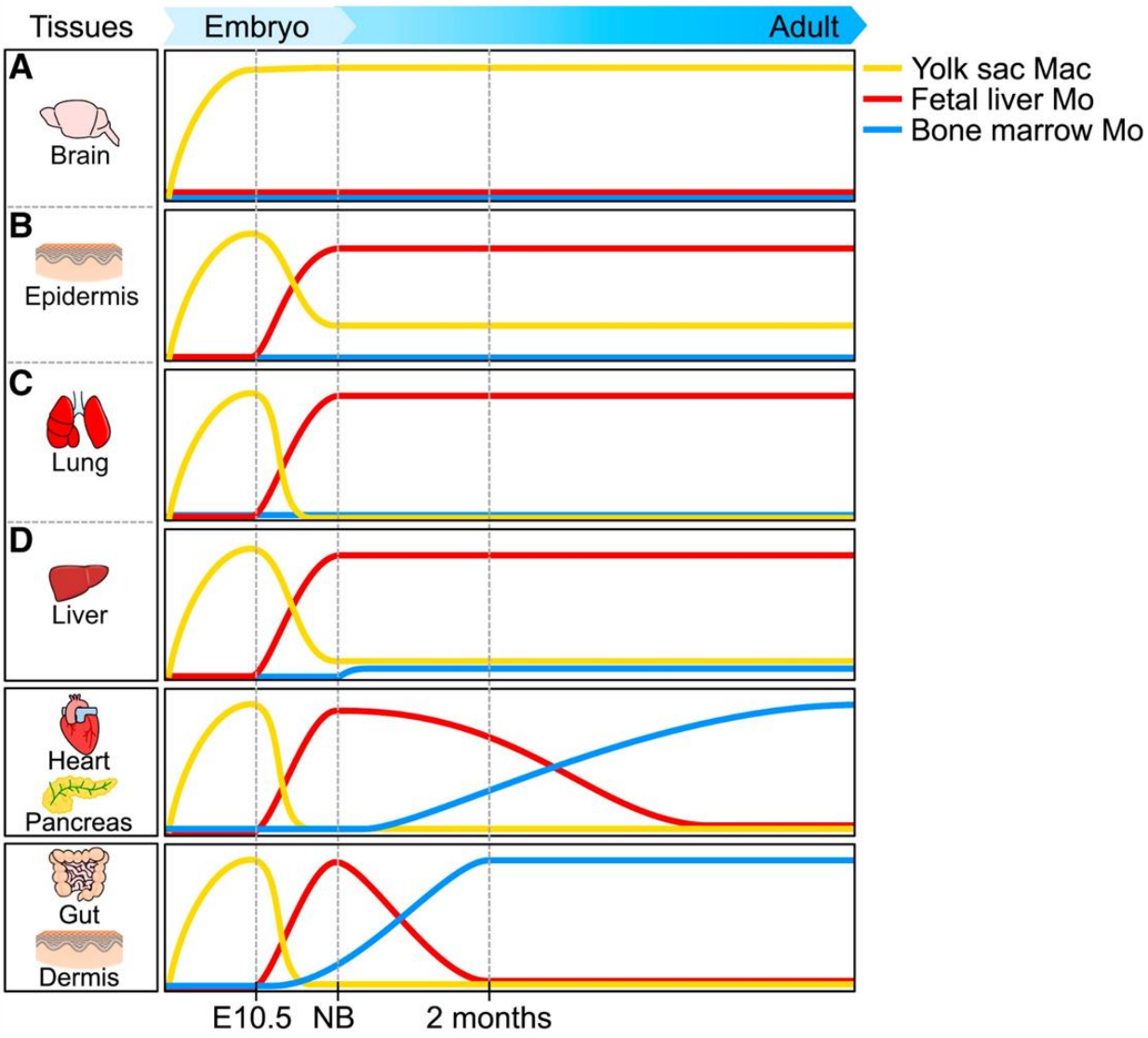

Figure 1.1: Origin and dynamics of tissue resident macrophage seeding.
The earliest embryonic yolk sac macrophages seed and persist in the brain into adulthood (Ginhoux and Guilliams, 2016). In contrast to the brain, epidermal macrophages are 100% yolk sac origin until fetal liver macrophages replace and outnumber them 80% vs 20% in adulthood. In addition, fetal liver macrophages replace yolk-sac macrophages almost completely in adult lung and liver. Interestingly, bone marrow derived macrophages dynamically replace the embryonic macrophages of tissues with distinct kinetics, slow (heart and pancreas) and fast (gut and dermis).

Figure 1.2

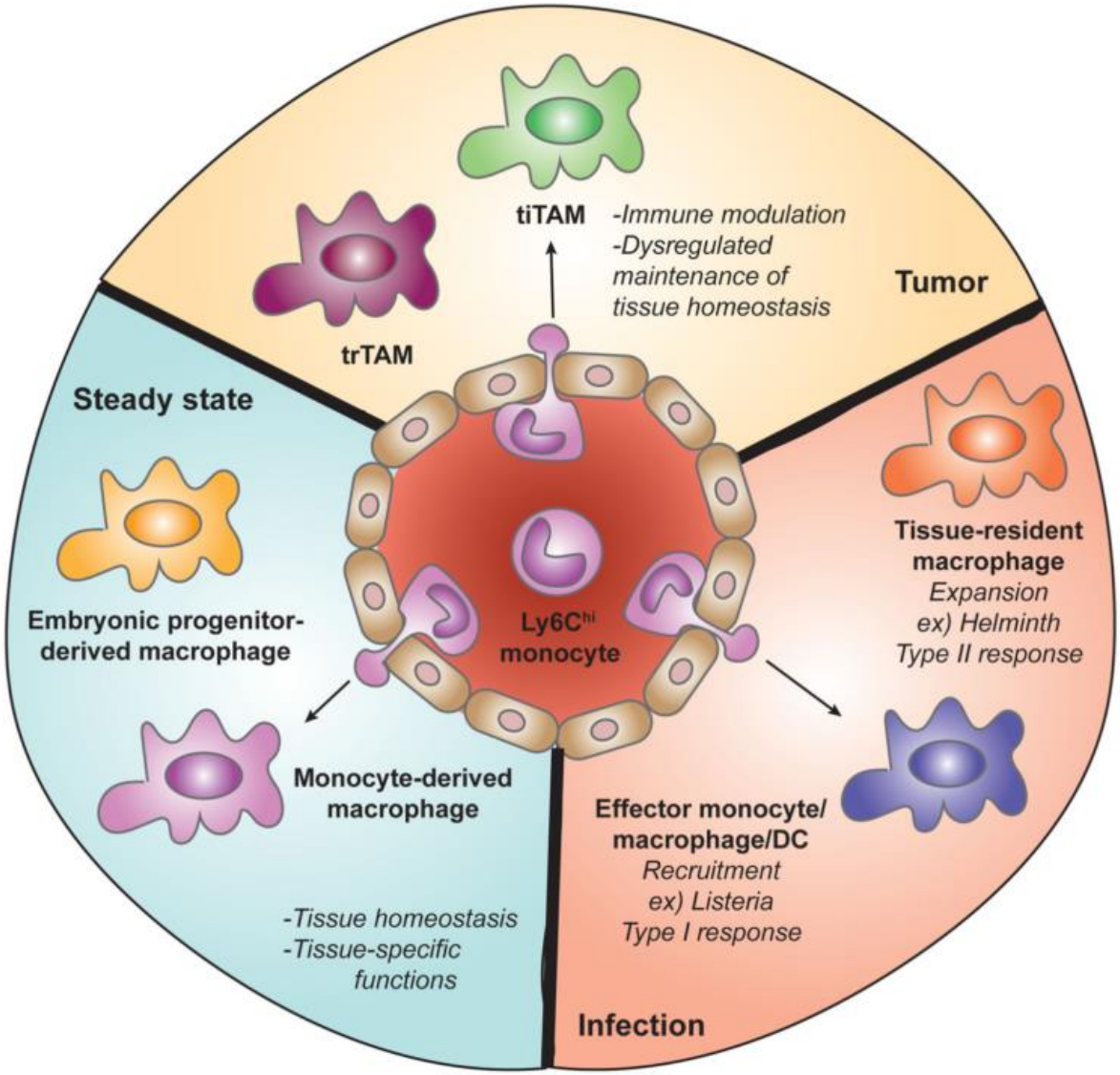

Figure 1.2: Bone marrow monocyte-derived macrophage activity.
During homeostasis embryonic progenitor-derived macrophages populate most tissues, with some exceptions for monocyte-derived tissue resident macrophages. Most infections are dominated by recruited monocyte-derived macrophages while less common parasitic helminths induce tissue-resident macrophage proliferation. Tumor progression is marked by the early influx and expansion of monocyte-derived macrophages (Franklin and Li, 2016).

Figure 1.3

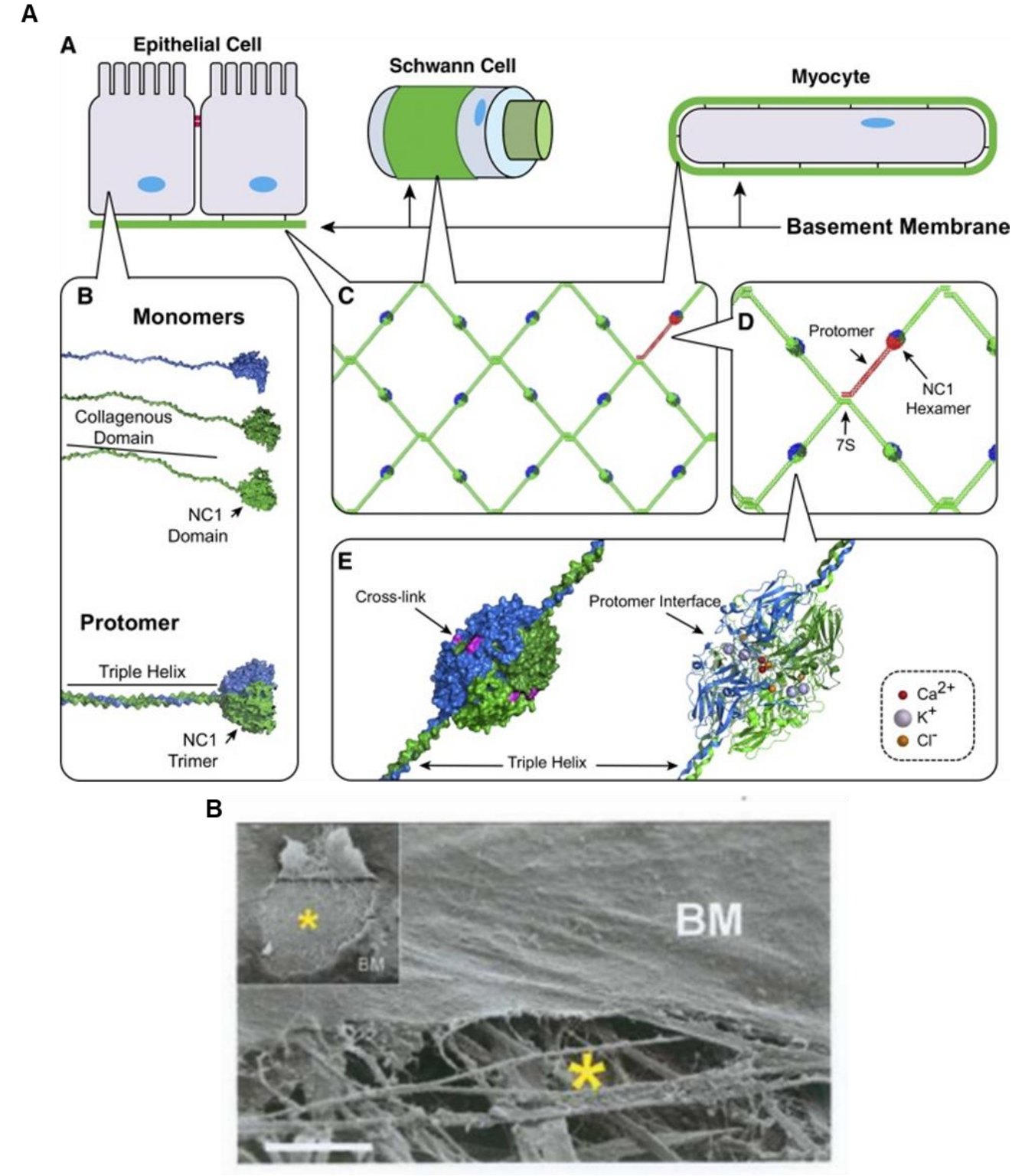
A
Epithelial Cell
Schwann Cell
Myocyte
Basement Membrane
B
Monomers
Collagenous Domain
NC1 Domain
Protomer
Triple Helix
NC1 Trimer
C
D
Protomer
NC1 Hexamer
7S
E
Cross-link
Protomer Interface
Triple Helix
Ca2+
K+
Cl-
B
BM
BM

Figure 1.3: Basement membrane structure and organization
(A) Basement membrane structures underlie epithelial cell layers as well as ensheathe Schwann cells and myocytes (Cummings et al., 2016). Type Ⅳ collagen α-chains form a triple-helical protomer. Protomers are assembled into a network extracellularly, cross-linking reinforces the NC1 hexamer junctions between protomers. **(B)** Scanning electron microscopy of denuded mesentery tissue reveals the thin, confluent, basement membrane layer overlying an interstitial matrix (yellow asterisk) (Hotary et al., 2006). Scale bar, 20 um.

Figure 1.4

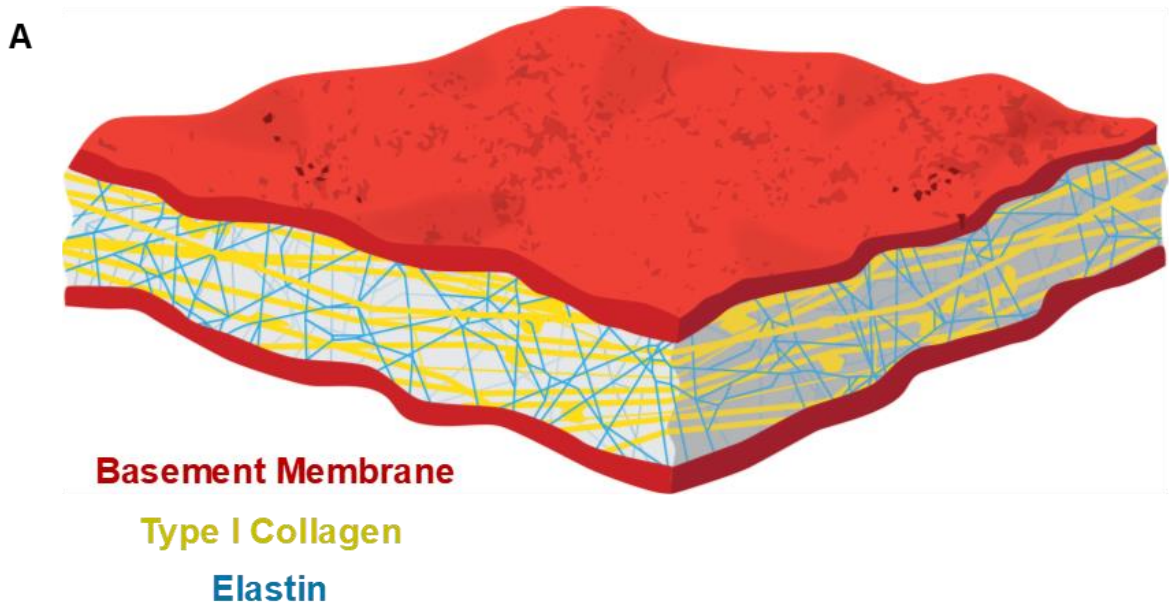

Figure 1.4: Interstitial matrix structure and organization.
(A) Schematic of 2D basement membrane and 3D interstitial matrix. **(B)** SEM of type I collagen fibers (arrowhead), bundles and tapes found in human subcutaneous tissue (left panel) and rat aorta (right panel). Scale bar: 5 um. **(C)** SEM of the elastin reticulation of the rat adventitia after formic acid digestion of collagen, including a 4-way junction (left panel, arrow). Elastin lamina of the rat aorta in a sheet-like pattern with large fenestrations (Ushiki, 2002).

Figure 1.5

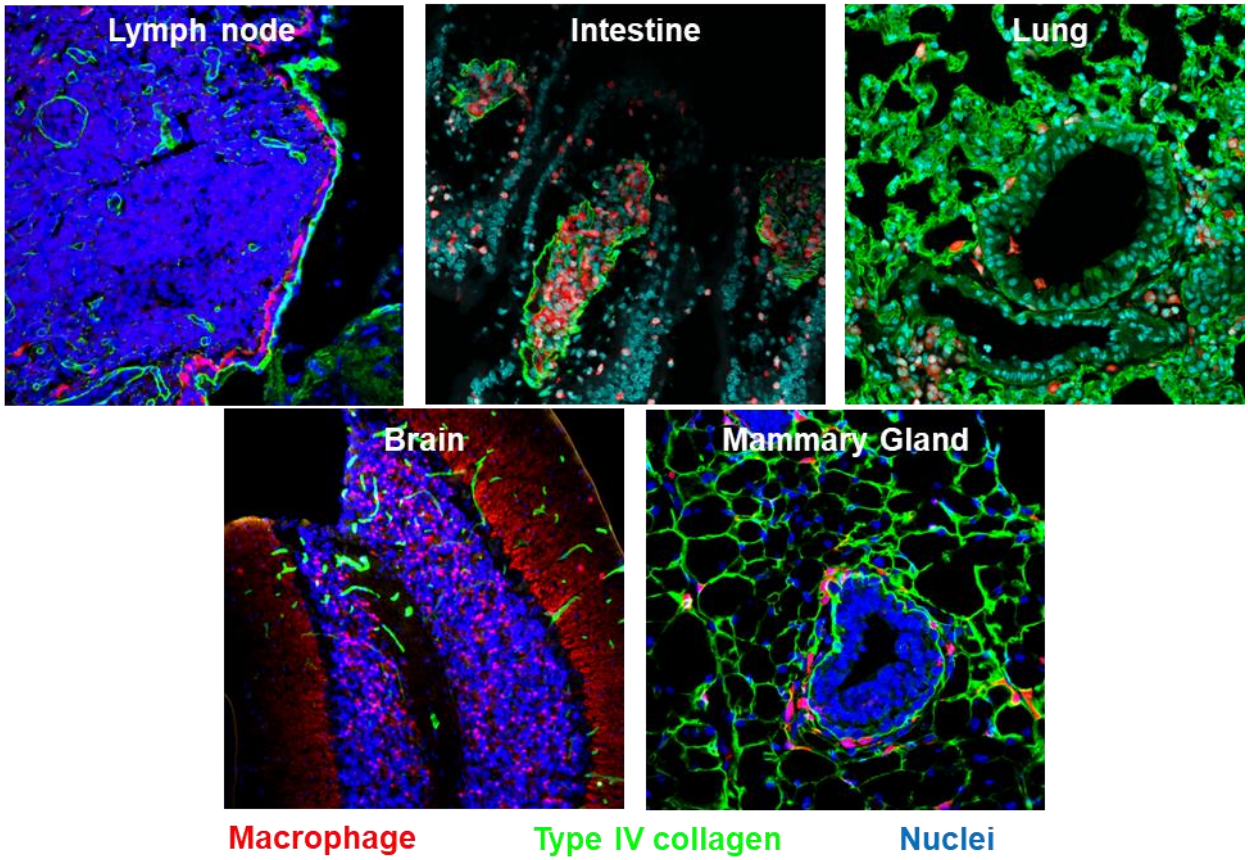

Figure 1.5: Macrophage-basement membrane co-localization *in vivo*.
Tissue resident macrophages indelibly labeled red in a Csf1r-Cre-Rosa26R-tdTomato mouse model colocalize with basement membrane (green) during homeostasis.

Figure 1.6

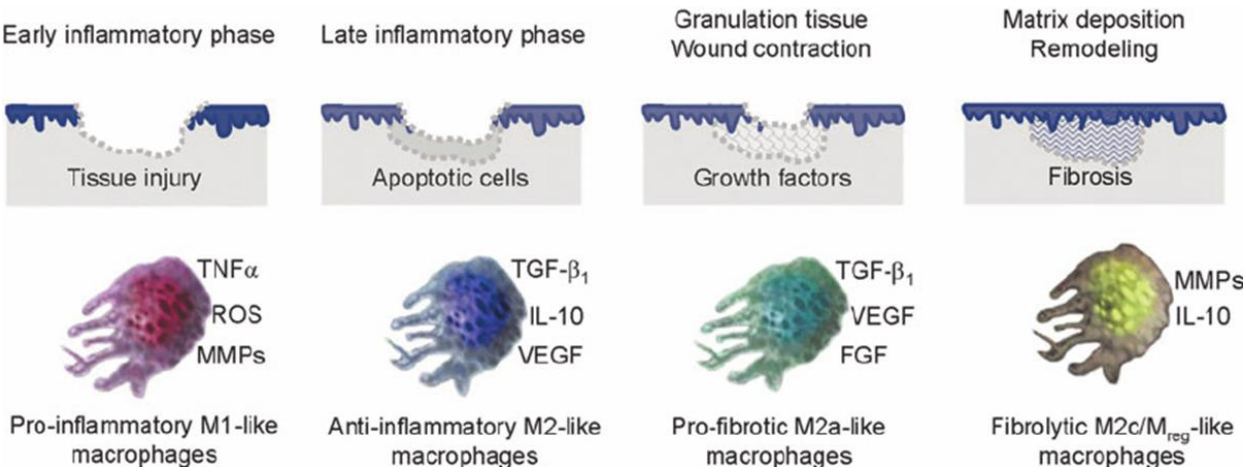

Figure 1.6: Dynamic macrophage functions during wound repair.
Macrophages mediate the wound microenvironment at every stage of the repair process. Initially, macrophages promote an immune response and upregulate the expression of proteolytic MMP enzymes. As the wound is sealed and foreign microbes cleared, macrophages dampen the host immune response and promote wound closure and fibrosis (Sindrilaru and Scharffetter-Kochanek, 2013).

Figure 1.7

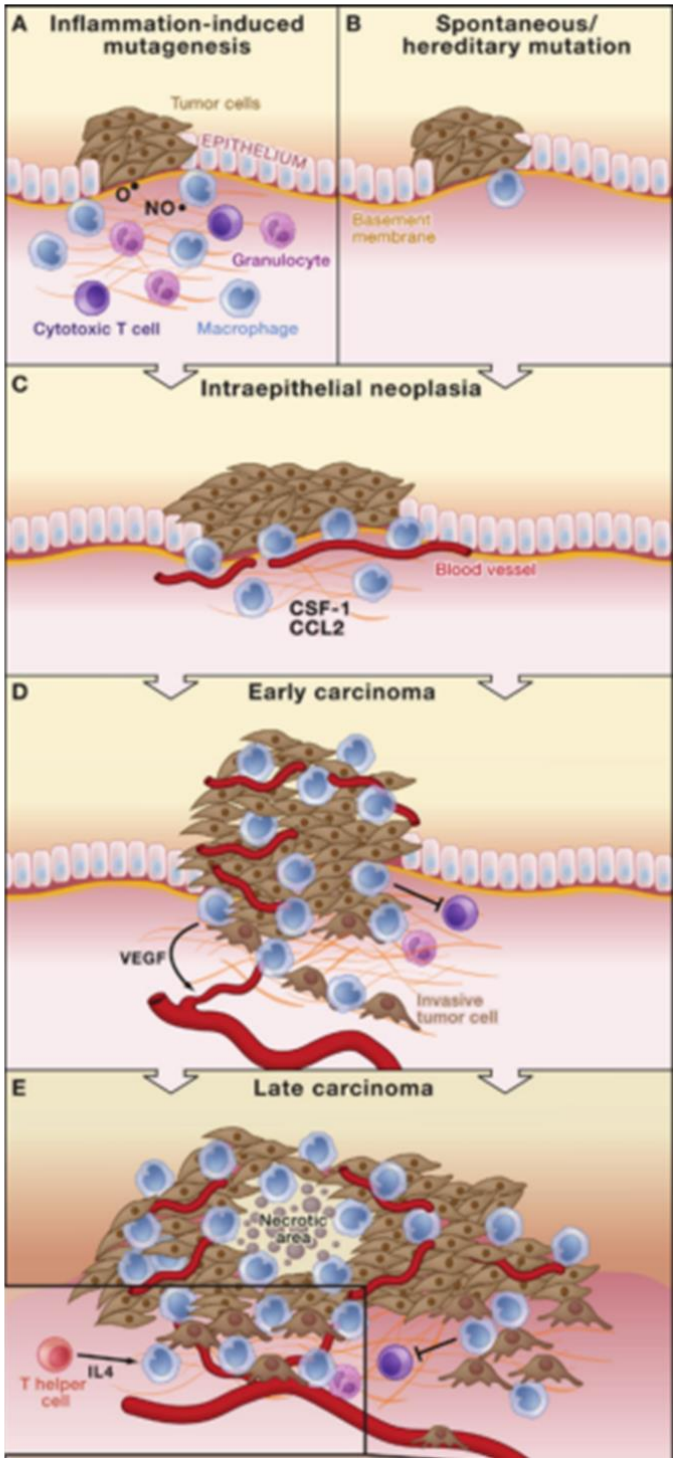

Figure 1.7: Macrophages promote tumor progression.
(A) Chronic inflammation or spontaneous mutations can initiate cancer growth. Chemoattractants such as CSF-1 and CCL-2 attract macrophages to the growing neoplasia where they are thought to promote tumor progression to an early invasive

carcinoma by promoting angiogenesis and remodeling basement membrane barriers (Qian and Pollard, 2010). Tumor-promoting macrophage activity continues into late-stage carcinomas and metastasis as macrophages promote cancer cell intravasation and the seeding of distant sites.

References

Afik, R., Zigmond, E., Vugman, M., Klepfish, M., Shimshoni, E., Pasmanik-Chor, M., … Varol, C. (2016). Tumor macrophages are pivotal constructors of tumor collagenous matrix. *The Journal of Experimental Medicine*, *213*(11), 2315–2331.

Akkari, L., Gocheva, V., Kester, J. C., Hunter, K. E., Quick, M. L., Sevenich, L., … Joyce, J. A. (2014). Distinct functions of macrophage-derived and cancer cell-derived cathepsin Z combine to promote tumor malignancy via interactions with the extracellular matrix. *Genes and Development*, *28*(19), 2134–2150.

Añazco, C., López-Jiménez, A. J., Rafi, M., Vega-Montoto, L., Zhang, M.-Z., Hudson, B. G., & Vanacore, R. M. (2016). Lysyl Oxidase-like-2 Cross-links Collagen IV of Glomerular Basement Membrane. *The Journal of Biological Chemistry*, *291*(50), 25999–26012.

Banys, M., Gruber, I., Krawczyk, N., Becker, S., Kurth, R., Wallwiener, D., … Fehm, T. (2012). Hematogenous and lymphatic tumor cell dissemination may be detected in patients diagnosed with ductal carcinoma in situ of the breast. *Breast Cancer Research and Treatment*, *131*(3), 801–808.

Barreiro, O., Cibrian, D., Clemente, C., Alvarez, D., Moreno, V., Valiente, Í., … Madrid, F. S. (2016). Pivotal role for skin transendothelial radio-resistant anti-inflammatory macrophages in tissue repair. *ELife*, *5*(JUN2016).

Benedek, G. B. (1971). Theory of Transparency of the Eye. *Applied Optics*, *10*(3), 459.

Beyer, M., Mallmann, M. R., Xue, J., Staratschek-Jox, A., & Vorholt, D. (2012). High-Resolution Transcriptome of Human Macrophages. *PLoS ONE*, *7*(9), 45466.

Buchmann, K. (2014). Evolution of Innate Immunity: Clues from Invertebrates via Fish to Mammals. *Frontiers in Immunology*, *5*, 459.

Candiello, J., Balasubramani, M., Schreiber, E. M., Cole, G. J., Mayer, U., Halfter, W., & Lin, H. (2007). Biomechanical properties of native basement membranes. *FEBS Journal*, *274*(11), 2897–2908.

Cummings, C. F., Pedchenko, V., Brown, K. L., Colon, S., Rafi, M., Jones-Paris, C., … Hudson, B. G. (2016). Extracellular chloride signals collagen IV network assembly during basement membrane formation. *Journal of Cell Biology*, *213*(4), 479–494.

Dahl, K. N. (2004). The nuclear envelope lamina network has elasticity and a compressibility limit suggestive of a molecular shock absorber. *Journal of Cell Science*, *117*(20), 4779–4786.

Davidson, P. M., Denais, C., Bakshi, M. C., & Lammerding, J. (2014). Nuclear deformability constitutes a rate-limiting step during cell migration in 3-D environments. *Cellular and Molecular Bioengineering*, *7*(3), 293–306.

Demou, Z. N., Awad, M., McKee, T., Perentes, J. Y., Wang, X., Munn, L. L., … Boucher, Y. (2005). Lack of Telopeptides in Fibrillar Collagen I Promotes the Invasion of a Metastatic Breast Tumor Cell Line. *Cancer Research*, *65*(13), 5674–5682.

Duffield, J. S., Forbes, S. J., Constandinou, C. M., Clay, S., Partolina, M., Vuthoori, S., … Iredale, J. P. (2005). Selective depletion of macrophages reveals distinct, opposing roles during liver injury and repair. *The Journal of Clinical Investigation*, *115*(1), 56–65.

Eming, S. A., Wynn, T. A., & Martin, P. (2017). Inflammation and metabolism in tissue repair and regeneration. *Science*.

Epelman, S., Lavine, K. J., Beaudin, A. E., Sojka, D. K., Carrero, J. A., Calderon, B., … Mann, D. L. (2014). Embryonic and Adult-Derived Resident Cardiac Macrophages Are Maintained through Distinct Mechanisms at Steady State and during Inflammation. *Immunity*, *40*(1), 91–104.

Fidler, A. L., Darris, C. E., Chetyrkin, S. V, Pedchenko, V. K., Boudko, S. P., Brown, K. L., … Hudson, B. G. (2017). Collagen iv and basement membrane at the evolutionary dawn of metazoan tissues. *ELife*, *6*.

Fidler, A. L., Vanacore, R. M., Chetyrkin, S. V, Pedchenko, V. K., Bhave, G., Yin, V. P., … Hudson, B. G. (2014). A unique covalent bond in basement membrane is a primordial innovation for tissue evolution. *Proceedings of the National Academy of Sciences*, *111*(1), 331–336.

Fleetwood, A. J., Achuthan, A., Schultz, H., Nansen, A., Almholt, K., Usher, P., & Hamilton, J. A. (2014). Urokinase plasminogen activator is a central regulator of macrophage three-dimensional invasion, matrix degradation, and adhesion. *Journal of Immunology (Baltimore, Md. : 1950)*, *192*(8), 3540–3547.

Franklin, R. A., & Li, M. O. (2016). Ontogeny of Tumor-associated Macrophages and Its Implication in Cancer Regulation. *Trends in Cancer*, *2*(1), 20–34.

Franklin, R. A., Liao, W., Sarkar, A., Kim, M. V, Bivona, M. R., Liu, K., … Li, M. O. (2014). The cellular and molecular origin of tumor-associated macrophages. *Science (New York, N.Y.)*, *344*(6186), 921–925.

Gautier, E. L., Shay, T., Miller, J., Greter, M., Jakubzick, C., Ivanov, S., … Randolph, G. J. (2012). Gene-expression profiles and transcriptional regulatory pathways that underlie the identity and diversity of mouse tissue macrophages. *Nature Immunology*, *13*(11), 1118–1128.

Gerlitz, G., & Bustin, M. (2011, January). The role of chromatin structure in cell migration. *Trends in Cell Biology*.

Ghosn, E. E. B., Cassado, A. A., Govoni, G. R., Fukuhara, T., Yang, Y., Monack, D. M., … Herzenberg, L. A. (2010). Two physically, functionally, and developmentally distinct peritoneal macrophage subsets. *Proceedings of the National Academy of Sciences of the United States of America*, *107*(6), 2568–2573.

Ginhoux, F., Greter, M., Leboeuf, M., Nandi, S., See, P., Gokhan, S., … Merad, M. (2010). Fate mapping analysis reveals that adult microglia derive from primitive macrophages. *Science (New York, N.Y.)*, *330*(6005), 841–845.

Ginhoux, F., & Guilliams, M. (2016, March 15). Tissue-Resident Macrophage Ontogeny

and Homeostasis. *Immunity*. Elsevier.

Gosselin, D., Link, V. M., Romanoski, C. E., Fonseca, G. J., Eichenfield, D. Z., Spann, N. J., … Glass, C. K. (2014). Environment drives selection and function of enhancers controlling tissue-specific macrophage identities. *Cell*, *159*(6), 1327–1340.

Gray, E. E., & Cyster, J. G. (2012). Lymph node macrophages. *Journal of Innate Immunity*, *4*(5–6), 424–436.

Gui, P., Labrousse, A., Van Goethem, E., Besson, A., Maridonneau-Parini, I., & Le Cabec, V. (2014). Rho/ROCK pathway inhibition by the CDK inhibitor p27(kip1) participates in the onset of macrophage 3D-mesenchymal migration. *Journal of Cell Science*, *127*(Pt 18), 4009–4023.

Gundra, U. M., Girgis, N. M., Ruckerl, D., Jenkins, S., Ward, L. N., Kurtz, Z. D., … Loke, P. (2014). Alternatively activated macrophages derived from monocytes and tissue macrophages are phenotypically and functionally distinct. *Blood*, *123*(20), e110-22.

Halfter, W., Oertle, P., Monnier, C. A., Camenzind, L., Reyes-Lua, M., Hu, H., … Plodinec, M. (2015). New concepts in basement membrane biology. *FEBS Journal*, *282*(23), 4466–4479.

Hanahan, D., & Weinberg, R. A. (2011, March 4). Hallmarks of cancer: The next generation. *Cell*. Elsevier.

Harney, A. S., Arwert, E. N., Entenberg, D., Wang, Y., Guo, P., Qian, B. Z., … Condeelis, J. S. (2015). Real-time imaging reveals local, transient vascular permeability, and tumor cell intravasation stimulated by TIE2himacrophage–derived VEGFA. *Cancer Discovery*, *5*(9), 932–943.

Hoeffel, G., Chen, J., Lavin, Y., Low, D., Almeida, F. F., See, P., … Ginhoux, F. (2015). C-Myb+ Erythro-Myeloid Progenitor-Derived Fetal Monocytes Give Rise to Adult Tissue-Resident Macrophages. *Immunity*, *42*(4), 665–678.

Holmbeck, K., Bianco, P., Caterina, J., Yamada, S., Kromer, M., Kuznetsov, S. A., … Birkedal-Hansen, H. (1999). MT1-MMP-deficient mice develop dwarfism, osteopenia, arthritis, and connective tissue disease due to inadequate collagen turnover. *Cell*, *99*(1), 81–92.

Hüsemann, Y., Geigl, J. B., Schubert, F., Musiani, P., Meyer, M., Burghart, E., … Klein, C. A. (2008). Systemic spread is an early step in breast cancer. *Cancer Cell*, *13*(1), 58–68.

Hynes, R. O. (2009, November 27). The extracellular matrix: Not just pretty fibrils. *Science*.

Hynes, R. O., & Naba, A. (2012). Overview of the matrisome-An inventory of extracellular matrix constituents and functions. *Cold Spring Harbor Perspectives in Biology*, *4*(1), a004903.

Iredale, J. P., Benyon, R. C., Pickering, J., McCullen, M., Northrop, M., Pawley, S., …

Arthur, M. J. P. (1998). Mechanisms of spontaneous resolution of rat liver fibrosis: Hepatic stellate cell apoptosis and reduced hepatic expression of metalloproteinase inhibitors. *Journal of Clinical Investigation*, *102*(3), 538–549.

Issa, R., Zhou, X., Constandinou, C. M., Fallowfield, J., Millward-Sadler, H., Gaca, M. D. A., … Iredale, J. P. (2004). Spontaneous recovery from micronodular cirrhosis: Evidence for incomplete resolution associated with matrix cross-linking. *Gastroenterology*, *126*(7), 1795–1808.

Itoh, Y. (2015). Membrane-type matrix metalloproteinases: Their functions and regulations. *Matrix Biology*, *44*, 207–223.

Jevnikar, Z., Mirković, B., Fonović, U. P., Zidar, N., Švajger, U., Kos, J., … Kos, J. (2012). Three-dimensional invasion of macrophages is mediated by cysteine cathepsins in protrusive podosomes. *European Journal of Immunology*, *42*(12), 3429–3441.

Kadler, K. E., Holmes, D. F., Trotter, J. A., & Chapman, J. A. (1996). *Collagen fibril formation*. *Biochem. J* (Vol. 316). Retrieved from https://www.ncbi.nlm.nih.gov/pmc/articles/PMC1217307/pdf/8645190.pdf

Kelleher, C. M., McLean, S. E., & Mecham, R. P. (2004). Vascular Extracellular Matrix and Aortic Development. *Current Topics in Developmental Biology*, *62*, 153–188.

Khoshnoodi, J., Pedchenko, V., & Hudson, B. G. (2008). Mammalian collagen IV. *Microscopy Research and Technique*, *71*(5), 357–370.

Kleinman, H. K., & Martin, G. R. (2005). Matrigel: Basement membrane matrix with biological activity. *Seminars in Cancer Biology*, *15*, 378–386.

Kohyama, M., Ise, W., Edelson, B. T., Wilker, P. R., Hildner, K., Mejia, C., … Murphy, K. M. (2009). Role for Spi-C in the development of red pulp macrophages and splenic iron homeostasis. *Nature*, *457*(7227), 318–321.

Lavin, Y., Winter, D., Blecher-Gonen, R., David, E., Keren-Shaul, H., Merad, M., … Amit, I. (2014). Tissue-Resident Macrophage Enhancer Landscapes Are Shaped by the Local Microenvironment. *Cell*, *159*(6), 1312–1326.

Lavine, K. J., Epelman, S., Uchida, K., Weber, K. J., Nichols, C. G., Schilling, J. D., … Mann, D. L. (2014). Distinct macrophage lineages contribute to disparate patterns of cardiac recovery and remodeling in the neonatal and adult heart. *Proceedings of the National Academy of Sciences of the United States of America*, *111*(45), 16029–16034.

Lewis, C. E., Harney, A. S., Pollard, J. W., Shi, H. S., Zeng, Y. H., Wang, X. Z., … Jones, J. G. (2016). The Multifaceted Role of Perivascular Macrophages in Tumors. *Cancer Cell*, *30*(1), 18–25.

Li, S., Liquari, P., McKee, K. K., Harrison, D., Patel, R., Lee, S., & Yurchenco, P. D. (2005). Laminin-sulfatide binding initiates basement membrane assembly and enables receptor signaling in Schwann cells and fibroblasts. *Journal of Cell Biology*, *169*(1), 179–189.

Lin, E. Y., Nguyen, A. V, Russell, R. G., & Pollard, J. W. (2001). Colony-stimulating factor 1 promotes progression of mammary tumors to malignancy. *The Journal of Experimental Medicine*, *193*(6), 727–740.

Linde, N., Casanova-Acebes, M., Sosa, M. S., Mortha, A., Rahman, A., Farias, E., … Aguirre-Ghiso, J. A. (2018). Macrophages orchestrate breast cancer early dissemination and metastasis. *Nature Communications*, *9*(1), 21.

Mansfield, J., Yu, J., Attenburrow, D., Moger, J., Tirlapur, U., Urban, J., … Winlove, P. (2009). The elastin network: Its relationship with collagen and cells in articular cartilage as visualized by multiphoton microscopy. *Journal of Anatomy*, *215*(6), 682–691.

Martinez-Santibanez, G., Singer, K., Cho, K. W., DelProposto, J. L., Mergian, T., & Lumeng, C. N. (2015). Obesity-induced remodeling of the adipose tissue elastin network is independent of the metalloelastase MMP-12. *Adipocyte*, *4*(4), 264–272.

Martinez, F. O., Gordon, S., Locati, M., & Mantovani, A. (2006). Transcriptional Profiling of the Human Monocyte-to-Macrophage Differentiation and Polarization: New Molecules and Patterns of Gene Expression. *The Journal of Immunology*, *177*(10), 7303–7311.

McClugage, S. G., Low, F. N., & Zimny, M. L. (1986). Porosity of the Basement Membrane Overlying Peyer's Patches in Rats and Monkeys. *Gastroenterology*, *91*(5), 1128–1133.

McKee, K. K., Harrison, D., Capizzi, S., & Yurchenco, P. D. (2007). Role of laminin terminal globular domains in basement membrane assembly. *Journal of Biological Chemistry*, *282*(29), 21437–21447.

Mebius, R. E., & Kraal, G. (2005, August 1). Structure and function of the spleen. *Nature Reviews Immunology*. Nature Publishing Group.

Meek, K. M., & Knupp, C. (2015, November 1). Corneal structure and transparency. *Progress in Retinal and Eye Research*. Pergamon.

Molawi, K., Wolf, Y., Kandalla, P. K., Favret, J., Hagemeyer, N., Frenzel, K., … Sieweke, M. H. (2014). Progressive replacement of embryo-derived cardiac macrophages with age. *The Journal of Experimental Medicine*, *211*(11), 2151–2158.

Mouw, J. K., Ou, G., & Weaver, V. M. (2014). Extracellular matrix assembly: A multiscale deconstruction. *Nature Reviews Molecular Cell Biology*.

Murray, M. Y., Birkland, T. P., Howe, J. D., Rowan, A. D., Fidock, M., Parks, W. C., & Gavrilovic, J. (2013). Macrophage migration and invasion is regulated by MMP10 expression. *PloS One*, *8*(5), e63555.

Murray, P. J., Allen, J. E., Biswas, S. K., Fisher, E. A., Gilroy, D. W., Goerdt, S., … Zhai, Y. (2014). Macrophage activation and polarization: nomenclature and experimental guidelines. *Immunity*, *41*(1), 14–20.

Murray, P. J., & Wynn, T. A. (2011, November 14). Protective and pathogenic functions of macrophage subsets. *Nature Reviews Immunology*.

Naglich, J. G., Metherall, J. E., Russell, D. W., & Eidels, L. (1992). Expression cloning of a diphtheria toxin receptor: Identity with a heparin-binding EGF-like growth factor precursor. *Cell*, *69*(6), 1051–1061.

Nathan, C., & Ding, A. (2010). Nonresolving inflammation. *Cell*, *140*(6), 871–882.

Noy, R., & Pollard, J. W. (2014). Tumor-Associated Macrophages: From Mechanisms to Therapy. *Immunity*, *41*(1), 49–61.

Ojalvo, L. S., King, W., Cox, D., & Pollard, J. W. (2009). High-density gene expression analysis of tumor-associated macrophages from mouse mammary tumors. *The American Journal of Pathology*, *174*(3), 1048–1064.

Ojalvo, L. S., Whittaker, C. A., Condeelis, J. S., & Pollard, J. W. (2010). Gene expression analysis of macrophages that facilitate tumor invasion supports a role for Wnt-signaling in mediating their activity in primary mammary tumors. *Journal of Immunology (Baltimore, Md. : 1950)*, *184*(2), 702–712.

Orgel, J. P., Wess, T. J., & Miller, A. (2000). The in situ conformation and axial location of the intermolecular cross-linked non-helical telopeptides of type I collagen. *Structure (London, England : 1993)*, *8*(2), 137–142.

Orkin, R. W., Gehron, P., McGoodwin, E. B., Martin, G. R., Valentine, T., & Swarm, R. (1977). A murine tumor producing a matrix of basement membrane. *The Journal of Experimental Medicine*, *145*(1), 204–220.

Orkin, S. H., & Zon, L. I. (2008). Hematopoiesis: an evolving paradigm for stem cell biology. *Cell*, *132*(4), 631–644.

Overall, C. M., & Blobel, C. P. (2007). In search of partners: Linking extracellular proteases to substrates. *Nature Reviews Molecular Cell Biology*.

Page-McCaw, A., Ewald, A. J., & Werb, Z. (2007). Matrix metalloproteinases and the regulation of tissue remodelling. *Nature Reviews. Molecular Cell Biology*, *8*(3), 221–233.

Palis, J., Robertson, S., Kennedy, M., Wall, C., & Keller, G. (1999). Development of erythroid and myeloid progenitors in the yolk sac and embryo proper of the mouse. *Development*, *126*(22).

Pei, D., & Weiss, S. J. (1995). Furin-dependent intracellular activation of the human stromelysin-3 zymogen. *Nature*, *375*(6528), 244–247.

Pei, D., & Weiss, S. J. (1996). Transmembrane-deletion mutants of the membrane-type matrix metalloproteinase-1 process progelatinase A and express intrinsic matrix-degrading activity. *The Journal of Biological Chemistry*, *271*(15), 9135–9140.

Perumal, S., Antipova, O., & Orgel, J. P. R. O. (2008). Collagen fibril architecture, domain organization, and triple-helical conformation govern its proteolysis.

Proceedings of the National Academy of Sciences, *105*(8), 2824–2829.

Qian, B.-Z., Li, J., Zhang, H., Kitamura, T., Zhang, J., Campion, L. R., … Pollard, J. W. (2011). CCL2 recruits inflammatory monocytes to facilitate breast-tumour metastasis. *Nature*, *475*(7355), 222–225.

Ricard-Blum, S. (2011). The Collagen Family. *Cold Spring Harbor Perspectives in Biology*, *3*(1), 1–19.

Ries, C. H., Cannarile, M. A., Hoves, S., Benz, J., Wartha, K., Runza, V., … Rüttinger, D. (2014). Targeting Tumor-Associated Macrophages with Anti-CSF-1R Antibody Reveals a Strategy for Cancer Therapy. *Cancer Cell*, *25*(6), 846–859.

Rockey, D. C., Bell, P. D., & Hill, J. A. (2015). Fibrosis — A Common Pathway to Organ Injury and Failure. *New England Journal of Medicine*, *372*(12), 1138–1149.

Roeder, B. A., Kokini, K., Sturgis, J. E., Robinson, J. P., & Voytik-Harbin, S. L. (2002). Tensile Mechanical Properties of Three-Dimensional Type I Collagen Extracellular Matrices With Varied Microstructure. *Journal of Biomechanical Engineering*, *124*(2), 214.

Rowe, R. G., Keena, D., Sabeh, F., Willis, A. L., & Weiss, S. J. (2011). Pulmonary fibroblasts mobilize the membrane-tethered matrix metalloprotease, MT1-MMP, to destructively remodel and invade interstitial type I collagen barriers. *American Journal of Physiology. Lung Cellular and Molecular Physiology*, *301*(5), L683-92.

Rowe, R. G., & Weiss, S. J. (2008). Breaching the basement membrane: who, when and how? *Trends in Cell Biology*, *18*(11), 560–574.

Rowe, R. G., & Weiss, S. J. (2009). Navigating ECM barriers at the invasive front: the cancer cell-stroma interface. *Annual Review of Cell and Developmental Biology*, *25*(1), 567–595.

Rozario, T., & DeSimone, D. W. (2010, May). The extracellular matrix in development and morphogenesis: A dynamic view. *Developmental Biology*.

Sabeh, F., Shimizu-Hirota, R., & Weiss, S. J. (2009). Protease-dependent versus-independent cancer cell invasion programs: Three-dimensional amoeboid movement revisited. *Journal of Cell Biology*, *185*(1), 11–19.

Saito, M., Iwawaki, T., Taya, C., Yonekawa, H., Noda, M., Inui, Y., … Kohno, K. (2001). Diphtheria toxin receptor-mediated conditional and targeted cell ablation in transgenic mice. *Nature Biotechnology*, *19*(8), 746–750.

Samokhvalov, I. M., Samokhvalova, N. I., & Nishikawa, S. (2007). Cell tracing shows the contribution of the yolk sac to adult haematopoiesis. *Nature*, *446*(7139), 1056–1061.

Sänger, N., Effenberger, K. E., Riethdorf, S., Van Haasteren, V., Gauwerky, J., Wiegratz, I., … Pantel, K. (2011). Disseminated tumor cells in the bone marrow of patients with ductal carcinoma in situ. *International Journal of Cancer*, *129*(10), 2522–2526.

Schenk, S., & Quaranta, V. (2003). Tales from the crypt[ic] sites of the extracellular matrix. *Trends in Cell Biology*, *13*(7), 366–375.

Schulz, C., Gomez Perdiguero, E., Chorro, L., Szabo-Rogers, H., Cagnard, N., Kierdorf, K., … Geissmann, F. (2012). A lineage of myeloid cells independent of Myb and hematopoietic stem cells. *Science (New York, N.Y.)*, *336*(6077), 86–90.

Sherratt, M. J. (2009). Tissue elasticity and the ageing elastic fibre. *Age (Dordrecht, Netherlands)*, *31*(4), 305–325.

Shifren, A., & Mecham, R. P. (2006). The Stumbling Block in Lung Repair of Emphysema: Elastic Fiber Assembly. *Proceedings of the American Thoracic Society*, *3*(5), 428–433.

Sodek, K. L., Brown, T. J., & Ringuette, M. J. (2008). Collagen I but not Matrigel matrices provide an MMP-dependent barrier to ovarian cancer cell penetration. *BMC Cancer*, *8*(1), 223.

Suzuki, T., Kono, T., Bochimoto, H., Hira, Y., Watanabe, T., & Furukawa, H. (2015). An injured tissue affects the opposite intact peritoneum during postoperative adhesion formation. *Scientific Reports*, *5*, 7668.

Tamoutounour, S., Guilliams, M., Montanana Sanchis, F., Liu, H., Terhorst, D., Malosse, C., … Henri, S. (2013). Origins and Functional Specialization of Macrophages and of Conventional and Monocyte-Derived Dendritic Cells in Mouse Skin. *Immunity*, *39*(5), 925–938.

Toner, P. G., Carr, K. E., Ferguson, A., & Mackay, C. (1970). Scanning and transmission electron microscopic studies of human intestinal mucosa. *Gut*, *11*(6), 471–481.

Turajlic, S., & Swanton, C. (2016). Metastasis as an evolutionary process. *Science (New York, N.Y.)*, *352*(6282), 169–175.

Ushiki, T. (2002). Collagen Fibers, Reticular Fibers and Elastic Fibers. A Comprehensive Understanding from a Morphological Viewpoint. *Archives of Histology and Cytology*, *65*(2), 109–126.

van Furth, R., Cohn, Z. A., Hirsch, J. G., Humphrey, J. H., Spector, W. G., & Langevoort, H. L. (1972). The mononuclear phagocyte system: a new classification of macrophages, monocytes, and their precursor cells. *Bulletin of the World Health Organization*, *46*(6), 845–852.

Van Goethem, E., Poincloux, R., Gauffre, F., Maridonneau-Parini, I., & Le Cabec, V. (2010). Matrix architecture dictates three-dimensional migration modes of human macrophages: differential involvement of proteases and podosome-like structures. *Journal of Immunology (Baltimore, Md. : 1950)*, *184*(2), 1049–1061.

van Rooijen, N., & Hendrikx, E. (2010). Liposomes for specific depletion of macrophages from organs and tissues. *Methods in Molecular Biology (Clifton, N.J.)*, *605*, 189–203.

Vanacore, R., Ham, A.-J. L., Voehler, M., Sanders, C. R., Conrads, T. P., Veenstra, T. D., … Hudson, B. G. (2009). A Sulfilimine Bond Identified in Collagen IV. *Science*, *325*(5945), 1230–1234.

Vannella, K. M., & Wynn, T. A. (2017). Mechanisms of Organ Injury and Repair by Macrophages. *Annual Review of Physiology*, *79*(1), 593–617.

Vérollet, C., Charrière, G. M., Labrousse, A., Cougoule, C., Le Cabec, V., & Maridonneau-Parini, I. (2011). Extracellular proteolysis in macrophage migration: losing grip for a breakthrough. *European Journal of Immunology*, *41*(10), 2805–2813.

Vracko, R. (1972). Significance of basal lamina for regeneration of injured lung. *Virchows Archiv Abteilung A Pathologische Anatomie*, *355*(3), 264–274.

Vracko, R., & Benditt, E. P. (1972). Basal lamina: The scaffold for orderly cell replacement: Observations on regeneration of injured skeletal muscle fibers and capillaries. *Journal of Cell Biology*, *55*(2), 406–419.

Wagenseil, J. E., Ciliberto, C. H., Knutsen, R. H., Levy, M. A., Kovacs, A., & Mecham, R. P. (2009). Reduced Vessel Elasticity Alters Cardiovascular Structure and Function in Newborn Mice. *Circulation Research*, *104*(10), 1217–1224.

Wagenseil, J. E., & Mecham, R. P. (2007, December 1). New insights into elastic fiber assembly. *Birth Defects Research Part C - Embryo Today: Reviews*. Wiley-Blackwell.

Weisberg, S. P., McCann, D., Desai, M., Rosenbaum, M., Leibel, R. L., Ferrante, A. W., & Jr. (2003). Obesity is associated with macrophage accumulation in adipose tissue. *The Journal of Clinical Investigation*, *112*(12), 1796–1808.

Wiesner, C., El Azzouzi, K., Linder, S., Lütcke, A., Zerial, M., Simons, K., & Olkkonen, V. M. (2013). A specific subset of RabGTPases controls cell surface exposure of MT1-MMP, extracellular matrix degradation and three-dimensional invasion of macrophages. *Journal of Cell Science*, *126*(Pt 13), 2820–2833.

Wiesner, C., Le-Cabec, V., El Azzouzi, K., Maridonneau-Parini, I., & Linder, S. (2014). Podosomes in space: Macrophage migration and matrix degradation in 2D and 3D settings. *Cell Adhesion and Migration*. Taylor & Francis.

Willis, A. L., Sabeh, F., Li, X. Y., & Weiss, S. J. (2013). Extracellular matrix determinants and the regulation of cancer cell invasion stratagems. *Journal of Microscopy*, *251*(3), 250–260.

Wolf, K., te Lindert, M., Krause, M., Alexander, S., te Riet, J., Willis, A. L., … Friedl, P. (2013). Physical limits of cell migration: Control by ECM space and nuclear deformation and tuning by proteolysis and traction force. *Journal of Cell Biology*, *201*(7), 1069–1084.

Wyckoff, J. B., Wang, Y., Lin, E. Y., Li, J., Goswami, S., Stanley, E. R., … Condeelis, J. (2007). Direct visualization of macrophage-assisted tumor cell intravasation in mammary tumors. *Cancer Research*, *67*(6), 2649–2656.

Wynn, T. A., Chawla, A., & Pollard, J. W. (2013). Macrophage biology in development, homeostasis and disease. *Nature*, *496*(7446), 445–455.

Wynn, T. A., & Vannella, K. M. Macrophages in Tissue Repair, Regeneration, and Fibrosis, 44 Immunity § (2016). Cell Press.

Xiong, W., Knispel, R., MacTaggart, J., Greiner, T. C., Weiss, S. J., & Baxter, B. T. (2009). Membrane-type 1 matrix metalloproteinase regulates macrophage-dependent elastolytic activity and aneurysm formation in vivo. *The Journal of Biological Chemistry*, *284*(3), 1765–1771.

Yana, I., & Weiss, S. J. (2000). Regulation of membrane type-1 matrix metalloproteinase activation by proprotein convertases. *Molecular Biology of the Cell*, *11*(7), 2387–2401.

Yona, S., & Gordon, S. (2015). From the Reticuloendothelial to Mononuclear Phagocyte System – The Unaccounted Years. *Frontiers in Immunology*, *6*, 328.

Yona, S., Kim, K.-W., Wolf, Y., Mildner, A., Varol, D., Breker, M., … Jung, S. (2013). Fate Mapping Reveals Origins and Dynamics of Monocytes and Tissue Macrophages under Homeostasis. *Immunity*, *38*(1), 79–91.

Yurchenco, P. D. (2011). Basement membranes: Cell scaffoldings and signaling platforms. *Cold Spring Harbor Perspectives in Biology*, *3*(2), 1–27.

Zbek, S., Balasubramanian, P. G., Chiquet-Ehrismann, R., Tucker, R. P., & Adams, J. C. (2010). The Evolution of Extracellular Matrix. *Molecular Biology of the Cell*, *21*, 4300–4305.

Zhou, Z., Apte, S. S., Soininen, R., Cao, R., Baaklini, G. Y., Rauser, R. W., … Tryggvason, K. (2000). Impaired endochondral ossification and angiogenesis in mice deficient in membrane-type matrix metalloproteinase I. *Proceedings of the National Academy of Sciences of the United States of America*, *97*(8), 4052–4057.

Chapter 2: Macrophage-Dependent Trafficking and Remodeling of the Basement Membrane-Interstitial Matrix Interface

Abstract

Macrophages dominate inflammatory environments where they modify the extracellular matrix by mobilizing complex repertoires of proteolytic enzymes. Nevertheless, the dominant proteinases used by macrophage as they confront physiologic tissue barriers remain undefined. Herein, we have characterized the molecular mechanisms that define human macrophage-extracellular matrix interactions *ex vivo*. Resting and immune-polarized macrophages are shown to proteolytically remodel basement membranes while infiltrating the underlying interstitial matrix. In an unbiased screen to identify key proteases, we find that the macrophage metalloproteinase, MT1-MMP, is the dominant effector of basement membrane degradation and invasion. Unexpectedly, macrophages can alternatively use actomyosin-dependent forces to transmigrate native basement membrane pores that provide cells with proteinase-independent access to the interstitial matrix. These studies not only identify MT1-MMP as a key proteolytic effector of extracellular matrix remodeling by human macrophages, but also define the invasive strategies used by macrophages to traverse native tissue barriers.

Introduction

Macrophages infiltrate and remodel the extracellular matrix (ECM) of native tissues under a wide variety of physiologic and pathologic conditions, ranging from post-parturition mammary gland involution to metastasis (Lewis et al., 2016; Wynn et al., 2013; Wynn & Vannella, 2016). In mediating these diverse effects, macrophages assume an array of differentially activated or polarized states that allow them to either degrade or repair the ECM (Afik et al., 2016; Murray et al., 2014; Talmi-Frank et al., 2016). Regardless of their activation state, however, macrophages interact with at least one of two distinct ECM compartments, i.e., the basement membrane or the interstitial matrix (Rowe & Weiss, 2008, 2009). As a specialized form of ECM, the basement membrane subtends all epithelial and endothelial cell layers, but also surrounds adipocytes, pericytes, nerves, and vascular smooth muscle cells (Fidler et al., 2017; Rowe & Weiss, 2008). Despite ranging in thickness from only 50-400 nm, basement membranes are mechanically rigid barriers in almost all tissues, largely owing to a covalently cross-linked network of tightly intertwined type IV collagen fibers that non-covalently associate with a laminin meshwork as well as a complex mix of more than 70 other components (Halfter et al., 2015; Randles et al., 2017). In turn, the underlying interstitial matrix is dominated by an interwoven composite of fibrillar type I/III collagen, elastin, glycoproteins, proteoglycans, and glycosaminoglycans (Rowe & Weiss, 2009).

In confronting the basement membrane-interstitial matrix continuum *in vivo*, current evidence suggests normal as well as neoplastic cells remodel the ECM interface in order to drive tissue-invasive activity (Chang et al., 2017; Kelley et al., 2014; Rowe & Weiss, 2008; Sabeh et al., 2009). To date, however, efforts to characterize human

macrophage-ECM interactions have largely been confined to the use of artificial matrix constructs that lack the critical structural organization and mechanical properties that characterize the ECM in vivo (Cougoule et al., 2012; Halfter et al., 2015; Jevnikar et al., 2012; Madsen et al., 2017; Randles et al., 2017; Rowe & Weiss, 2008, 2009; Starnes et al., 2014; Van Goethem et al., 2010; Wiesner et al., 2014). Hence, despite the fact that macrophages can mobilize a complex repertoire of proteolytic enzymes belonging to the aspartyl-, serine-, cysteine- and metallo- proteinase families, which, if any, of these systems participate in tissue remodeling and invasion remains undefined (Akkari et al., 2014; Nathan & Ding, 2010; Newby, 2016; Sevenich & Joyce, 2014; Vérollet et al., 2011). To this end, we now characterize the molecular mechanisms that underlie macrophage-dependent remodeling of native ECM barriers. Unlike other cell populations characterized to date, we find that human macrophages display a unique hybrid ability to penetrate native tissues by either mobilizing the membrane-anchored matrix metalloproteinase, MT1-MMP, that serves to dissolve intervening matrix barriers or alternatively, generating actomyosin-dependent mechanical forces that drive a shape shifting phenotype that permits invasion to proceed independently of matrix-degradative activity.

Results

Primary human macrophages remodel native basement membrane

Following gentle decellularization of native mesenteric sheets, 3-dimensional (3D) reconstructions of immunofluorescent and second harmonic generation images allow visualization of a reflected basement membrane bilayer that ensheaths an intervening interstitial matrix (Figure 2.1A,B and Video 1-2) (Hotary et al., 2006; Witz et al., 2001). At higher magnification, en face confocal images of excised tissue incubated with anti-laminin or anti-type IV collagen antibodies highlight the confluent nature of the basement membrane sheets (Figure 2.1C). By imaging through the labeled tissue, orthogonal xz and yz reconstructions permit visualization of the apical and basal basement membrane layers that are separated by the ~50 μm-thick (unstained) interstitial matrix (Figure 2.1C). Given that the mechanical integrity of basement membranes is largely defined by a variable number of intermolecular sulfilimine bonds formed between the C-terminal domains of opposing type IV collagen trimers (Figure 2.1D) (Fidler et al., 2018), we sought to determine the relative frequency of these covalent cross-links in the isolated basement membranes. Following digestion with bacterial collagenase, the C-terminal domains of type IV collagen molecules (termed NC1 domains) remain associated as either non-covalently or covalently-associated dimers (Boudko et al., 2018; Fidler et al., 2014). However, following SDS-PAGE, only the covalently cross-linked dimers remain intact, whereas non-covalently cross-linked dimers dissociate into monomers (Figure 2.1E) (Boudko et al., 2018). In the specific case of the peritoneal basement membrane, analyses of NC1 dimer structure demonstrate that its type IV collagen network is

dominated by covalent cross-links (Figure 2.1E), thereby highlighting the fact that tissue-invasive cell populations confront a mechanically stable barrier.

Given the compositional and structural integrity of our *ex vivo* tissue construct, we next sought to characterize the nature of its interactions with primary human macrophages. As such, carboxyfluorescein diacetate succinimidyl ester (CFSE)-labeled monocyte-derived macrophages were cultured atop basement membranes that were pre-labeled with fluorescently-tagged anti-laminin antibodies in the presence of F_c receptor blocking reagents to prevent direct interactions between the macrophages and the antibody-coated surface (Güç et al., 2014; Kilarski et al., 2013). After a 48 h time period, the macrophage-tissue constructs were imaged for 160 mins using real-time spinning disc confocal microscopy. As shown, macrophages (green) are found adherent to the basement membrane in association with the appearance of distinct 5-10 μm diameter perforations in the labeled matrix (Figure 2.1F, arrows). While real-time imaging of macrophage membrane contours over this timespan demonstrates only small changes in lateral cell spreading (Figure 2.1G), cells are observed that are actively traversing the apical face of the *ex vivo* construct with macrophage membrane protrusions found breaching the basement membrane surface (Figure 2.1H and Video 3). Indeed, under high magnification, real-time imaging of a single basement membrane pore in association with an overlying macrophage over this time span demonstrates an increase in perforation size from ~11 μm^2 to ~17 μm^2 in the absence of noticeable changes in the fluorescent intensity of the pore edge (Figure 2.1I and Video 4), a finding consistent with the active proteolytic remodeling of the cell-matrix interface. Hence, by 48 h, human

macrophages are able to remodel native basement membranes while breaching the surface with invasive membrane protrusions.

Inflammatory stimuli alter the basement membrane remodeling potential of human macrophages

Given that macrophages serve discrete functions during the initiation and resolution of inflammatory responses (Wynn & Vannella, 2016), we sought to characterize the effect of immune polarizing stimuli on basement membrane remodeling. Consistent with recent studies, macrophages stimulated with purified E. coli lipopolysaccharide (LPS) upregulate *TNFα* and downregulate *MRC1* transcript levels (Figure 2.2A) (Martinez et al., 2013; Murray et al., 2014). Conversely, polarizing macrophages with the cytokine, IL-4, downregulates *TNFα* and upregulates *MRC1* transcript levels (Figure 2.2A) (Martinez et al., 2013; Murray et al., 2014). As such, variably polarized macrophages were cultured atop ex vivo tissue constructs before staining with anti-laminin antibodies to assess basement membrane integrity. After a 6-day culture period, unstimulated macrophages are observed atop the apical basement membrane in association with large numbers of ~10 μm diameter perforations (Figure 2.2B, arrowheads). Over this timeframe, orthogonal reconstructions demonstrate that macrophages not only remodel the basement membrane interface, but also proceed to infiltrate the underlying interstitial matrix (Figure 2.2B, xz and yz images). Of note, a subset of the tissue-invasive macrophages also begins to traverse the opposing reflected basement membrane, demonstrating that the remodeling program occurs regardless of basement membrane symmetry (Halfter et al., 2013) (Figure 2.2B arrowheads).

In a manner similar to unstimulated macrophages, LPS-polarized cells likewise remodel the basement membrane, but the percent surface area degraded increases ~2-fold as does the average size of the perforations (Figure 2.2C,E). Interestingly, while IL-4-dependent polarization is commonly linked to a tissue remodeling phenotype (Madsen et al., 2013; Mantovani et al., 2013), these macrophages fail to affect remodeling beyond that observed with unstimulated macrophages (Figure 2.2D,E).

Given that LPS-stimulated macrophages mount the most robust remodeling program, we used these cells to characterize the dynamic characteristics underlying the formation of basement membrane perforations. Macrophages actively engaged in the remodeling of adjacent perforations adopt two distinct morphologies, i.e., either encircling the border of the perforation without extending obvious protrusions into the cavity or sending small cell processes through the perforation into the underlying interstitial matrix (Video 5 and 6). Coincident with this activity, macrophages can be observed to 'tug' on the underlying basement membrane with force sufficient to contort the matrix (Video 6). As basement membrane perforations can be generated – or enlarged – as a function of reversible mechanical distortions (Kelley et al., 2014), we assessed basement membrane structure by SEM following the 6-day culture period. As shown, clearly demarcated perforations that are ~10 μm diameter can readily be found in macrophage-exposed, but not control, constructs (Figure 2.2F). In tandem with basement membrane denudation, type IV collagen is solubilized as assessed by ELISA (Figure 2.2G).

While recent studies have highlighted the ability of human and mouse macrophages to respond to specific inflammatory stimuli in transcriptionally and phenotypically distinct fashion (Martinez et al., 2013; Seok et al., 2013), we find that

mouse bone marrow-derived macrophages (BMDM) also perforate the basement membrane in response to LPS and IL-4 polarization, as well as infiltrate the interstitial compartment (Figure 2.3A). Under these conditions, LPS-stimulated BMDM remodel an area three times larger than unstimulated or IL-4 stimulated BMDM, and form modestly, although not significantly, larger perforations (Figure 2.3C). Interestingly, mouse multinucleated giant cells are occasionally formed in response to IL-4 (McNally & Anderson, 1995), but they express only minimal basement membrane remodeling activity and fail to invade the interstitial matrix (Figure 2.3B). Taken together, these data demonstrate that human as well as mouse macrophages proteolytically remodel and actively transmigrate native tissue barriers through processes responsive to immune polarization.

Macrophage polarization and basement membrane remodeling correlates with protease expression

As both mouse and human macrophages display similar matrix-remodeling phenotypes, we sought to first use mouse BMDM as a genetically-modifiable system to identify the underlying mechanisms responsible for basement membrane remodeling. To this end, we transcriptionally profiled mouse BMDM after a 24 h culture period under either unstimulated, LPS-stimulated or IL-4-stimulated conditions. As expected, the upregulation of mouse-specific polarization markers, *Nos2* and *Arg1* (Gundra et al., 2014; Murray et al., 2014), correlated with LPS and IL-4 stimulation, respectively (Figure 2.3D). In addition, a large number of proteases belonging to the metalloproteinase, cathepsin and serine proteinase family thought to be essential for ECM remodeling are expressed under these conditions (Figure 2.3E) (Fleetwood et al., 2014; Jevnikar et al., 2012;

Madsen et al., 2013; Murray et al., 2013). Of note, however, only a relatively small number of these proteases are differentially expressed in response to LPS or IL-4, with a smaller subset of these enzymes altering their transcript levels in a pattern that correlated with the matrix-remodeling phenotype, including the metalloproteases, *Mt1-mmp* and *Adamts4*; serine proteases, *Htra4* and *Ctrl;* and serine protease receptor, *Pluar* (Figure 2.3F).

Matrix metalloproteases are required for basement membrane remodeling

Cognizant of the fact that correlative changes in transcripts level may – or may not – correlate with matrix degradation activity, we next sought to identify effector proteases responsible for matrix remodeling by culturing BMDM atop tissue explants in the presence of broad spectrum inhibitors directed against cysteine, serine, or metalloprotease family members (Fleetwood et al., 2014; Hotary et al., 2006; Pflicke & Sixt, 2009; Van Goethem et al., 2010; Wolf et al., 2013). Despite the expression of multiple proteases by LPS-stimulated BMDMs, the addition of high concentrations of validated cysteine or serine protease inhibitors fail to inhibit basement membrane remodeling to a significant degree (Figure 2.4A) (Punturieri et al., 2000; Reddy et al., 1995). In contrast, the metalloprotease inhibitor, BB-94, that targets MMP, ADAM and ADAM-TS family members (Baker et al., 2002; Seals & Courtneidge, 2003) significantly blocks basement membrane degradation without affecting macrophage-basement membrane adhesion or cell viability (Figure 2.4A and data not shown). To further narrow the number of candidate proteases, we took advantage of the fact that endogenous protease inhibitors, known as tissue inhibitor of metalloproteinases (TIMPs), can be used to preferentially block the proteolytic activity of secreted versus membrane-anchored MMPs (Brew & Nagase, 2010; English et al., 2006;

Hotary et al., 2006). In the presence of TIMP-1, a more specific inhibitor of secreted MMPs (English et al., 2006; Sabeh et al., 2009), the remodeling program is unaffected (Figure 4A). By contrast, TIMP-2, an endogenous inhibitor of both secreted and type I membrane-anchored MMPs (English et al., 2006; Hotary et al., 2006; Sabeh et al., 2009), abrogates basement membrane degradation completely (Figure 2.4A). As BB-94 and TIMP-2 are the only inhibitors that effectively block basement membrane degradation, these results support the conclusion that a membrane-type MMP (MT-MMP) is likely the sole protease required for basement membrane remodeling (Figure 2.4B).

MT1-MMP is the dominant effector responsible for macrophage-mediated remodeling of the basement membrane

While at least four members of the MT-MMP family are sensitive to TIMP-2 (i.e. MT1-MMP, MT2-MMP, MT3-MMP and MT5-MMP) (English et al., 2006; Rowe & Weiss, 2009), transcriptional profiling of LPS-stimulated macrophages identified MT1-MMP as the sole membrane-anchored MMP expressed under these conditions (Figure 2.3E,F). Given that the increase in MT1-MMP transcript levels most closely correlated with the basement membrane remodeling phenotype, we confirmed by Western blot and qPCR that MT1-MMP is significantly upregulated following polarization with LPS (Figure 2.5A). As such, to directly define the impact of MT1-MMP on the matrix remodeling program, BMDM were prepared from *Mt1-mmp*$^{-/-}$ mice and cultured atop native explants. Underlining an essential requirement for MT1-MMP in basement membrane remodeling, *Mt1-mmp*$^{-/-}$ BMDM fail to display matrix-degradative activity under basal, LPS-, or IL-4-stimulated conditions (Figure 2.5B,D), despite maintaining identical expression of non-targeted cysteine, serine, and metallo-proteases (data not shown). Importantly, following

transduction of *Mt1-mmp*$^{-/-}$ macrophages with an MT1-MMP/mCherry-tagged construct (Sakurai-Yageta et al., 2008), basement membrane perforations materialize coincident with macrophages extending MT1-MMP/mCherry-positive protrusions into the underlying interstitial stroma (Figure 2.5C,D).

To next determine whether the mouse MT1-MMP-dependent regulation of basement membrane remodeling can be extended to human macrophages, we first confirmed that primary human macrophages express MT1-MMP and upregulate its expression following LPS polarization (Figure 2.6A). However, while LPS increased *MT1-MMP* transcript levels, protein expression remains largely unchanged (Figure 2.6A). Nevertheless, as assessed by confocal imaging, while endogenous MT1-MMP was found to localize in permeabilized cells to the peri-nuclear ER/Golgi region as well as trafficking vesicles throughout the cell, under non-permeabilized conditions, the levels of cell surface-associated MT1-MMP increase in response to LPS polarization (Figure 2.6B). Consistent with these findings, when human macrophages are cultured atop the basement membrane in the presence of BB-94 or a monoclonal antibody directed against the catalytic domain of MT1-MMP (Ager et al., 2015; Devy et al., 2009), matrix degradation is almost completely ablated (Figure 2.6C-F). Hence, MT1-MMP is required for both mouse and human macrophage-mediated basement membrane degradation.

Macrophages can traverse the basement membrane–interstitial matrix interface independently of proteolysis

While multiple normal as well as neoplastic cell populations degrade native tissue barriers as a prerequisite for supporting tissue-invasive activity (Hanahan & Weinberg, 2011; Rowe & Weiss, 2009; Wolf et al., 2013), the mechanisms underlying the ability of

macrophages to cross native tissue interfaces remains undefined. Confirming the barrier properties of our *ex vivo* model, the highly invasive human breast cancer cell line, MDA-MB-231 (Ota et al., 2009; Sabeh et al., 2004; Sabeh et al., 2009), rapidly degrades the underlying basement membrane barrier and infiltrates the interstitial space (Figure 2.7A,E). By contrast, when MDA-MB-231 cells are cultured in the presence of BB-94, basement membrane remodeling is curtailed and invasion into the interstitium completely blocked (Figure 2.7A,E). To determine whether macrophage invasion is similarly linked to basement membrane proteolysis, wild-type and MT1-MMP-targeted mouse or human macrophages were cultured atop explants for 6 d and infiltration monitored. As expected, both mouse and human macrophages degrade the subjacent membrane coincident with the expression of tissue-invasive activity (Figure 2.7B). Interestingly, macrophages accessing the interstitial matrix are found to adhere tightly to elastin fibrils while also infiltrating basement membrane sleeves that ensheathed the peritoneal vasculature (Figure 2.7C-D). However, in contrast to the protease-dependent invasion program deployed by carcinoma cells, when basement membrane remodeling by macrophages is blocked by targeting MT1-MMP, macrophages continue to infiltrate the interstitial matrix, bind to elastin fibers and invade vascular basement membranes (Figure 2.7B-E). Similar, if not identical, results are obtained when macrophages are cultured in the presence of protease inhibitors directed against each of the major proteinase classes in tandem, ruling out the possibility that alternate proteolytic systems required for invasion are engaged following MT1-MMP targeting (Figure 2.7B,E).

Basement membrane pores provide macrophages with proteinase-independent access to the interstitium

While carcinoma cells mobilize proteinases to degrade the pericellular ECM in order to invade the interstitial matrix, the question remains as to the means by which macrophages traverse an identical barrier independently of proteolytic remodeling. Interestingly, earlier reports have described basement membrane "pores" that exist in almost every tissue where they have been proposed allow for epithelial-mesenchymal or mesodermal-stromal contact – and possibly, myeloid cell trafficking (Barreiro et al., 2016; Bluemink et al., 1976; Howat et al., 2001; Oakford et al., 2011; Takahashi-Iwanaga et al., 1999; Takeuchi & Gonda, 2004). As such, we considered the possibility that macrophages might gain access to the interstitium through similar structures via a non-proteolytic process (Howat et al., 2001; McClugage et al., 1986; Oakford et al., 2011; Pflicke & Sixt, 2009; Toner et al., 1970). Indeed, under higher resolution, the peritoneal basement membrane can be shown to harbor a series of ~1 μm diameter pores (Figure 2.8A). Importantly, these pores are visible in intact tissue prior to decellularization, ruling out pore formation as an unintended consequence of tissue processing (Figure 2.S1). Hence, basement membranes and primary human macrophages were fluorescently pre-labeled and transmigration captured by live imaging in the presence of the MT1-MMP-blocking antibody (Figure 2.8B). Over a 7-hour time-course, macrophages were observed moving in a 2-dimenstional orientation towards a group of preformed portals (Figure 2.8B, Video 7). Orthogonal reconstructions over this timeframe demonstrate that macrophages first move laterally towards these perforations in an MT1-MMP-independent fashion before migrating vertically through the basement membrane and into the interstitial matrix (Figure 2.8B, Video 8). Hence, macrophages - unlike carcinoma cells - do not require

MT1-MMP to penetrate the basement membrane-interstitial interface or invade the underlying interstitial matrix.

In other cell systems, non-proteolytic mechanisms of invasion have been linked to the transfer of mechanical forces from the cell body to either the surrounding matrix or the perinuclear compartment as a means to shape the rigid nucleus to a size that allows small ECM pores to be negotiated (Chang et al., 2017; Harunaga et al., 2014; Hung et al., 2013; Paul et al., 2017; Ruprecht et al., 2015). In an effort to define the contribution of actomyosin-dependent contractility to macrophage invasion, human macrophage infiltration into the interstitial matrix was assessed in the presence of the Rho kinase inhibitor, Y27632, or the myosin II inhibitor, blebbistatin (Harunaga et al., 2014; Hung et al., 2013; Ruprecht et al., 2015). While human macrophages cultured in the presence of BB-94 actively cross the basement membrane and infiltrate the interstitial matrix, the addition of either Y27632 or blebbistatin significantly blocks invasion (Figure 2.8C,D), highlighting the importance actomyosin-dependent forces in supporting motility responses though physiologic tissue barriers. To next determine if proteolysis might generate larger pore sizes in the ECM that potentially preclude a requirement for the actomyosin network, macrophages were cultured atop the ex vivo construct with either Y27632 or blebbistatin; but in the absence of BB-94 (Figure 2.8C,D). Interestingly, neither inhibitor affects the ability of macrophages to proteolytically remodel the underlying basement membrane (Figure 2.8C,D). Nevertheless, interstitial matrix invasion remains inhibited, demonstrating a continued requirement for actomyosin-dependent forces as the macrophages traverse the exposed interstitial ECM compartment, presumably as a consequence of negotiating restrictive pore sizes in this matrix compartment as well.

Hence, these data are consistent with a heretofore undescribed dual ability of macrophages to infiltrate interstitial matrix by either proteolytically degrading the basement membrane barrier or alternatively, mobilizing actomyosin-dependent pathways to non-proteolytically traverse basement membrane portals.

Discussion

In postnatal states, macrophage patrol or infiltrate host tissue where they remodel the ECM in order to either exert palliative effects, e.g., during host defense and wound repair, or participate in deleterious outcomes, e.g., chronic inflammatory disease states and cancer (Nathan & Ding, 2010; Noy & Pollard, 2014; Wynn & Vannella, 2016). However, the precise mechanisms that allow macrophages to remodel native tissue barriers have remained largely undefined. To date, almost all studies have relied on the use of model systems to characterize macrophage interactions with either basement membrane or interstitial matrix barriers (Cougoule et al., 2012; Fleetwood et al., 2014; Gui et al., 2011, 2012, 2014; Jevnikar et al., 2012; Murray et al., 2013; Ogura et al., 2017; Starnes et al., 2014; Van Goethem et al., 2010; Werb et al., 1980). However, given increased appreciation that these constructs cannot recapitulate the more complex structure of the ECM in vivo, and that the composition and mechanical properties of the ECM can each affect cell function (Liu et al., 2015; Previtera & Sengupta, 2015; Wiesner et al., 2014), the utility of these systems for predicting macrophage function in vivo is subject to debate. For example, whereas basement membranes in vivo are type IV collagen-rich and mechanically rigid as a consequence of lysyl oxidase- and peroxidasin-mediated covalent crosslinks, in vitro constructs that rely on EHS carcinoma extracts (i.e., Matrigel) are alternatively enriched with laminin, mechanically soft and largely devoid of the critical type IV collagen crosslinks that define basement membrane structure (Halfter et al., 2015; Rowe & Weiss, 2008, 2009; Willis et al., 2013). Likewise, given the fact that the interstitial matrix, though dominated by type I/III collagen, is comprised of hundreds of distinct components, attempts to recapitulate its structure with relatively simple collagen hydrogels is problematic (Naba et al., 2016; Sabeh et al., 2009; Wolf et al.,

2013). While these systems as well as synthetic polyethylene glycol- or alginate- based substrates engineered in 2-D, 3-D or microchannel format can nevertheless yield valuable insights (Hung et al., 2013; Liu et al., 2015; Paul et al., 2017; Previtera & Sengupta, 2015; Thiam et al., 2016), none of these constructs recapitulate the structural complexity or architecture of native tissues. Given these limitations, we selected a matrix explant model for characterizing cell-matrix interactions, thereby allowing us to gauge the ability of non-polarized as well as polarized macrophages to remodel and transmigrate native basement membrane barriers while gaining access to an underlying interstitial matrix.

In considering the potential proteolytic mechanisms that might be responsible for macrophage-dependent basement membrane remodeling, we chose an unbiased transcriptional screen as a means to identify candidate proteinases. Consistent with reports implicating cysteine proteinases, serine proteinases as well as secreted MMPs in conferring macrophages with the ability to invade Matrigel-based constructs, each of these proteolytic systems were expressed by polarized macrophages (Jevnikar et al., 2012; Murray et al., 2013). However, when macrophage interactions with native basement membranes were examined, targeting these proteinases with class-specific inhibitors failed to block matrix remodeling. Instead, both human and mouse macrophages deployed the membrane-anchored MMP, MT1-MMP, as the dominant effector of basement membrane remodeling. Interestingly, in a manner similar to that observed during podosome-mediated proteolysis (Wiesner et al., 2013; Wiesner et al., 2014), MT1-MMP actively trafficked to invasive membrane protrusions as the macrophages penetrated the basement membrane. While we have not examined this exocytotic process in detail, MT1-MMP trafficking most likely involves the RabGTPase-

microtubule system previously detailed by Linder and colleagues (Wiesner et al., 2013; Wiesner et al., 2010).

Following MT1-MMP deletion or inhibition, we anticipated that macrophages would be unable to cross the basement membrane or infiltrate the interstitial matrix. While cells can potentially use cytoskeletal-generated forces to displace non-covalently cross-linked ECM fibers (Gjorevski et al., 2015; Pflicke & Sixt, 2009; Sabeh et al., 2009), the basement membrane used here is heavily cross-linked by sulfilimine bonds that would be predicted to render the type IV collagen backbone resistant to mechanical displacement (McCall et al., 2014). Further, while migrating cells can negotiate fixed pores whose size exceeds 10% of the nuclear cross-sectional area, the type IV collagen network has been estimated to limit interfibrillar pore size to ~50 nm in diameter, dimensions that would effectively preclude cellular transmigration (Fidler et al., 2017; Hallmann et al., 2015; Kelley et al., 2014; Wolf et al., 2013). Indeed, while human breast carcinoma cells were able to degrade and penetrate the basement membrane, invasion was, as expected (Hanahan & Weinberg, 2011; Hotary et al., 2006; Ota et al., 2009; Paul et al., 2017; Rowe & Weiss, 2008), inhibited completely when MMP activity was blocked. Though recent reports have emphasized the ability of human carcinoma cells, including MDA-MB-231 cells, to alternatively adopt an amoeboid phenotype to negotiate ECM barriers via non-proteolytic mechanisms, these studies consistently rely on artificial matrix models whose relevance to native tissue barriers remains to be determined (Aung et al., 2014; Haeger et al., 2015; He & Wirtz, 2014; Liu et al., 2015). Using tissue explants, carcinoma cells were, by contrast, wholly dependent on MMP-dependent proteolysis. Nevertheless, in the absence of MT1-MMP activity, both human and mouse macrophages retained the ability to cross

the basement membrane-interstitial matrix interface via a process that is dependent on actomyosin-generated forces. In our efforts to visualize the sites permissive for proteinase-independent transmigration, our attention focused on discrete ~3 μm^2 pores that decorate the basement membrane surface (Figure 2.8A, arrowheads; Figure 2.S1). Importantly, micrometer-sized basement pores have been identified in lung, skin, blood vessel and colon tissues, raising the distinct possibility that these structures are purposefully generated during embryogenesis not only to allow epithelial/mesodermal-stromal crosstalk, but also to serve as permissive passageways for cell movement (Howat et al., 2001; McClugage et al., 1986; Oakford et al., 2011; Pflicke & Sixt, 2009; Toner et al., 1970). Given their relatively small pore size - at least relative the nuclear dimensions of most cell populations - the engagement of the macrophage actomyosin network is consistent with recent studies demonstrating similar requirements as cells negotiate space-restrictive environments (Hung et al., 2013; Paul et al., 2017; Thiam et al., 2016). Interestingly, although the basement membrane surrounding lymphatic vessels are less well-organized than those found subtending epithelial cells or the vascular endothelium, Sixt and colleagues recently demonstrated that basement membrane portals similar to those described here are permissive for non-proteolytic dendritic cell trafficking (Pflicke & Sixt, 2009). It should be stressed however, that basement membrane pores do not provide proteinase-independent access to all cell populations, as exemplified by the inability of MDA-MB-231 cells to usurp these passageways in their efforts to access the interstitial compartment. Furthermore, the trafficking mechanisms outlined here for macrophages cannot be extended to all myeloid population as we have found that human neutrophils are unable to cross the peritoneal basement membrane – either in the

absence or presence of chemotactic gradients (unpublished observation). While Glentis et al have recently proposed that cancer-associated fibroblasts can induce cancer cell invasion through the peritoneal basement membrane by a metalloproteinase-independent process (Glentis et al., 2017), SEM images of their constructs appear to be devoid of an intact basement membrane and only show the fibrillar matrix of interstitial collagen (i.e., the diameter of type IV collagen fibrils is only on the order of 2 nm and requires high resolution metal shadow casting for visualization) (Yurchenco & Ruben, 1987). As the ability of cell-generated mechanical forces to guide carcinoma cells through stromal collagen hydrogels has been described (Aung et al., 2014), their model is most consistent with the ability of cancer-associated fibroblasts to accelerate cancer cell invasion through a porous collagen network. These issues notwithstanding, macrophages may well represent a unique cell population that can traverse basement membranes in a cell autonomous fashion by alternatively mobilizing MT1-MMP-dependent or proteinase-independent mechanisms. In this regard, we note that recent live imaging studies of macrophage migration within zebrafish larvae describe a dual requirement for proteinases and ROCK-dependent traction forces (Barros-Becker et al., 2017). However, as a cocktail of proteinase inhibitors was used in this study, the identity of the targeted proteinases remains to be determined.

Having gained access to the interstitial matrix, we noted that macrophages were not randomly arrayed within the stroma, but instead were closely associated with the underlying network of elastin fibrils. Interestingly, inflammatory macrophage infiltrating adipose tissues *in vivo* were recently reported to be similarly positioned, raising the possibility that elastin networks may provide a 1-dimensional ‘highway’ for macrophage

trafficking through stromal tissues (Martinez-Santibanez et al., 2015). Of note, we also observed that macrophage-associated elastin fibrils were frequently fragmented (Figure 2.7C). As elastin networks were disrupted in the absence or presence of MT1-MMP, alternate proteolytic systems must be in play here. Indeed, we have previously described the ability of human macrophages to degrade insoluble elastin fibers by mobilizing the cysteine proteinases, cathepsin L and S, and the role of these proteinases in this more physiologic model of elastinolytic activity remains to be determined (Filippov et al., 2003; Punturieri et al., 2000; Reddy et al., 1995). Finally, we also note that macrophages, having gained access to the interstitial matrix, establish contact with the stromal face of both vascular basement membranes and the inner face of the reflected basement membrane. Recent studies demonstrate that basement membranes are not homogenous, but instead are asymmetrically organized with marked differences in rigidity and matrix composition on the epithelial versus stromal sides, raising the possibility that macrophage-basement membrane trafficking might be unidirectionally favored (Halfter et al., 2013). However, we find that macrophages are able to transmigrate basement membranes in either direction, a finding consistent with recent reports demonstrating the ability of macrophages to remodel vascular basement membranes during carcinoma cell intravasation or the alveolar basement membrane following lung injury (Harney et al., 2015; Misharin et al., 2017; Wyckoff et al., 2007).

In sum, we find that human as well as mouse macrophages mobilize MT1-MMP as the dominant effector of basement membrane remodeling. While MT1-MMP confers non-polarized as well as polarized macrophages with the ability to resorb native tissues during tissue trafficking, these cells can also adopt an alternate phenotype that allows

them to traffic through tissue barriers in a proteinase-independent mode that is not conserved in carcinoma cells. As such, we posit that macrophages, unlike other normal or neoplastic cell populations, have the ability to infiltrate tissues wherein the ECM is purposefully left unscathed during reparative states or irreversibly remodeled in association with tissue-destructive events.

Materials and Methods

Isolation of primary macrophages

Bone marrow macrophages were isolated as previously described from 2-8 week old wild-type (*Mt1-mmp*$^{+/+}$) or MT1-MMP-null (*Mt1-mmp*$^{-/-}$) Swiss Black mice (Holmbeck et al 1999; Sakamoto and Seiki 2009). Briefly, long bones were flushed with PBS, red cells were lysed with ACK buffer (ThermoFisher) and the remaining cells were cultured in alpha-MEM with 10% heat-inactivated fetal bovine serum (HI-FBS), 1% penicillin-streptomycin solution (ThermoFisher), and 10 ng/mL M-CSF (R&D Systems) overnight on tissue culture dishes. Nonadherent cells were plated onto non-tissue culture-treated dishes in media with M-CSF for an additional 5-7 days; media was replaced every 48 hours.

Human peripheral blood monocytes were isolated from whole blood of volunteers in accordance with institutional review board (IRB) approval and the patient's informed consent. PBMCs were separated by Lymphocyte Separation Medium (Corning) by density centrifugation, purified by CD14 selection (Miltenyi Biotec) and cultured at 2 x 10^6 in 6-well plates containing RPMI 1640 without serum. After 2 h, media was replaced with RPMI 1640 with 1% penicillin-streptomycin solution and 20% autologous serum for 5-7 days. Autologous serum was prepared by incubating non-heparinized whole blood at 37 °C for 1 h followed by centrifugation at 2,850 g for 15 minutes, and sterile filtration of the serum fraction.

Ex vivo mesentery ECM preparation

Mesentery tissue were prepared as previously described (Witz et al., 2001; Hotary et al., 2006). Briefly, rat mesentery was mounted on 6.5 or 12-mm diameter Transwells (Sigma) with sterile surgical thread and decellularized with 0.1 N ammonium hydroxide. 1-2 x 10^5 mouse or human macrophages were cultured atop the tissue for six days with media changes every 48 hours. All experiments were performed in complete medium in the absence or presence of the following inhibitors 100 µM E-64d, 100 µg/mL aprotinin, 100 µg/mL soybean trypsin inhibitor (SBTI), 20 µM Y-27632, 20 µM Blebbistatin (Sigma), 5 µM BB-94 (Tocris Bioscience), 12.5 µg/mL TIMP-1, 5 µg/mL TIMP-2 (Peprotech). Protease inhibitor mix contained 100 µM E-64d, 100 µg/mL aprotinin, 100 µg/mL SBTI, 5 µM BB-94, 2 µM leupeptin, 10 µM pepstatin A. Human macrophages were also cultured with 75 µg/mL human isotype control IgG antibody or anti-MT1-MMP antibody DX-2400 (Ager et al., 2015) in medium with 20% heat-inactivated autologous human serum and 1% penicillin-streptomycin in the presence of 5 µL F_c-receptor blocking antibody TruStain FcX (Biolegend). DX-2400 was provided by the Kadmon Corporation. Macrophages were polarized with 1 µg/mL LPS from *Escherichia coli* O111:B4 (Sigma) or 20 ng/mL recombinant mouse or human IL-4 (Peprotech). After six days of culture, tissue constructs were washed with PBS, fixed with 4% PFA, and stained as described.

Lentiviral gene transfer

A mCherry-tagged MT1-MMP construct (Sakurai-Yageta 2008) was cloned into pLenti lox IRES EGFP vector and subsequently transfected into 293T cells using Lipofectamine 2000 (ThermoFisher) to generate lentiviral particles. BMDM at 5 days post-isolation were incubated with the lentivirus-containing supernatant in the presence of 8 µg/mL polybrene

for 6 h before media was replaced. 48 h later transduced macrophages were cultured atop the tissue construct as described.

Tumor cell culture

MDA-MB-231 were cultured in DMEM supplemented with 10% heat-inactivated fetal bovine serum (HI-FBS) and a 1% penicillin-streptomycin solution. Cells were cultured on the basement membrane construct for 48 hours before processing.

Confocal fluorescence microscopy and analysis

PFA-fixed constructs were incubated with polyclonal antibodies targeting laminin (Sigma, cat #: L9393), type IV collagen (Abcam, cat #: ab19808), and elastin (EMD Millipore cat #: 2039), at 1:150 dilution in a blocking solution of 1% bovine serum albumin-PBS for 1 h room temperature. Constructs were then incubated with secondary fluorescent antibodies at 1:250 dilution while cells were labeled with Alexa Fluor 488 phalloidin and DAPI (Sigma) for 1 h in blocking solution. Image acquisition was performed using a spinning disc confocal CSU-WI (Yokogawa) on a Nikon Eclipse TI inverted microscope with a 60x oil-immersion objective and the Micro-Manager software (Open Imaging). Fluorescent images were processed with ImageJ (National Institutes of Health) with 3D viewer plugin for orthogonal and 3D reconstructions. Confocal imaging of the collagen I matrix was captured by second harmonic generation on a Leica SP5 inverted confocal microscope with a 60x oil-immersion objective.

For immunofluorescence of endogenous MT1-MMP, fixed primary human macrophages were incubated on glass coverslips with 1:50 rabbit monoclonal anti-MT1-MMP (Abcam)

overnight at 4°C in 3% BSA-PBS with or without 0.1% Triton X-100 to permeabilize the cells, followed by incubation with 1:200 Alexa Fluor-488 secondary antibody for 1 h 37°C.

Live image microscopy

Live imaging was performed on unfixed tissue constructs pre-labeled with fluorescent antibodies as above. Macrophages were incubated with 5 µM CFSE (Life Technologies) in PBS for 20 minutes at 37°C, quenched with a 5x volume of medium with 1% HI-autologous serum, resuspended in PBS-F_c receptor block for 5 minutes at room temperature, and plated on the pre-labeled tissue construct. Z-stacks or single slices were captured in a 37°C 5% CO_2 humidified chamber (Livecell Pathology Devices) as described. Cell outlines were generated and overlaid using the binary and outline functions of ImageJ.

Electron microscopy

Tissue constructs were processed for SEM as follows, fix in 2% glutaraldehyde/1.5% paraformaldehyde in 0.1 M cacodylate buffer, post-fix in 1% osmium tetroxide, and dehydrated through a graded ethanol series as described (Hotary et al. 2003). Image acquisition was performed using an AMRAY 1910 field emission scanning electron microscope at 5.0 kV.

ELISA

Anti-Rat COL4A1 ELISA kits were purchased from LSBio. Tissue constructs were cultured for 72 hours in the presence of media alone or with LPS-stimulated human macrophages and LPS before cell-free media was analyzed according to the manufacturer's instructions.

qPCR and transcriptional profiling

RNA was isolated from macrophages using the NucleoSpin RNA kit (Macherey Nagel) as instructed. Day 5-7 macrophages were polarized for 24 hours as described. cDNA synthesis was performed with Superscript III enzyme (Invitrogen). qPCR reactions were performed in triplicate with SYBR green PCR master mix on a 7900HT fast Real-Time PCR machine (Applied Biosystems). Data were analyzed using the comparative threshold cycle method with mRNA levels normalized to GAPDH.

For transcriptional profiling, total mRNA was isolated as above, and labeled and hybridized to Mouse Gene ST 2.1 strips (Affymetrix). Three replicates of each sample were analyzed by the University of Michigan Microarray Core. BMDM proteases with expression values greater than 2^4 in any condition were tabulated and further analyzed for relative fold differences across conditions.

Western Blot

Western blots were performed as described with antibodies targeting MT1-MMP (Epitomics), alpha 2 (IV) NC1, Clone H22 (Chondrex), and β-actin (Cell Signaling). Primary antibodies were labeled with horseradish peroxidase-conjugated species-specific secondary antibodies (Santa Cruz) and detected by the SuperSignal West Pico system (Pierce). For type IV collagen dimer-monomer content analysis, isolated tissue was first digested with bacterial collagenase type IV (Worthington Biochemical Corporation) overnight at 37 °C with occasional vortexing. Samples were pelleted at 15,000 g for 20 minutes and analyzed by SDS-PAGE without heat-denaturation.

Statistical Analysis

The area of basement membrane degraded as well as basement membrane perforation size were calculated using ImageJ as follows; image intensity was enhanced and background subtracted using default settings, the images converted to black and white via binary function, inverted, and particles larger than a 1 μm^2 minimum cut off analyzed. For percent invasion, cells were considered traversed if the cell body including nucleus were located between the two basement membrane layers. Results are expressed as mean ± SEM and comparisons were made with one-way ANOVA.

Notes and Acknowledgements

A version of Chapter 2 has been submitted for publication by the following authors: Julian C. Bahr and Stephen J. Weiss.

We thank the Kadmon Corporation for providing the anti-MT1-MMP antibody, licensed to the Kadmon Corporation by the Dyax Corporation. We acknowledge Stephanie King (Life Sciences Institute) for assistance with illustrations and Craig Johnson (University of Michigan) for assistance with microarray analysis. We thank Stefan Linder for helpful discussions. This work was supported by grants from the NIH to SJW (AI105068) and the Cancer Biology Training Grant (NCI Training Grant T32-CA009676).

Figure 2.1

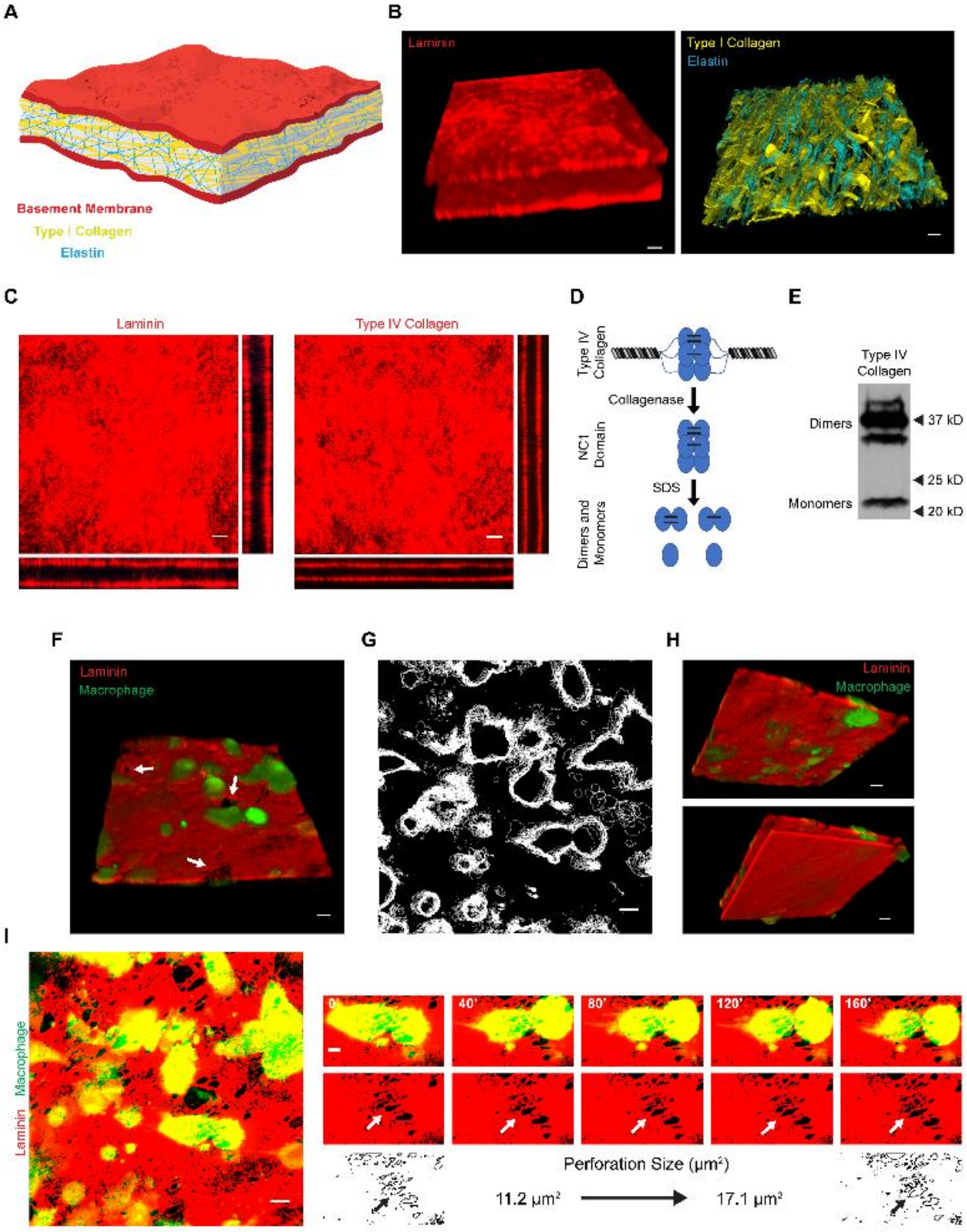
A
Basement Membrane
Type I Collagen
Elastin
B
Laminin
Type I Collagen
Elastin
C
Laminin
Type IV Collagen
D
Type IV Collagen
Collagenase
NC1 Domain
SDS
Dimers and Monomers
E
Type IV Collagen
Dimers
Monomers
37 kD
25 kD
20 kD
F
Laminin
Macrophage
G
H
Laminin
Macrophage
I
Laminin
Macrophage
0'
40'
80'
120'
160'
Perforation Size (μm²)
11.2 μm²
17.1 μm²

Figure 2.1. Human macrophage interactions with native basement membrane.
(A) Schematic illustration of the mesentery extracellular matrix. **(B)** 3D confocal reconstructions of laminin (red, left panel) and elastin (blue, right panel), with second harmonic generation of type I collagen (yellow, right panel) in rat mesentery constructs. **(C)** *En face* and orthogonal immunofluorescence of laminin and type IV collagen. **(D)** Schematic of type IV collagen dimer-monomer content analysis. After collagenase digestion of type IV collagen, the hexameric NC1 domain remains intact. The hexamer can be dissociated via non-reducing SDS-PAGE into sulfilimine-crosslinked dimers and non-crosslinked monomers. **(E)** Type IV collagen dimer-monomer content analysis as determined by Western blotting. **(F)** 3D confocal reconstruction of human macrophages (green) atop the apical face of a basement membrane (red) with adjacent perforations (arrow) after 48 h. **(G)** Overlay of macrophage outlines captured every 10 minutes for 160 minutes. **(H)** 3D reconstruction from (F) rotated 180° showing the apical basement membrane surface (top panel) and the reflected basal face (bottom panel). **(I)** Immunofluorescence of the apical basement membrane layer and macrophages (left panel) with a macrophage actively expanding a perforation in the basement membrane (small panels, arrows) from an area of 11.2 μm^2 to 17.1 μm^2 over 160 minutes. Bars: 20 µm (B, F, H); 10 µm (C, G, I left panel); 5 µm (I right panel).

Figure 2.2

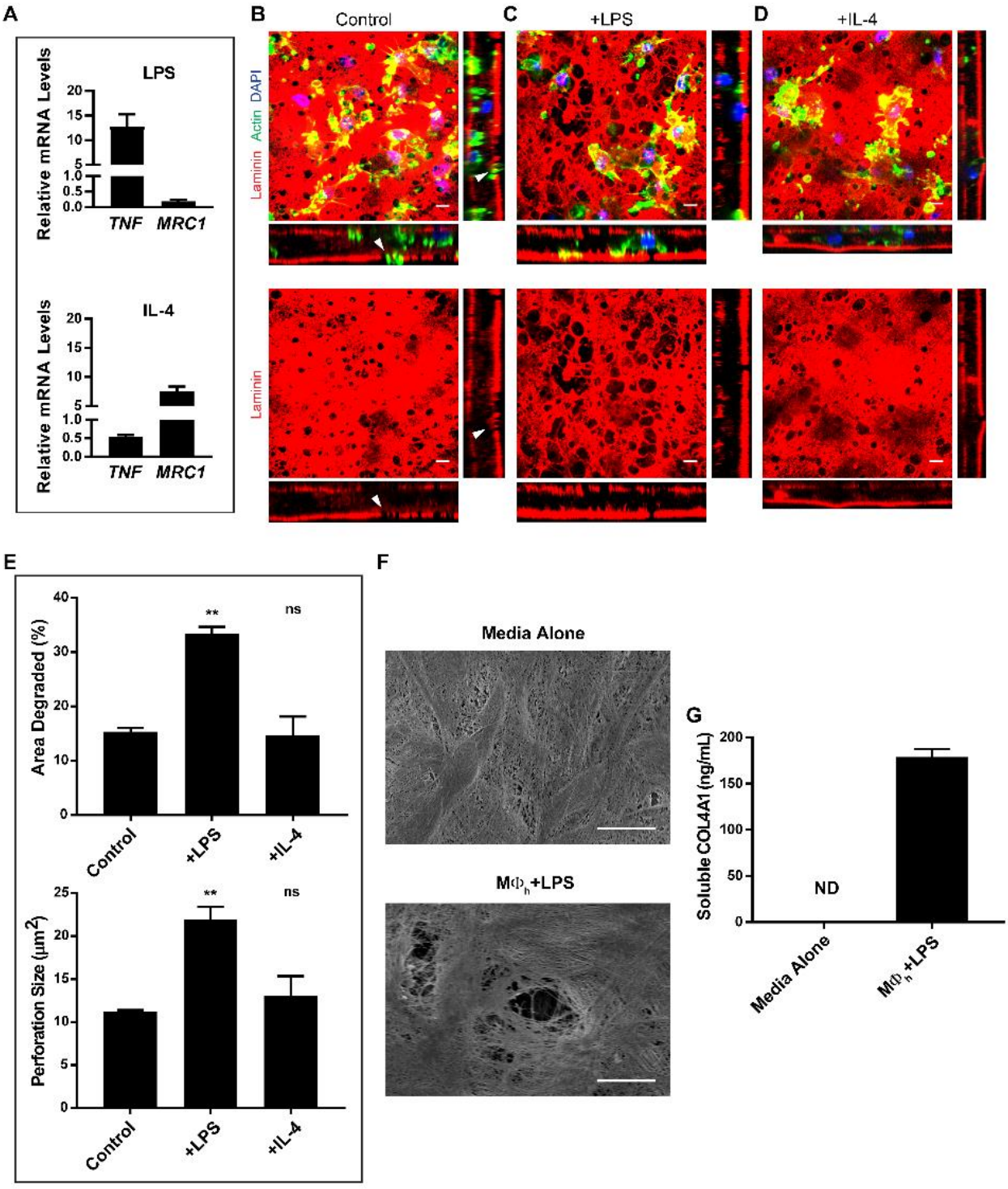
A
LPS
Relative mRNA Levels
TNF
MRC1
IL-4
B
Control
C
+LPS
D
+IL-4
Laminin
Actin
DAPI
E
Area Degraded (%)
Perforation Size (μm2)
ns
F
Media Alone
MΦh+LPS
G
Soluble COL4A1 (ng/mL)
ND

Figure 2.2. Polarized human macrophage-dependent remodeling of the basement membrane.

(A) Transcript expression of immune response genes was analyzed by qPCR in human macrophages polarized with LPS (1 µg/mL) or recombinant human IL-4 (20 ng/mL). Results are expressed as mean ± SEM, n = 3, fold-change relative to control. **(B)** Immunofluorescence of unstimulated macrophages cultured for 6 days on the basement membrane surface. Orthogonal reconstructions reveal cells that infiltrated the interstitial matrix and perforated the basal basement membrane (arrows). **(C)** Immunofluorescence of macrophages polarized with LPS (1 µg/mL) or **(D)** recombinant human IL-4 (20 ng/mL). Images shown in (B-D) are representative of three replicates. **(E)** Quantification of the area of basement membrane degraded and basement membrane perforation size as analyzed by ImageJ pixel analysis of each condition from (B-D). Results are expressed as mean ± SEM; (**) $P < .001$; ns, not significant; n = 3. **(F)** Scanning electron micrograph of basement membrane stripped of cells either after culture with medium alone or with LPS-polarized macrophages for 6 days. **(G)** Quantification of soluble type IV collagen detected in cell-free media on day 3 of (F); results are expressed as mean ± SEM, n = 4. Bars: (B-D, F) 10 µm.

Figure 2.3

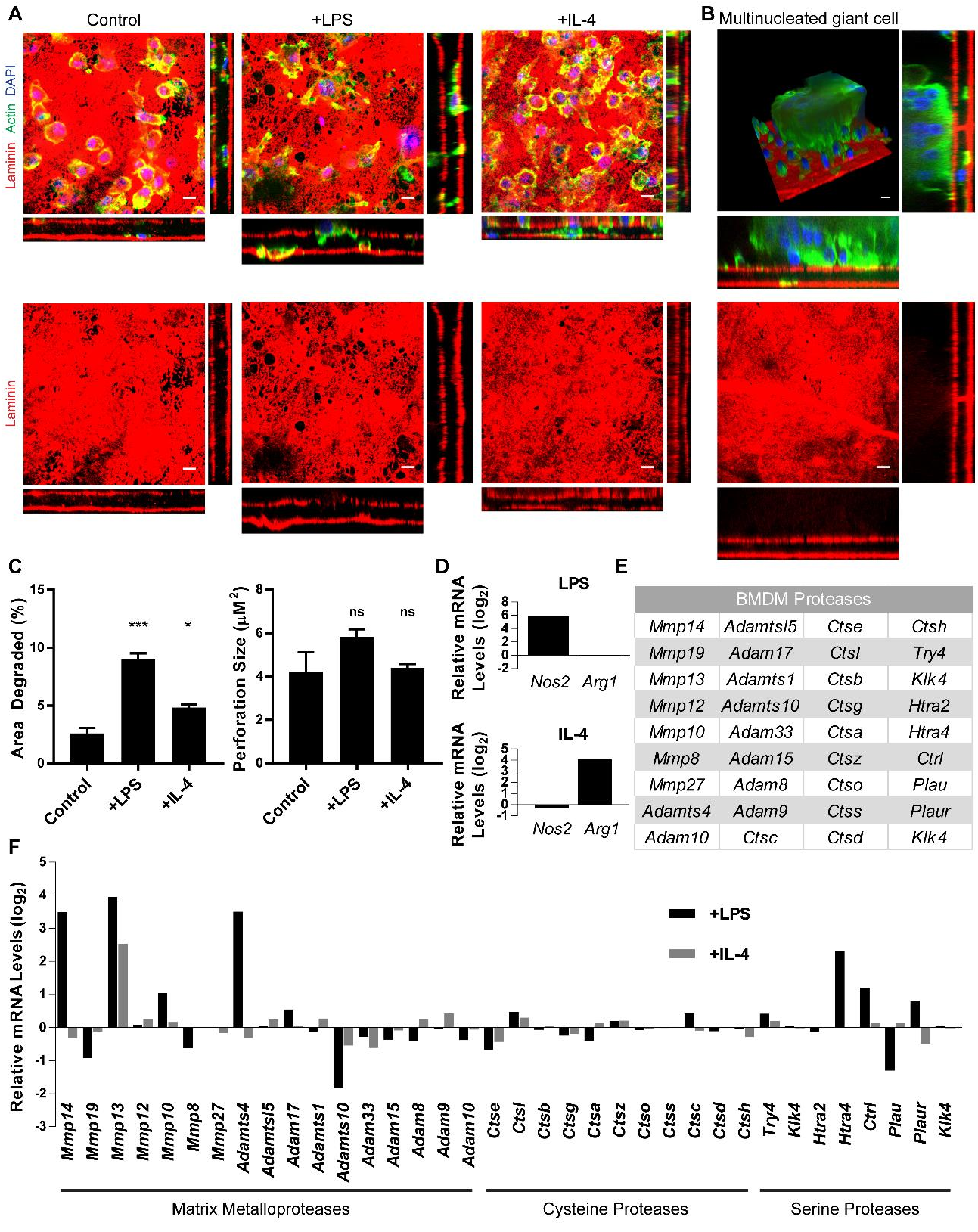
A
Control
+LPS
+IL-4
Laminin Actin DAPI
Laminin
B Multinucleated giant cell
C
Area Degraded (%)
***
*
Perforation Size (μM²)
ns
ns
Control
+LPS
+IL-4
D
Relative mRNA Levels (log2)
LPS
Nos2 Arg1
IL-4
Nos2 Arg1
E
BMDM Proteases
Mmp14 Adamtsl5 Ctse Ctsh
Mmp19 Adam17 Ctsl Try4
Mmp13 Adamts1 Ctsb Klk4
Mmp12 Adamts10 Ctsg Htra2
Mmp10 Adam33 Ctsa Htra4
Mmp8 Adam15 Ctsz Ctrl
Mmp27 Adam8 Ctso Plau
Adamts4 Adam9 Ctss Plaur
Adam10 Ctsc Ctsd Klk4
F
Relative mRNA Levels (log2)
+LPS
+IL-4
Mmp14 Mmp19 Mmp13 Mmp12 Mmp10 Mmp8 Mmp27 Adamts4 Adamtsl5 Adam17 Adamts1 Adamts10 Adam33 Adam15 Adam8 Adam9 Adam10
Ctse Ctsl Ctsb Ctsg Ctsa Ctsz Ctso Ctss Ctsc Ctsd Ctsh
Try4 Klk4 Htra2 Htra4 Ctrl Plau Plaur Klk4
Matrix Metalloproteases
Cysteine Proteases
Serine Proteases

Figure 2.3. Polarized mouse macrophages express a suite of proteases.
(A) Immunofluorescence of mouse BMDM cultured for 6 days on basement membrane constructs in the presence of media alone, LPS (1 μg/mL), or recombinant mouse IL-4 (20 ng/mL) . Images shown are representative of three replicates. **(B)** 3D, *en face*, and orthogonal images of a multinucleated giant cell formed in response to IL-4. **(C)** Quantification of the area of basement membrane degraded and basement membrane perforation size as analyzed by ImageJ pixel analysis of each condition from (A). Results are expressed as mean ± SEM; (***) $P < .0001$, (*) $P < .01$; ns, not significant; $n = 3$. **(D)** Microarray data for two biological replicates of mouse BMDM left unstimulated, polarized with LPS (1 μg/mL), or polarized with recombinant mouse IL-4 (20 ng/mL) for 24 h. Relative expression levels of mouse-specific immune response genes (D), proteases with an absolute gene expression value of at least 2^4 **(E)**, and the relative expression of those proteases in response to LPS and IL-4 **(F)** are presented. (D, F) are on a $\log_2$ scale.

Figure 2.4

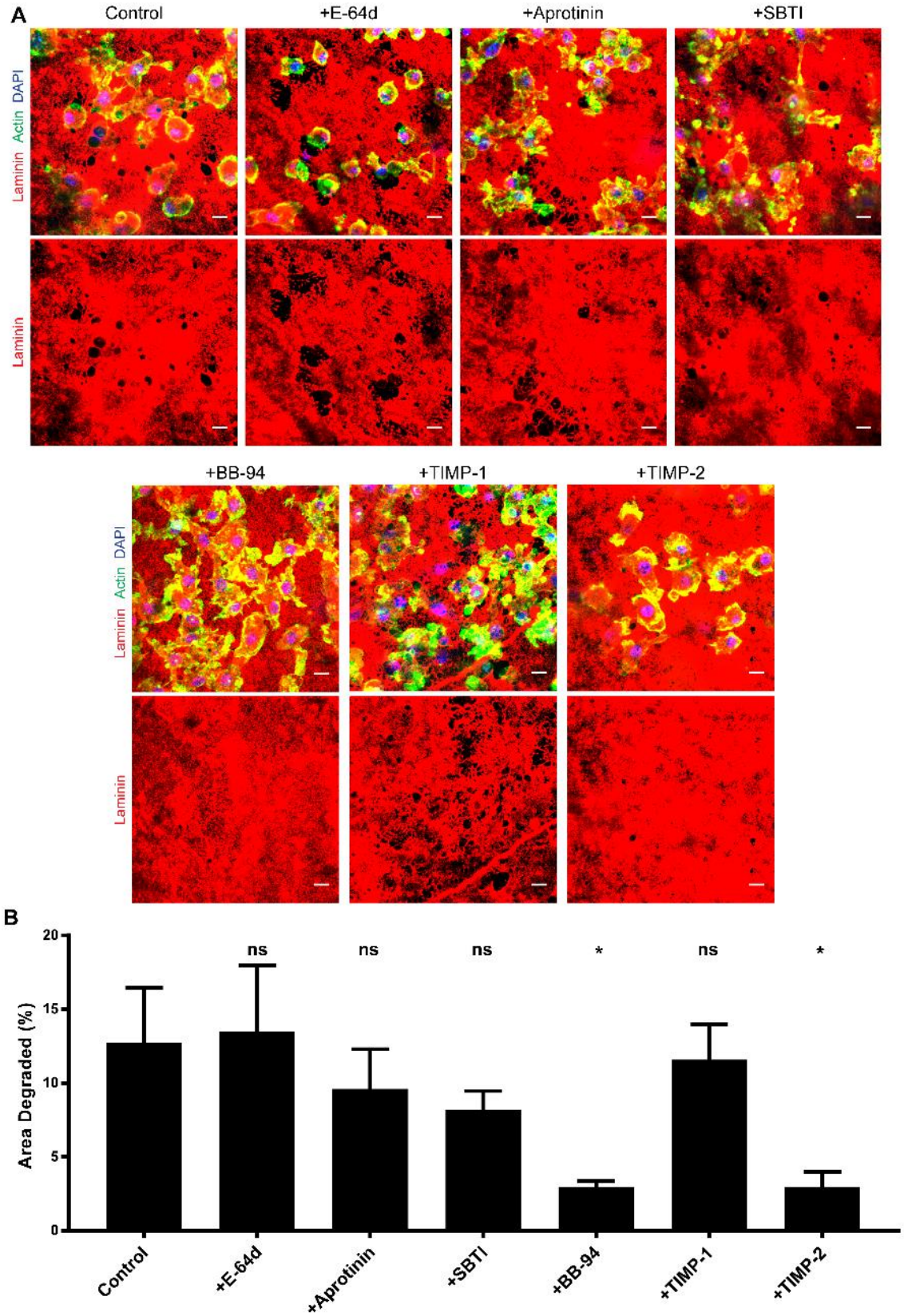
A
Control
+E-64d
+Aprotinin
+SBTI
Laminin Actin DAPI
Laminin
+BB-94
+TIMP-1
+TIMP-2
Laminin Actin DAPI
Laminin
B
Area Degraded (%)
20
15
10
5
0
ns
ns
ns
*
ns
*
Control
+E-64d
+Aprotinin
+SBTI
+BB-94
+TIMP-1
+TIMP-2

Figure 2.4. Mouse macrophages require matrix metalloproteinases for basement membrane remodeling.
(A) Macrophages were cultured atop basement membrane constructs for 6 days with LPS (1 µg/mL) in the absence or presence of inhibitors directed against cysteine proteinases (100 µM E-64d), serine proteinases (100 µg/mL aprotinin; 100 µg/mL soybean trypsin inhibitor, SBTI), matrix metalloproteinases (5 µM BB-94), 12.5 µg/mL TIMP-1, or 5 µg/mL TIMP-2. Images are representative of three replicates. Bars: 10 µm. **(B)** Quantification of the area of basement membrane degraded as analyzed by ImageJ pixel analysis under each set of conditions. Results are expressed as mean ± SEM; (*) $P < .01$; ns, not significant; $n = 3$.

Figure 2.5

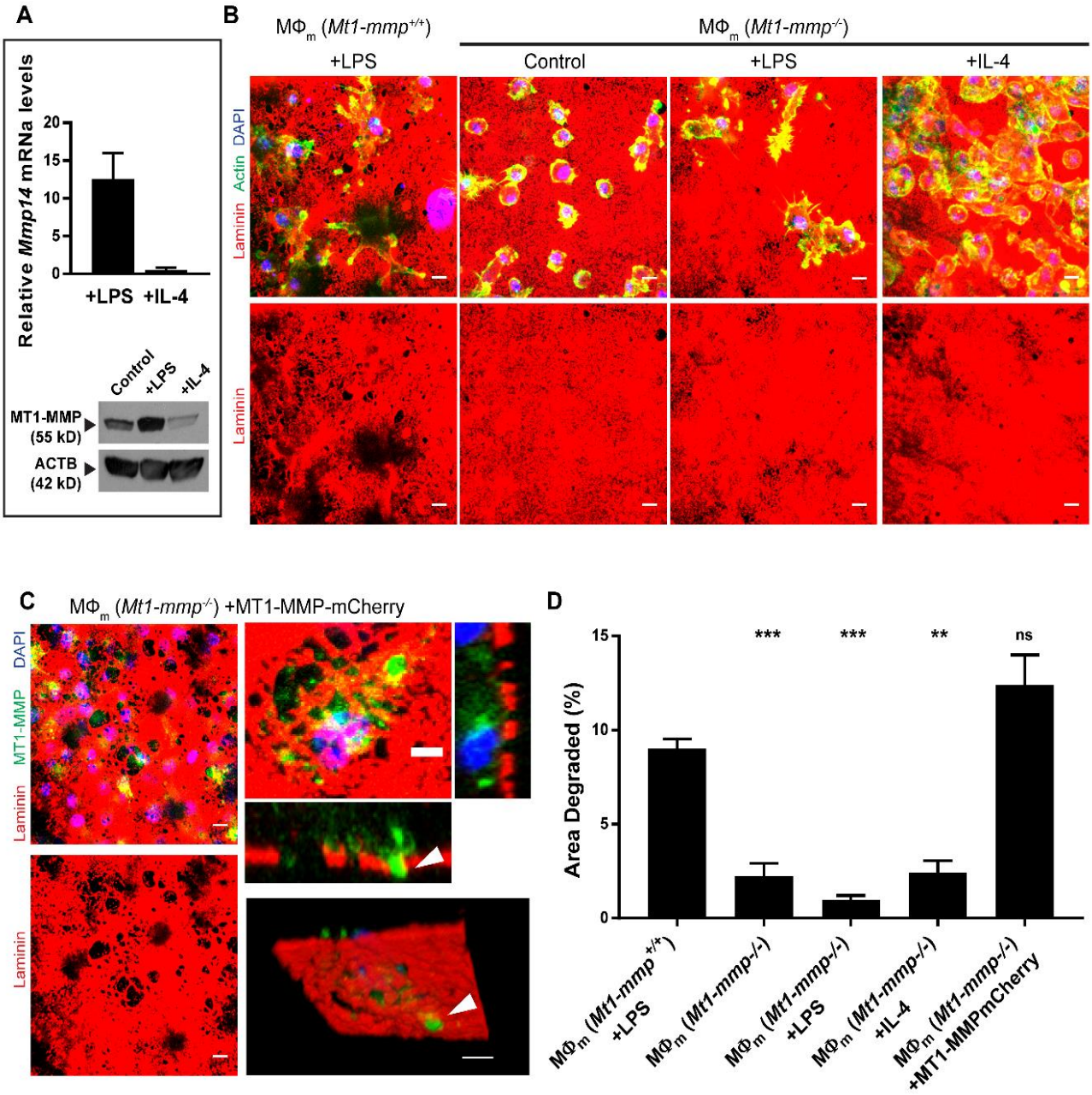

Figure 2.5. MT1-MMP-dependent mouse BMDM-mediated basement membrane remodeling.

(A) Relative MT1-MMP expression in mouse BMDM left unstimulated or polarized with LPS (1 µg/mL), or recombinant mouse IL-4 (20 ng/mL), as determined by qPCR (top panel) or Western blot (bottom panel). **(B)** Immunofluorescence basement membranes exposed to either LPS-polarized MT1-MMP$^{+/+}$ mouse BMDM or unstimulated, LPS-, and IL-4-polarized MT1-MMP$^{-/-}$ mouse BMDM. **(C)** Immunofluorescence of MT1-MMP$^{-/-}$

mouse BMDM transduced with a lentiviral MT1-MMP-mCherry vector (pseudo-colored green) for 48 h before culture on the basement membrane construct (pseudo-colored red). MT1-MMP-mCherry-positive protrusions are localized to basement membrane perforations (arrowheads). Images shown in (B-C) are representative of three replicates. Bars: (B; C, left panels) 10 µm, (C, right panels) 5 µm. **(D)** Quantification of the area of basement membrane degraded as analyzed by ImageJ pixel analysis under each set of conditions from (B-C). Results are expressed as mean ± SEM; (***) $P < .0001$, (**) $P < .001$; ns, not significant; $n = 3$.

Figure 2.6

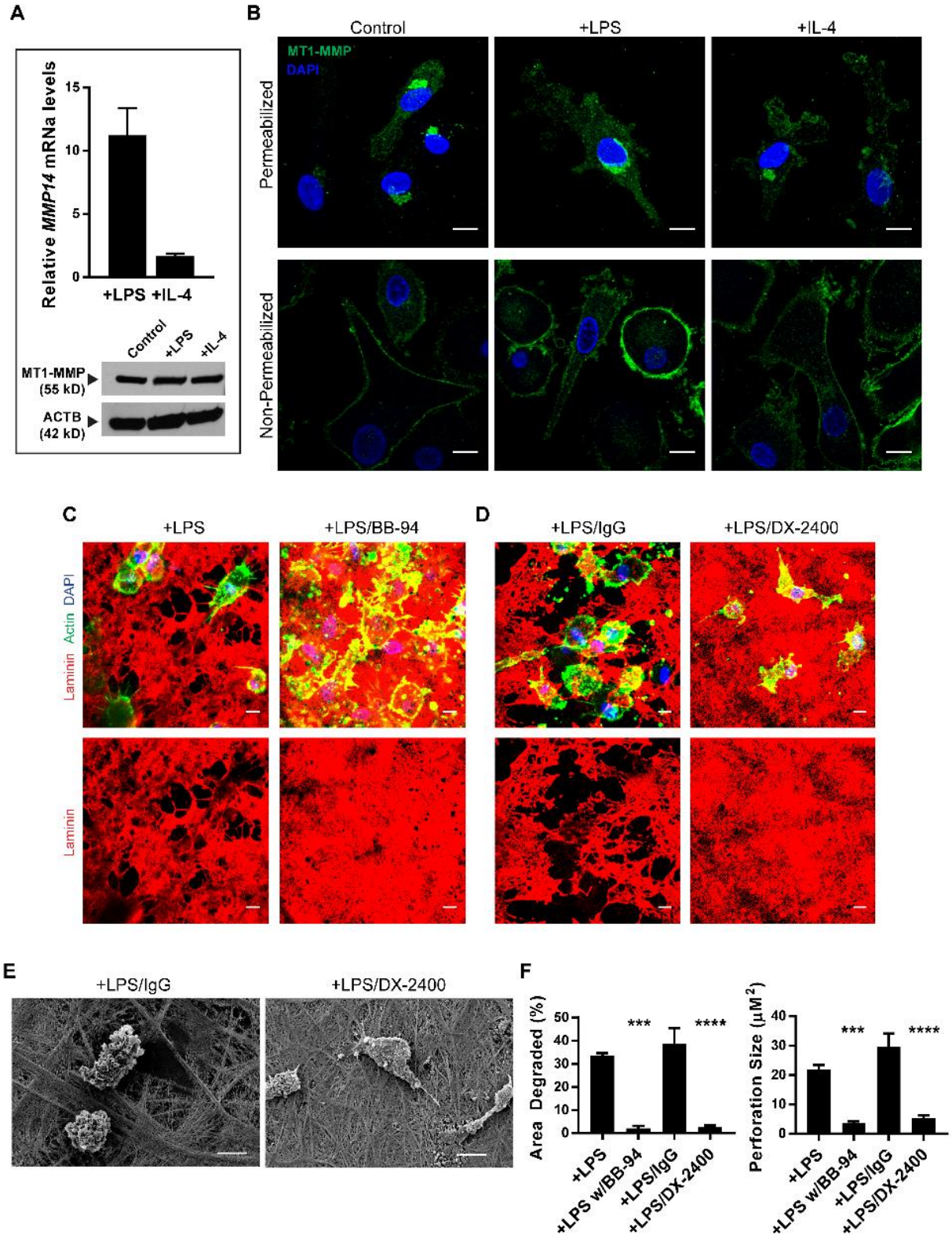
A
Relative MMP14 mRNA levels
15
10
5
0
+LPS +IL-4
Control
+LPS
+IL-4
MT1-MMP (55 kD)
ACTB (42 kD)
B
Control
+LPS
+IL-4
MT1-MMP
DAPI
Permeabilized
Non-Permeabilized
C
+LPS
+LPS/BB-94
Laminin Actin DAPI
Laminin
D
+LPS/IgG
+LPS/DX-2400
E
+LPS/IgG
+LPS/DX-2400
F
Area Degraded (%)
50
40
30
20
10
0
***
****
+LPS
+LPS w/BB-94
+LPS/IgG
+LPS/DX-2400
Perforation Size (μM²)
40
30
20
10
0
***
****
+LPS
+LPS w/BB-94
+LPS/IgG
+LPS/DX-2400

Figure 2.6. Human macrophages require MT1-MMP to degrade the basement membrane.

(A) Relative MT1-MMP expression in human macrophages left unstimulated, polarized with LPS (1 µg/mL), or recombinant human IL-4 (20 ng/mL) as determined by qPCR (top panel) or Western blot (bottom panel). **(B)** High-magnification confocal images of endogenous MT1-MMP immunofluorescence in permeabilized (top 3 panels) or non-permeabilized (bottom 3 panels) human macrophages. **(C)** Immunofluorescence of macrophages on basement membrane constructs in the presence of LPS (1 µg/mL) without or with 5 µm BB-94, **(D)** 75 µg/mL IgG control antibody or 75 µg/mL of MT1-MMP blocking antibody, DX-2400. **(E)** Scanning electron micrograph of mesentery basement membrane after culture with macrophages in the presence of LPS (1 µg/mL) and either 75 µg/mL IgG or 75 µg/mL DX-2400 for 6 days. Images shown in (B-D) are representative of three replicates. Bars: (B-E) 10 µm. **(F)** Quantification of the area of basement membrane degraded as analyzed by ImageJ pixel analysis of each condition from (C-D). Results are expressed as mean ± SEM; (****) $P < .00001$, (***) $P < .0001$; $n = 3$.

Figure 2.7

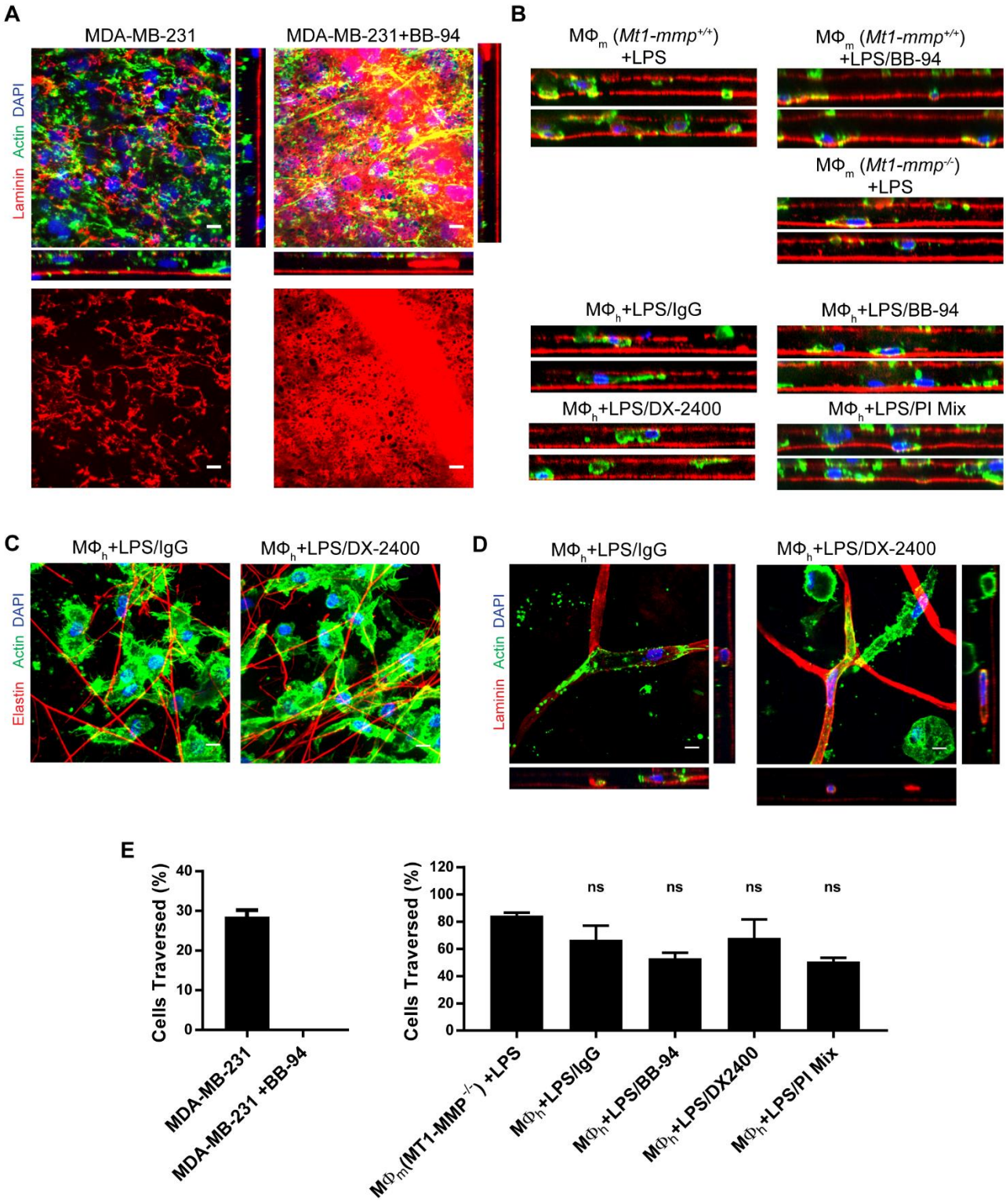
A
MDA-MB-231
MDA-MB-231+BB-94
Laminin Actin DAPI
B
MΦm (Mt1-mmp+/+) +LPS
MΦm (Mt1-mmp+/+) +LPS/BB-94
MΦm (Mt1-mmp-/-) +LPS
MΦh+LPS/IgG
MΦh+LPS/BB-94
MΦh+LPS/DX-2400
MΦh+LPS/PI Mix
C
MΦh+LPS/IgG
MΦh+LPS/DX-2400
Elastin Actin DAPI
D
MΦh+LPS/IgG
MΦh+LPS/DX-2400
Laminin Actin DAPI
E
Cells Traversed (%)
40
30
20
10
0
MDA-MB-231
MDA-MB-231 +BB-94
Cells Traversed (%)
120
100
80
60
40
20
0
ns
ns
ns
ns
MΦm(MT1-MMP-/-) +LPS
MΦh+LPS/IgG
MΦh+LPS/BB-94
MΦh+LPS/DX2400
MΦh+LPS/PI Mix

Figure 2.7. Macrophages can mobilize a proteinase-independent tissue invasion program.
(A) *En face* and orthogonal immunofluorescence of basement membranes cultured with human MDA-MB-231 breast carcinoma cells for 48 h without or with 5 µm BB-94. **(B)** Orthogonal view reconstructions of LPS (1 µg/mL) -polarized MT1-MMP$^{+/+}$ or MT1-MMP$^{-/-}$ mouse BMDM in the absence or presence of 5 µm BB-94 (top 3 panels), and LPS (1 µg/mL) -polarized human macrophages in the presence or absence of 75 µg/mL IgG, 5 µm BB-94, 75 µg/mL DX-2400, or a protease inhibitor mix (100 µm E-64d, 100 µg/ml aprotinin, 10 µm pepstatin A, 100 µg/ml SBTI, 5 µm BB-94, 2 µm leupeptin) (bottom 4 panels). Images shown are representative of three replicates. **(C)** Immunofluorescence of human macrophages polarized with LPS (1 µg/mL) adhering to the interstitial elastin network in the presence or absence of 75 µg/mL IgG or 75 µg/mL DX-2400 for 6 days. **(D)** *En face* and orthogonal immunofluorescence of human macrophages infiltrating laminin-stained vascular basement membranes in the presence or absence of 75 µg/mL IgG or 75 µg/mL DX-2400 for 6 days. **(E)** Quantification of cell bodies (including nuclei) of MDA-MB-231 (left panel) or macrophages (right panel), located between the two basement membrane layers from (A-B) as a percentage of the total number of cells. Bars: (A, C-D) 10 µm.

Figure 2.8

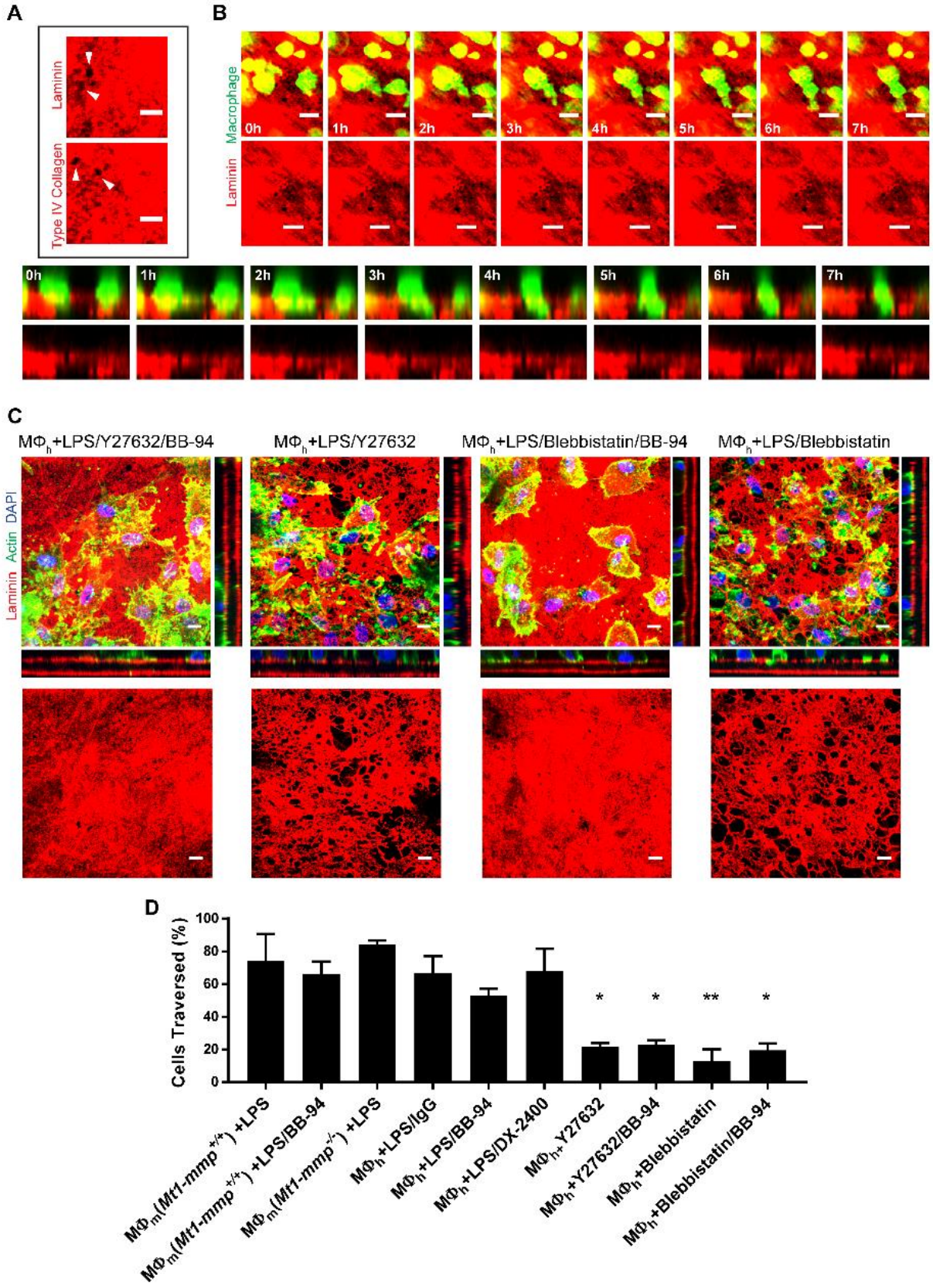
A
Laminin
Type IV Collagen
B
Macrophage
Laminin
0h
1h
2h
3h
4h
5h
6h
7h
C
MΦh+LPS/Y27632/BB-94
MΦh+LPS/Y27632
MΦh+LPS/Blebbistatin/BB-94
MΦh+LPS/Blebbistatin
Laminin
Actin
DAPI
D
Cells Traversed (%)
100
80
60
40
20
0
*
*
**
*
MΦm(Mt1-mmp+/+)+LPS
MΦm(Mt1-mmp+/+)+LPS/BB-94
MΦm(Mt1-mmp-/-)+LPS
MΦh+LPS/IgG
MΦh+LPS/BB-94
MΦh+LPS/DX-2400
MΦh+Y27632
MΦh+Y27632/BB-94
MΦh+Blebbistatin
MΦh+Blebbistatin/BB-94

Figure 2.8. Macrophages traverse preformed portals in the basement membrane in an actomyosin-dependent fashion.

(A) Magnified confocal immunofluorescence of pores (arrowheads) in laminin- and type IV collagen-labeled basement membranes (B) Time-lapse series of CFSE-labeled human macrophages (green) and laminin-prelabeled basement membrane (red) captured every hour for 7 h immediately after plating. A macrophage moves towards preformed portals and distorts its shape (top two rows) while traversing the basement membrane en route to the interstitial matrix (bottom two rows). **(B)** *En face* and orthogonal immunofluorescence of basement membranes cultured with human macrophages polarized with LPS (1 µg/mL) in the absence or presence of Y-27632 (20 µM) and BB-94 (5 µm) (left panels), or Blebbistatin (20 µM) and BB-94 (5 µm) (right panels). Images shown are representative of three replicates. **(C)** Quantification of cell bodies (including nuclei) of macrophages, located between the two basement membrane layers (from Figure 7B and Figure 8B) as a percentage of the total number of cells. Bars: (A, B) 5 µm, (C) 10 µm. Results are expressed as mean ± SEM; (**) $P < .001$, (*) $P < .01$; $n = 3$.

Figure 2.S1

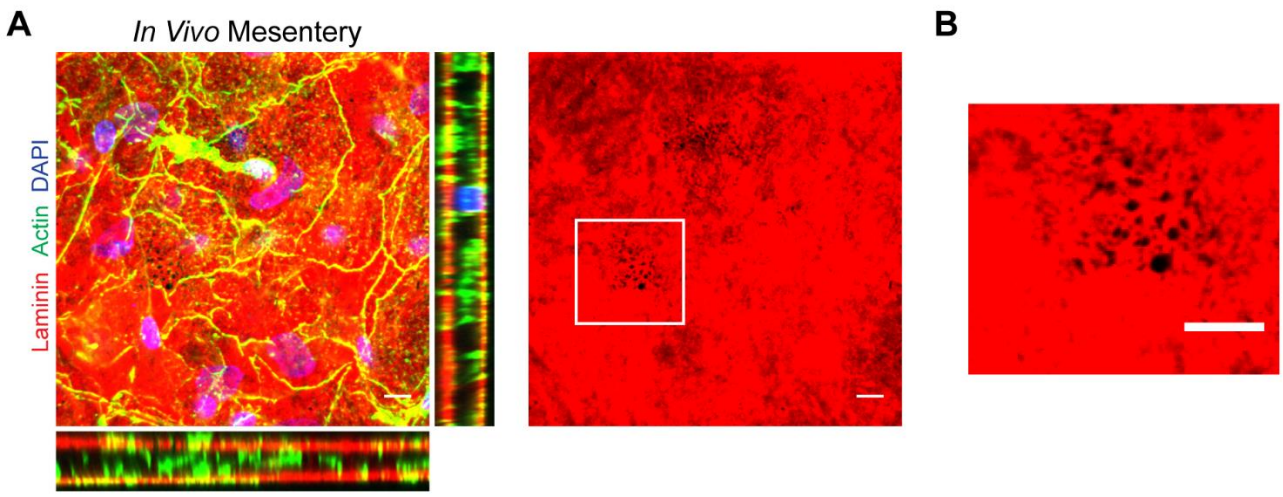

Figure 2.S1. **Preformed portals in basement membrane prior to decellularization.** **(A)** *En face* and orthogonal immunofluorescence of mesentery fixed in 4% PFA prior to decellularization. **(B)** Magnification of boxed region in (A) showing a grouping of preformed portals in the basement membrane. Bars: (A, B) 10 µm.

Video 1

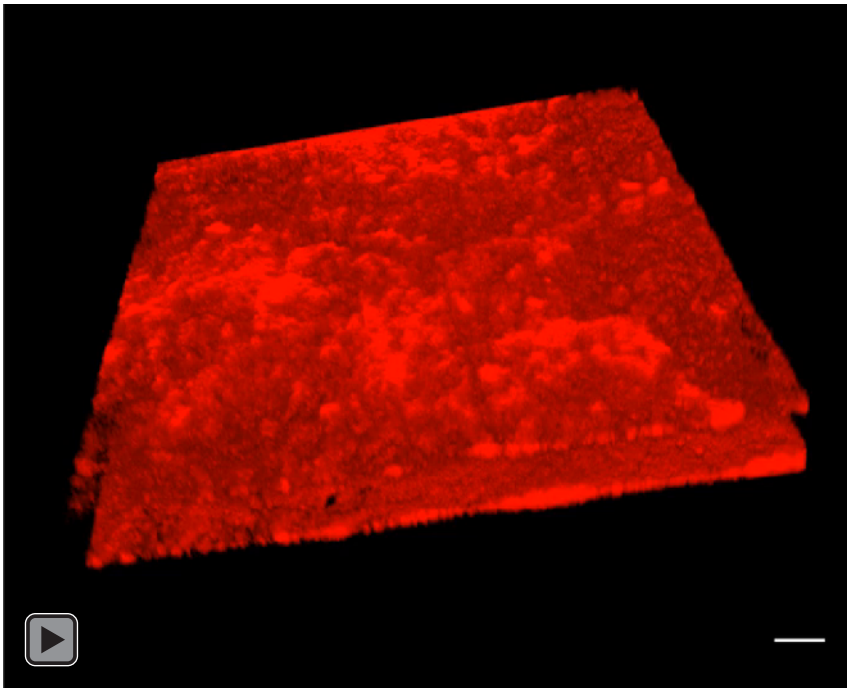

Video 1. **3D rotation of rat mesentery basement membrane.**
Laminin-stained (red) apical and reflected basal basement membrane surfaces in a 360° rotation. Depicted as a 3D-rendered confocal z-stack. Bar 20 µm. Refers to Figure 2.1B.

Video 2

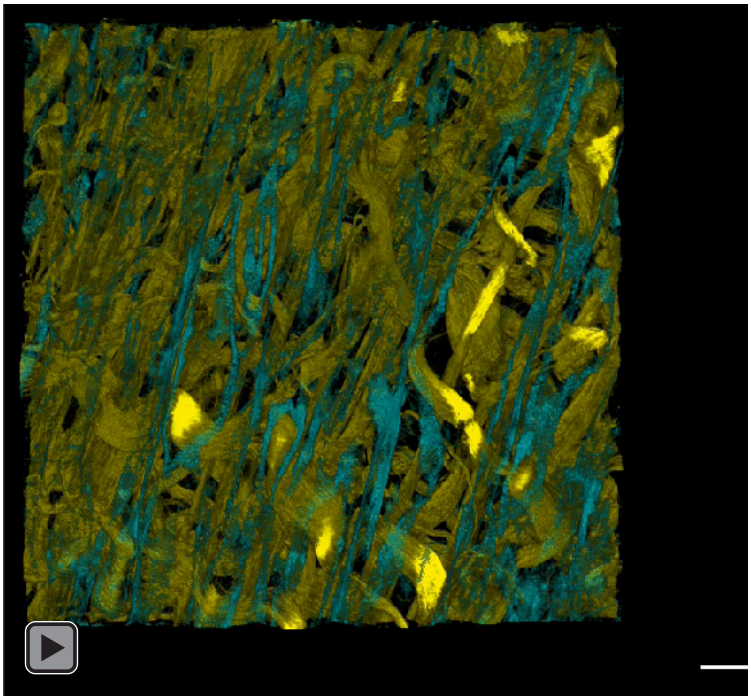

Video 2. **3D rotation of rat mesentery interstitial matrix.**
Elastin (blue) with second harmonic generation of type I collagen (yellow) in a 360° rotation. Depicted as a 3D-rendered confocal z-stack. Bar 20 µm. Refers to Figure 2.1B.

Video 3

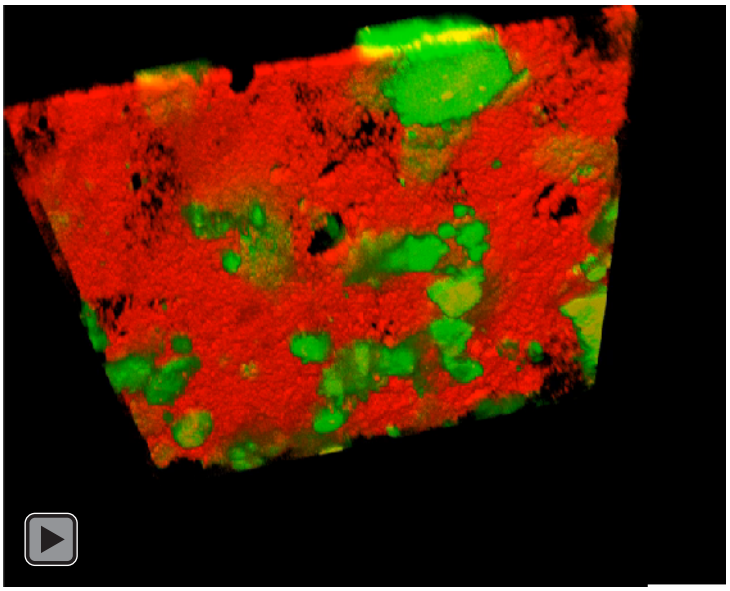

Video 3. Human macrophages dynamically protrude through the basement membrane.

3D confocal time-lapse view of the interstitium-facing side of the apical basement membrane (red) as human macrophages (green) actively protrude through it. Time of observation: 160 minutes, captured every 10 minutes. Playback: 6 frames/s. Bar 20 µm. Refers to Figure 2.1H.

Video 4

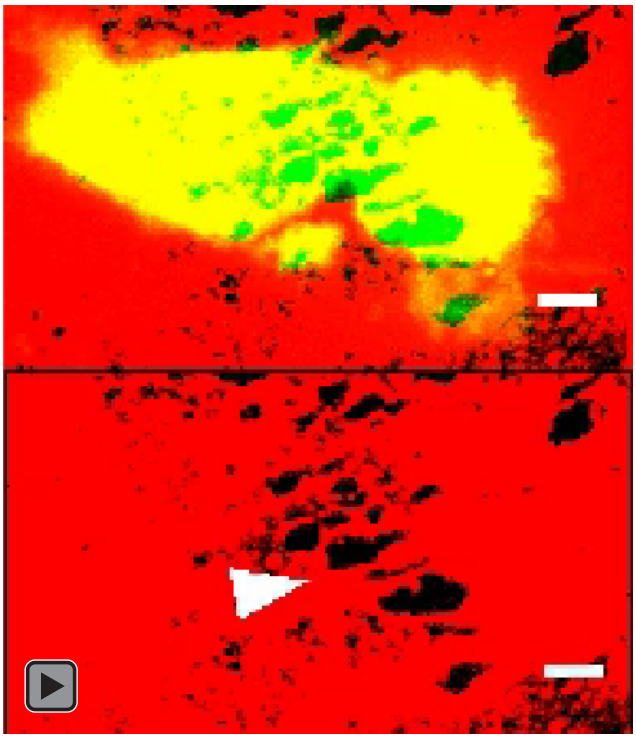

Video 4. **Human macrophages expand basement membrane perforations.** Enlarged max intensity projection confocal time-lapse of human macrophages (green) atop the apical basement membrane face (red) in the presence of LPS (1 µg/mL) actively expanding a perforation (arrowhead) in the basement membrane. Time of observation: 160 minutes, captured every 10 minutes. Playback: 6 frames/s. Bar 10 µm. Refers to Figure 2.1I.

Video 5

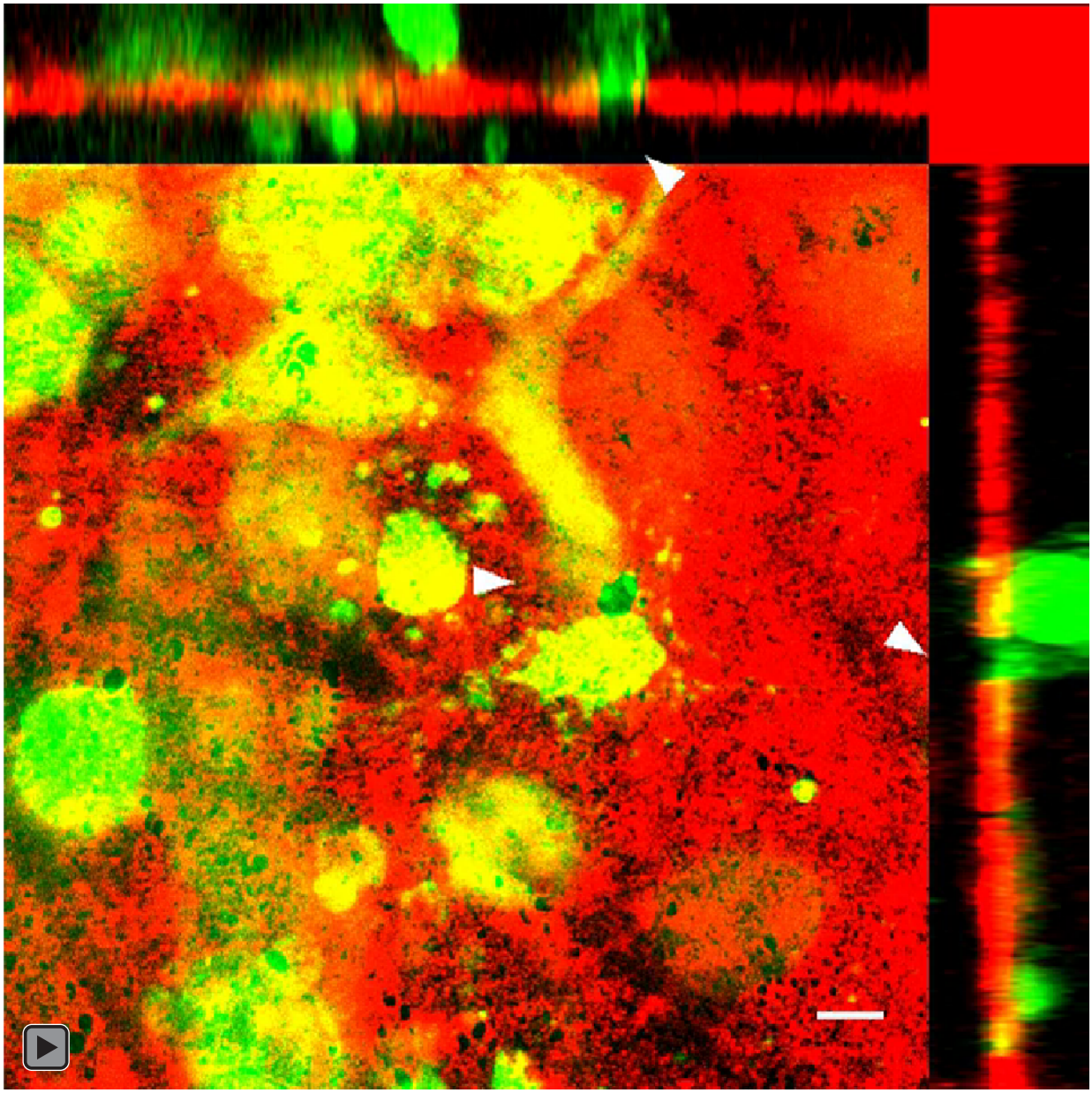

Video 5. Human macrophages encircle expanding basement membrane perforations.
Max intensity projection and orthogonal reconstruction confocal time-lapse of human macrophages (green) atop the apical basement membrane face (red) in the presence of LPS (1 µg/mL) actively expanding a perforation in the basement membrane (arrowhead). Time of observation: 11 h, captured every 1 h. Playback: 6 frames/s. Bar 10 µm. Refers to Figure 2.2.

Video 6

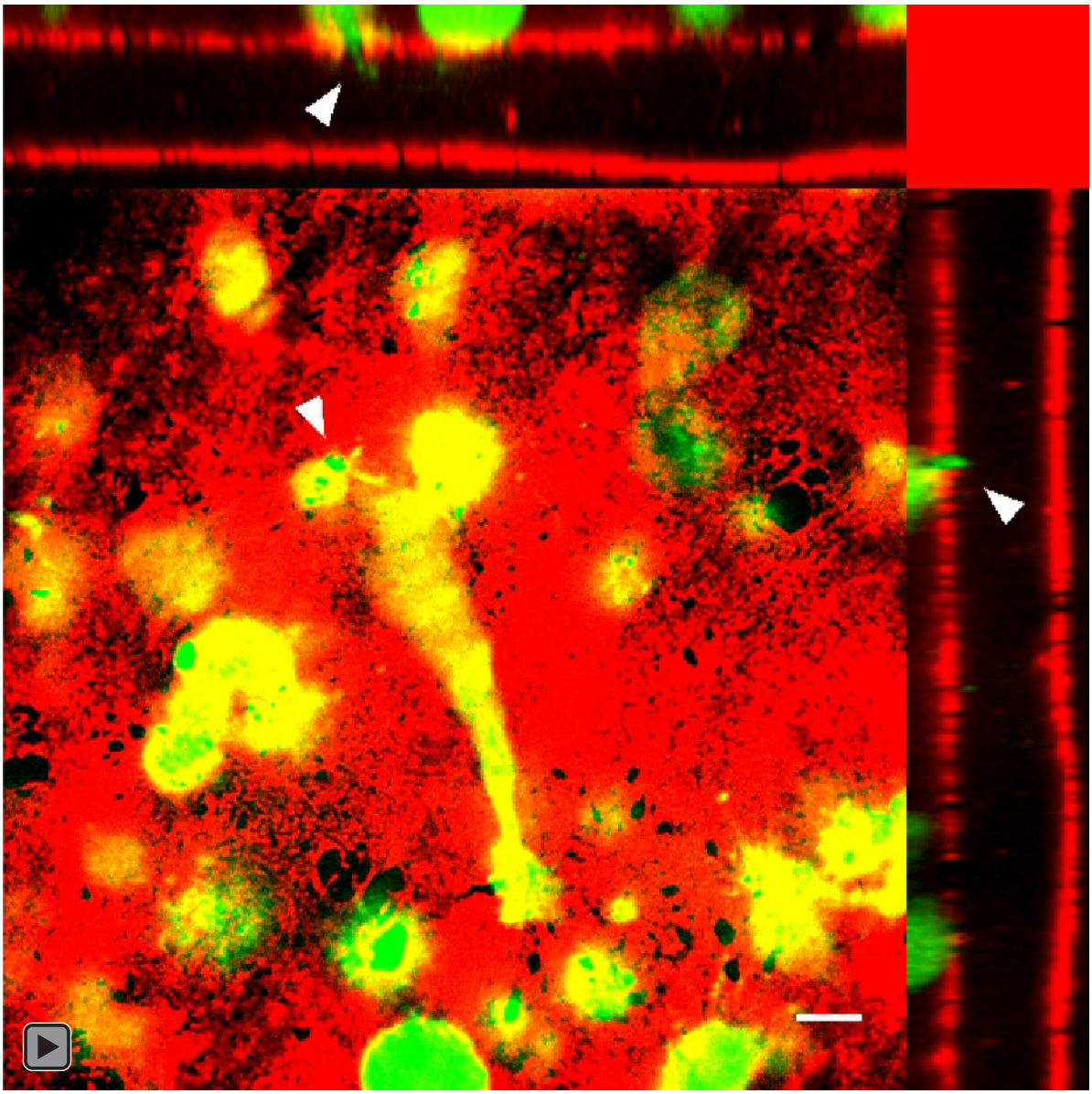

Video 6. Human macrophages protrude through expanding basement membrane perforations.

Max intensity projection confocal time-lapse combined with static confocal orthogonal reconstructions of human macrophages (green) atop the apical basement membrane face (red) in the presence of LPS (1 µg/mL) actively expanding a perforation in the basement membrane (arrowhead). Time of observation: 90 minutes, captured every 3 minutes. Playback: 10 frames/s. Bar 10 µm. Refers to Figure 2.2.

Video 7

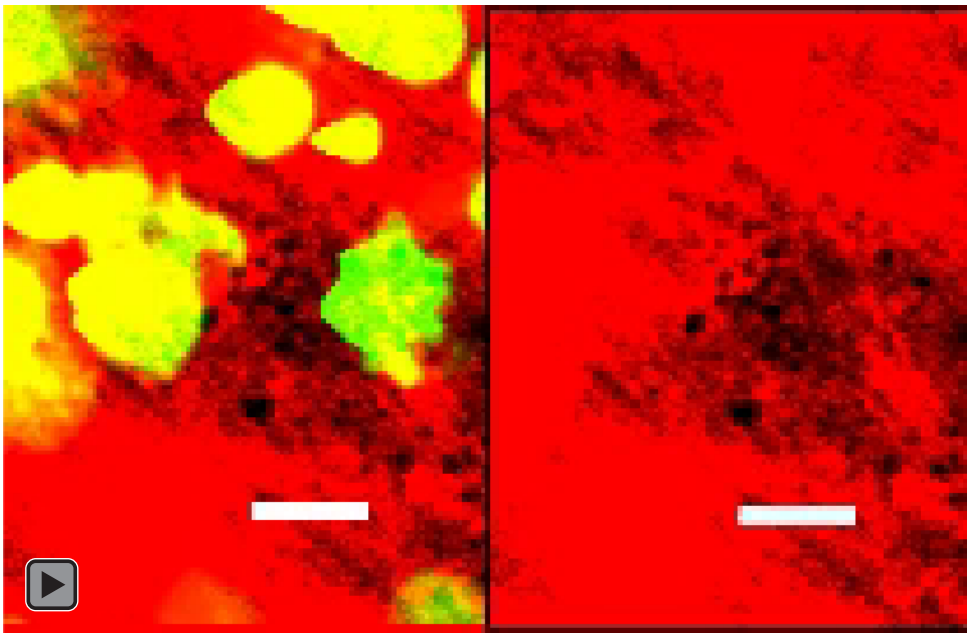

Video 7. Human macrophages engage with preformed basement membrane portals.
Enlarged max intensity projection confocal time-lapse of human macrophages (green) atop the apical basement membrane face (red) in the presence of LPS (1 µg/mL) and 75 µg/mL DX-2400. Time of observation: 460 minutes, captured every 20 minutes. Playback: 6 frames/s. Bar 5µm. Refers to Figure 2.8A.

Video 8

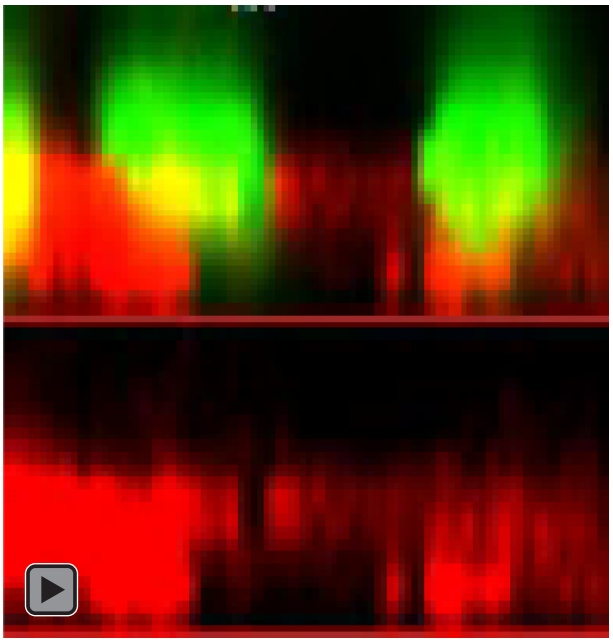

Video 8. **Human macrophages traverse preformed basement membrane portals.** Enlarged orthogonal reconstruction confocal time-lapse of human macrophages (green) atop the apical basement membrane face (red) in the presence of LPS (1 µg/mL) and 75 µg/mL DX-2400. Time of observation: 520 minutes, captured every 20 minutes. Playback: 8 frames/s. Refers to Figure 2.8A.

References

Afik, R., Zigmond, E., Vugman, M., Klepfish, M., Shimshoni, E., Pasmanik-Chor, M., . . . Varol, C. (2016). Tumor macrophages are pivotal constructors of tumor collagenous matrix. *The Journal of Experimental Medicine, 213*, 2315-2331.

Ager, E. I., Kozin, S. V., Kirkpatrick, N. D., Seano, G., Kodack, D. P., Askoxylakis, V., . . . Jain, R. K. (2015). Blockade of MMP14 activity in murine breast carcinomas: Implications for macrophages, vessels, and radiotherapy. *Journal of the National Cancer Institute, 107*, djv017.

Akkari, L., Gocheva, V., Kester, J. C., Hunter, K. E., Quick, M. L., Sevenich, L., . . . Joyce, J. A. (2014). Distinct functions of macrophage-derived and cancer cell-derived cathepsin Z combine to promote tumor malignancy via interactions with the extracellular matrix. *Genes & Development, 28*, 2134-2150.

Aung, A., Seo, Young N., Lu, S., Wang, Y., Jamora, C., del Álamo, Juan C., & Varghese, S. (2014). 3D traction stresses activate protease-dependent invasion of cancer cells. *Biophysical Journal, 107*, 2528-2537.

Baker, A. H., Edwards, D. R., & Murphy, G. (2002). Metalloproteinase inhibitors: biological actions and therapeutic opportunities. *Journal of Cell Science, 115*, 3719-3727.

Barreiro, O., Cibrian, D., Clemente, C., Alvarez, D., Moreno, V., Valiente, Í., . . . Sánchez Madrid, F. (2016). Pivotal role for skin transendothelial radio-resistant anti-inflammatory macrophages in tissue repair. *eLife, 5*, pii: e15251.

Barros-Becker, F., Lam, P.-Y., Fisher, R., & Huttenlocher, A. (2017). Live imaging reveals distinct modes of neutrophil and macrophage migration within interstitial tissues. *Journal of Cell Science, 130*, 3801-3808.

Bluemink, J. G., van Maurik, P., & Lawson, K. A. (1976). Intimate cell contacts at the epithelial/mesenchymal interface in embryonic mouse lung. *Journal of Ultrastructure Research, 55*, 257-270.

Boudko, S. P., Danylevych, N., Hudson, B. G., & Pedchenko, V. K. (2018). Basement membrane collagen IV: Isolation of functional domains. *Methods in Cell Biology, 143*, 171-185.

Brew, K., & Nagase, H. (2010). The tissue inhibitors of metalloproteinases (TIMPs): An ancient family with structural and functional diversity. *Biochimica et Biophysica Acta (BBA) - Molecular Cell Research, 1803*, 55-71.

Chang, T. T., Thakar, D., & Weaver, V. M. (2017). Force-dependent breaching of the basement membrane. *Matrix Biology, 57-58*, 178-189.

Cougoule, C., Van Goethem, E., Le Cabec, V., Lafouresse, F., Dupré, L., Mehraj, V., . . . Maridonneau-Parini, I. (2012). Blood leukocytes and macrophages of various

phenotypes have distinct abilities to form podosomes and to migrate in 3D environments. *European Journal of Cell Biology, 91*, 938-949.

Devy, L., Huang, L., Naa, L., Yanamandra, N., Pieters, H., Frans, N., . . . Dransfield, D. T. (2009). Selective inhibition of matrix metalloproteinase-14 blocks tumor growth, invasion, and angiogenesis. *Cancer Research, 69*, 1517-1526.

English, J. L., Kassiri, Z., Koskivirta, I., Atkinson, S. J., Di Grappa, M., Soloway, P. D., . . . Khokha, R. (2006). Individual TIMP deficiencies differentially impact pro-MMP-2 activation. *The Journal of Biological Chemistry, 281*, 10337-10346.

Fidler, A. L., Boudko, S. P., Rokas, A., & Hudson, B. G. (2018). The triple helix of collagens - an ancient protein structure that enabled animal multicellularity and tissue evolution. *Journal of Cell Science, 131*, jcs203950-jcs203950.

Fidler, A. L., Darris, C. E., Chetyrkin, S. V., Pedchenko, V. K., Boudko, S. P., Brown, K. L., . . . Hudson, B. G. (2017). Collagen iv and basement membrane at the evolutionary dawn of metazoan tissues. *eLife, 6*, pii: e24176.

Fidler, A. L., Vanacore, R. M., Chetyrkin, S. V., Pedchenko, V. K., Bhave, G., Yin, V. P., . . . Hudson, B. G. (2014). A unique covalent bond in basement membrane is a primordial innovation for tissue evolution. *Proceedings of the National Academy of Sciences, 111*, 331-336.

Filippov, S., Caras, I., Murray, R., Matrisian, L. M., Chapman, H. A., Shapiro, S., & Weiss, S. J. (2003). Matrilysin-dependent Elastolysis by Human Macrophages. *The Journal of Experimental Medicine, 198*, 925-935.

Fleetwood, A. J., Achuthan, A., Schultz, H., Nansen, A., Almholt, K., Usher, P., & Hamilton, J. A. (2014). Urokinase plasminogen activator is a central regulator of macrophage three-dimensional invasion, matrix degradation, and adhesion. *Journal of immunology (Baltimore, Md.: 1950), 192*, 3540-3547.

Gjorevski, N., S. Piotrowski, A., Varner, V. D., & Nelson, C. M. (2015). Dynamic tensile forces drive collective cell migration through three-dimensional extracellular matrices. *Scientific Reports, 5*, 11458-11458.

Glentis, A., Oertle, P., Mariani, P., Chikina, A., El Marjou, F., Attieh, Y., . . . Vignjevic, D. M. (2017). Cancer-associated fibroblasts induce metalloprotease-independent cancer cell invasion of the basement membrane. *Nature Communications, 8*, 924-924.

Güç, E., Fankhauser, M., Lund, A. W., Swartz, M. A., & Kilarski, W. W. (2014). Long-term intravital immunofluorescence imaging of tissue matrix components with epifluorescence and two-photon microscopy. *Journal of Visualized Experiments*, 51388.

Gui, P., Labrousse, A., Van Goethem, E., Besson, A., Maridonneau-Parini, I., & Le Cabec, V. (2014). Rho/ROCK pathway inhibition by the CDK inhibitor p27(kip1) participates in the onset of macrophage 3D-mesenchymal migration. *Journal of Cell Science, 127*, 4009-4023.

Guiet, R., Van Goethem, E., Cougoule, C., Balor, S., Valette, A., Al Saati, T., . . . Maridonneau-Parini, I. (2011). The process of macrophage migration promotes matrix metalloproteinase-independent invasion by tumor cells. *Journal of immunology (Baltimore, Md. : 1950), 187*, 3806-3814.

Guiet, R., Vérollet, C., Lamsoul, I., Cougoule, C., Poincloux, R., Labrousse, A., . . . Maridonneau-Parini, I. (2012). Macrophage mesenchymal migration requires podosome stabilization by filamin A. *The Journal of Biological Chemistry, 287*, 13051-13062.

Gundra, U. M., Girgis, N. M., Ruckerl, D., Jenkins, S., Ward, L. N., Kurtz, Z. D., . . . Loke, P. n. (2014). Alternatively activated macrophages derived from monocytes and tissue macrophages are phenotypically and functionally distinct. *Blood, 123*, e110-122.

Haeger, A., Wolf, K., Zegers, M. M., & Friedl, P. (2015). Collective cell migration: guidance principles and hierarchies. *Trends in Cell Biology, 25*, 556-566.

Halfter, W., Candiello, J., Hu, H., Zhang, P., Schreiber, E., & Balasubramani, M. (2013). Protein composition and biomechanical properties of in vivo-derived basement membranes. *Cell Adhesion & Migration, 7*, 64-71.

Halfter, W., Monnier, C., Müller, D., Oertle, P., Uechi, G., Balasubramani, M., . . . Henrich, P. B. (2013). The bi-functional organization of human basement membranes. *PLoS ONE, 8*, e67660-e67660.

Halfter, W., Oertle, P., Monnier, C. A., Camenzind, L., Reyes-Lua, M., Hu, H., . . . Plodinec, M. (2015). New concepts in basement membrane biology. *FEBS Journal, 282*, 4466-4479.

Hallmann, R., Zhang, X., Di Russo, J., Li, L., Song, J., Hannocks, M.-J., & Sorokin, L. (2015). The regulation of immune cell trafficking by the extracellular matrix. *Current Opinion in Cell Biology, 36*, 54-61.

Hanahan, D., & Weinberg, R. A. (2011). Hallmarks of cancer: the next generation. *Cell, 144*, 646-674.

Harney, A. S., Arwert, E. N., Entenberg, D., Wang, Y., Guo, P., Qian, B. Z., . . . Condeelis, J. S. (2015). Real-time imaging reveals local, transient vascular permeability, and tumor cell intravasation stimulated by TIE2hi macrophage–derived VEGFA. *Cancer Discovery, 5*, 932-943.

Harunaga, J. S., Doyle, A. D., & Yamada, K. M. (2014). Local and global dynamics of the basement membrane during branching morphogenesis require protease activity and actomyosin contractility. *Developmental Biology, 394*, 197-205.

He, L., & Wirtz, D. (2014). Switching from protease-independent to protease-dependent cancer cell invasion. *Biophysical Journal, 107*, 2484-2485.

Hotary, K., Li, X.-Y., Allen, E., Stevens, S. L., & Weiss, S. J. (2006). A cancer cell metalloprotease triad regulates the basement membrane transmigration program. *Genes & Development, 20*, 2673-2686.

Howat, W. J., Holmes, J. A., Holgate, S. T., & Lackie, P. M. (2001). Basement membrane pores in human bronchial epithelium: a conduit for infiltrating cells? *The American Journal of Pathology, 158*, 673-680.

Hung, W.-C., Chen, S.-H., Paul, C. D., Stroka, K. M., Lo, Y.-C., Yang, J. T., & Konstantopoulos, K. (2013). Distinct signaling mechanisms regulate migration in unconfined versus confined spaces. *The Journal of Cell Biology, 202*, 807-824.

Jevnikar, Z., Mirkovi, B., Fonovi, U. P., Zidar, N., Svajger, U., & Kos, J. (2012). Three-dimensional invasion of macrophages is mediated by cysteine cathepsins in protrusive podosomes. *Eur. J. Immunol, 42*, 3429-3441.

Kelley, L. C., Lohmer, L. L., Hagedorn, E. J., & Sherwood, D. R. (2014). Traversing the basement membrane in vivo: a diversity of strategies. *The Journal of Cell Biology, 204*, 291-302.

Kilarski, W. W., Güç, E., Teo, J. C. M., Oliver, S. R., Lund, A. W., & Swartz, M. A. (2013). Intravital immunofluorescence for visualizing the microcirculatory and immune microenvironments in the mouse ear dermis. *PLoS ONE, 8*, e57135-e57135.

Lewis, C. E., Harney, A. S., Pollard, J. W., Shi, H. S., Zeng, Y. H., Wang, X. Z., . . . Jones, J. G. (2016). The multifaceted role of perivascular macrophages in tumors. *Cancer Cell, 30*, 18-25.

Liu, Y.-J., Le Berre, M., Lautenschlaeger, F., Maiuri, P., Callan-Jones, A., Heuzé, M., . . . Piel, M. (2015). Confinement and low adhesion induce fast amoeboid migration of slow mesenchymal cells. *Cell, 160*, 659-672.

Madsen, D. H., Jürgensen, H. J., Siersbæk, M. S., Kuczek, D. E., Grey Cloud, L., Liu, S., . . . Bugge, T. H. (2017). Tumor-associated macrophages derived from circulating inflammatory monocytes degrade collagen through cellular uptake. *Cell Reports, 21*, 3662-3671.

Madsen, D. H., Leonard, D., Masedunskas, A., Moyer, A., Jürgensen, H. J., Peters, D. E., . . . Bugge, T. H. (2013). M2-like macrophages are responsible for collagen degradation through a mannose receptor-mediated pathway. *The Journal of Cell Biology, 202*, 951-966.

Mantovani, A., Biswas, S. K., Galdiero, M. R., Sica, A., & Locati, M. (2013). Macrophage plasticity and polarization in tissue repair and remodelling. *Journal of Pathology, 229*, 176-185.

Martinez-Santibanez, G., Singer, K., Cho, K. W., DelProposto, J. L., Mergian, T., & Lumeng, C. N. (2015). Obesity-induced remodeling of the adipose tissue elastin network is independent of the metalloelastase MMP-12. *Adipocyte, 4*, 264-272.

Martinez, F. O., Helming, L., Milde, R., Varin, A., Melgert, B. N., Draijer, C., . . . Gordon, S. (2013). Genetic programs expressed in resting and IL-4 alternatively activated mouse and human macrophages: similarities and differences. *Blood, 121*, e57-69.

McCall, A. S., Cummings, C. F., Bhave, G., Vanacore, R., Page-Mccaw, A., & Hudson, B. G. (2014). Bromine is an essential trace element for assembly of collagen IV scaffolds in tissue development and architecture. *Cell, 157*, 1380-1392.

McClugage, S. G., Low, F. N., & Zimny, M. L. (1986). Porosity of the Basement Membrane Overlying Peyer's Patches in Rats and Monkeys. *Gastroenterology, 91*, 1128-1133.

McNally, A. K., & Anderson, J. M. (1995). Interleukin-4 induces foreign body giant cells from human monocytes/macrophages. Differential lymphokine regulation of macrophage fusion leads to morphological variants of multinucleated giant cells. *The American Journal of Pathology, 147*, 1487-1499.

Misharin, A. V., Morales-Nebreda, L., Reyfman, P. A., Cuda, C. M., Walter, J. M., McQuattie-Pimentel, A. C., . . . Perlman, H. (2017). Monocyte-derived alveolar macrophages drive lung fibrosis and persist in the lung over the life span. *The Journal of Experimental Medicine, 214*, 2387-2404..

Murray, M. Y., Birkland, T. P., Howe, J. D., Rowan, A. D., Fidock, M., Parks, W. C., & Gavrilovic, J. (2013). Macrophage migration and invasion is regulated by MMP10 expression. *PLoS ONE, 8*, e63555-e63555.

Murray, P. J., Allen, J. E., Biswas, S. K., Fisher, E. A., Gilroy, D. W., Goerdt, S., . . . Zhai, Y. (2014). Macrophage activation and polarization: nomenclature and experimental guidelines. *Immunity, 41*, 14-20.

Naba, A., Clauser, K. R., Ding, H., Whittaker, C. A., Carr, S. A., & Hynes, R. O. (2016). The extracellular matrix: Tools and insights for the "omics" era. *Matrix Biology, 49*, 10-24..

Nathan, C., & Ding, A. (2010). Nonresolving inflammation. *Cell, 140*, 871-882.

Newby, A. C. (2016). Metalloproteinase production from macrophages - a perfect storm leading to atherosclerotic plaque rupture and myocardial infarction. *Experimental Physiology, 101*, 1327-1337.

Noy, R., & Pollard, Jeffrey W. (2014). Tumor-associated macrophages: from mechanisms to therapy. *Immunity, 41*, 49-61.

Oakford, M. E., Dixon, S. V., August, S., Pickard, C., Ardern-Jones, M., Lackie, P., . . . Healy, E. (2011). Migration of Immunocytes across the Basement Membrane in Skin: The Role of Basement Membrane Pores. *The Journal of Investigative Dermatology, 131*, 1950-1953.

Ogura, M., Bridgeman, V. L., & Malanchi, I. (2017). Macrophages unlock progression of breast cancer cells experiencing matrigel-segregation in transplantation models. *Scientific Reports, 7*, 11028-11028.

Ota, I., Li, X.-Y., Hu, Y., & Weiss, S. J. (2009). Induction of a MT1-MMP and MT2-MMP-dependent basement membrane transmigration program in cancer cells by Snail1. *Proceedings of the National Academy of Sciences of the United States of America, 106*, 20318-20323.

Paul, C. D., Mistriotis, P., & Konstantopoulos, K. (2017). Cancer cell motility: Lessons from migration in confined spaces. *Nature Reviews Cancer, 17*, 131-140.

Pflicke, H., & Sixt, M. (2009). Preformed portals facilitate dendritic cell entry into afferent lymphatic vessels. *The Journal of Experimental Medicine, 206*, 2925-2935.

Previtera, M. L., & Sengupta, A. (2015). Substrate stiffness regulates proinflammatory mediator production through TLR4 activity in macrophages. *PLoS ONE, 10*, e0145813-e0145813.

Punturieri, A., Filippov, S., Allen, E., Caras, I., Murray, R., Reddy, V., & Weiss, S. J. (2000). Regulation of elastinolytic cysteine proteinase activity in normal and cathepsin K-deficient human macrophages. *The Journal of Experimental Medicine, 192*, 789-799.

Randles, M. J., Humphries, M. J., & Lennon, R. (2017). Proteomic definitions of basement membrane composition in health and disease. *Matrix Biology, 57*, 12-28.

Reddy, V. Y., Zhang, Q. Y., & Weiss, S. J. (1995). Pericellular mobilization of the tissue-destructive cysteine proteinases, cathepsins B, L, and S, by human monocyte-derived macrophages. *Proceedings of the National Academy of Sciences of the United States of America, 92*, 3849-3853.

Rowe, R. G., & Weiss, S. J. (2008). Breaching the basement membrane: who, when and how? *Trends in Cell Biology, 18*, 560-574.

Rowe, R. G., & Weiss, S. J. (2009). Navigating ECM barriers at the invasive front: the cancer cell-stroma interface. *Annual Review of Cell and Developmental Biology, 25*, 567-595.

Ruprecht, V., Wieser, S., Callan-Jones, A., Smutny, M., Morita, H., Sako, K., . . . Heisenberg, C.-P. (2015). Cortical contractility triggers a stochastic switch to fast amoeboid cell motility. *Cell, 160*, 673-685.

Sabeh, F., Li, X.-Y., Saunders, T. L., Rowe, R. G., & Weiss, S. J. (2009). Secreted versus membrane-anchored collagenases: relative roles in fibroblast-dependent collagenolysis and invasion. *The Journal of Biological Chemistry, 284*, 23001-23011.

Sabeh, F., Ota, I., Holmbeck, K., Birkedal-Hansen, H., Soloway, P., Balbin, M., . . . Weiss, S. J. (2004). Tumor cell traffic through the extracellular matrix is controlled by the membrane-anchored collagenase MT1-MMP. *The Journal of Cell Biology, 167*, 769-781.

Sabeh, F., Shimizu-Hirota, R., & Weiss, S. J. (2009). Protease-dependent versus -independent cancer cell invasion programs: three-dimensional amoeboid movement revisited. *The Journal of Cell Biology, 185*, 11-19.

Sakurai-Yageta, M., Recchi, C., Le Dez, G., Sibarita, J.-B., Daviet, L., Camonis, J., . . . Chavrier, P. (2008). The interaction of IQGAP1 with the exocyst complex is required for tumor cell invasion downstream of Cdc42 and RhoA. *The Journal of Cell Biology, 181*, 985-998.

Seals, D. F., & Courtneidge, S. A. (2003). The ADAMs family of metalloproteases: Multidomain proteins with multiple functions. *Genes & Development, 17*, 7-30.

Seok, J., Warren, H. S., Cuenca, A. G., Mindrinos, M. N., Baker, H. V., Xu, W., . . . Host Response to Injury, L. S. C. R. P. L. S. C. R. P. (2013). Genomic responses in mouse models poorly mimic human inflammatory diseases. *Proceedings of the National Academy of Sciences of the United States of America, 110*, 3507-3512.

Sevenich, L., & Joyce, J. A. (2014). Pericellular proteolysis in cancer. *Genes & Development, 28*, 2331-2347.

Starnes, T. W., Bennin, D. A., Bing, X., Eickhoff, J. C., Grahf, D. C., Bellak, J. M., . . . Huttenlocher, A. (2014). The F-BAR protein PSTPIP1 controls extracellular matrix degradation and filopodia formation in macrophages. *Blood, 123*, 2703-2714.

Takahashi-Iwanaga, H., Iwanaga, T., & Isayama, H. (1999). Porosity of the epithelial basement membrane as an indicator of macrophage-enterocyte interaction in the intestinal mucosa. *Archives of Histology and Cytology, 62*, 471-481.

Takeuchi, T., & Gonda, T. (2004). Distribution of the pores of epithelial basement membrane in the rat small intestine. *Journal of Veterinary Medical Science, 66*, 695-700.

Talmi-Frank, D., Altboum, Z., Solomonov, I., Udi, Y., Jaitin, D. A., Klepfish, M., . . . Sagi, I. (2016). Extracellular matrix proteolysis by MT1-MMP contributes to influenza-related tissue damage and mortality. *Cell Host and Microbe, 20*, 458-470.

Thiam, H. R., Vargas, P., Carpi, N., Crespo, C. L., Raab, M., Terriac, E., . . . Piel, M. (2016). Perinuclear Arp2/3-driven actin polymerization enables nuclear deformation to facilitate cell migration through complex environments. *Nature Communications, 7*, 10997-10997.

Toner, P. G., Carr, K. E., Ferguson, A., & Mackay, C. (1970). Scanning and transmission electron microscopic studies of human intestinal mucosa. *Gut, 11*, 471-481.

Van Goethem, E., Poincloux, R., Gauffre, F., Maridonneau-Parini, I., & Le Cabec, V. (2010). Matrix architecture dictates three-dimensional migration modes of human macrophages: differential involvement of proteases and podosome-like structures. *Journal of immunology (Baltimore, Md.: 1950), 184*, 1049-1061.

Vérollet, C., Charrière, G. M., Labrousse, A., Cougoule, C., Le Cabec, V., & Maridonneau-Parini, I. (2011). Extracellular proteolysis in macrophage migration: losing grip for a breakthrough. *European Journal of Immunology, 41*, 2805-2813.

Werb, Z., Bainton, D. F., & Jones, P. A. (1980). Degradation of connective tissue matrices by macrophages. III. Morphological and biochemical studies on extracellular, pericellular, and intracellular events in matrix proteolysis by macrophages in culture. *The Journal of Experimental Medicine, 152*, 1537-1553.

Wiesner, C., El Azzouzi, K., Linder, S., Lütcke, A., Zerial, M., Simons, K., & Olkkonen, V. M. (2013). A specific subset of RabGTPases controls cell surface exposure of MT1-MMP, extracellular matrix degradation and three-dimensional invasion of macrophages. *Journal of Cell Science, 126*, 2820-2833.

Wiesner, C., Faix, J., Himmel, M., Bentzien, F., & Linder, S. (2010). KIF5B and KIF3A/KIF3B kinesins drive MT1-MMP surface exposure, CD44 shedding, and extracellular matrix degradation in primary macrophages. *Blood, 116*, 1559-1569.

Wiesner, C., Le-Cabec, V., El Azzouzi, K., Maridonneau-Parini, I., & Linder, S. (2014). Podosomes in space: Macrophage migration and matrix degradation in 2D and 3D settings. *Cell Adhesion & Migration, 8*, 179-191.

Willis, A. L., Sabeh, F., Li, X. Y., & Weiss, S. J. (2013). Extracellular matrix determinants and the regulation of cancer cell invasion stratagems. *Journal of Microscopy, 251*, 250-260.

Witz, C. A., Montoya-Rodriguez, I. A., Cho, S., Centonze, V. E., Bonewald, L. F., & Schenken, R. S. (2001). Composition of the extracellular matrix of the peritoneum. *Journal of the Society for Gynecologic Investigation, 8*, 299-304.

Wolf, K., Te Lindert, M., Krause, M., Alexander, S., Te Riet, J., Willis, A. L., . . . Friedl, P. (2013). Physical limits of cell migration: control by ECM space and nuclear deformation and tuning by proteolysis and traction force. *The Journal of Cell Biology, 201*, 1069-1084.

Wyckoff, J. B., Wang, Y., Lin, E. Y., Li, J.-f., Goswami, S., Stanley, E. R., . . . Condeelis, J. (2007). Direct visualization of macrophage-assisted tumor cell intravasation in mammary tumors. *Cancer Research, 67*, 2649-2656.

Wynn, T. A., Chawla, A., & Pollard, J. W. (2013). Macrophage biology in development, homeostasis and disease. *Nature, 496*, 445-455.

Wynn, T. A., & Vannella, K. M. (2016). Macrophages in tissue repair, regeneration, and fibrosis. *Immunity, 44*, 450-462.

Yurchenco, P. D., & Ruben, G. C. (1987). Basement membrane structure in situ: Evidence for lateral associations in the type IV collagen network. *Journal of Cell Biology, 105*, 2559-2568.

Chapter 3: MT1-MMP-Dependent Human Macrophage Transmigration Across Interstitial Matrix Barriers

Abstract

Macrophage migration across interstitial matrix barriers is an essential early step of the human immune response. Migration along and through 3-dimensional interstitial matrices is governed by matrix pore dimensions that are either large enough to traverse non-proteolytically, or alternatively, sufficiently small that the matrix must be remodeled to permit the passage of the cell's rigid nucleus. However, to date, interactions between stimulated macrophages and interstitial matrix barriers, and the proteolytic requirements engaged therein, have not been defined. Here, we characterize macrophage cell body and nuclear morphology during migration across acellular mesenteric tissue and type I collagen gels. We observe that independent of MMP catalytic activity, macrophages infiltrate the low-density mesenteric interstitial matrix and tightly associate with, and degrade, the elastin network. In a similar fashion, macrophages traverse and displace low-density type I collagen gels in the absence of MMP activity. In contrast, when confronting high-density type I collagen gels, macrophages mobilize MT1-MMP to proteolytically remodel restrictive collagen pores to generate "passageways" that are permissive for transiting the rigid nuclear body. By contrast, in the absence of MT1-MMP, macrophages mount a futile invasive program wherein the cell body, but not the nucleus,

traverse the collagen barrier. These data not only define human macrophage interactions with physiologically relevant interstitial matrix barriers, but also reveal a requirement of MT1-MMP for successful nuclear body migration across restrictive type I collagen matrices.

Introduction

In mediating host-wide immune responses, macrophages mobilize an array of proteolytic enzymes to remodel and traverse tissues that display a diverse composition of interstitial matrix macromolecules (Eming et al., 2017; Lin et al., 2001; Murray et al., 2013; Ojalvo et al., 2009; Wynn and Vannella, 2016). Although the interstitial matrix is commonly dominated by networks of interwoven elastin and type I collagen, as well as dozens of glycoproteins, proteoglycans, and glycosaminoglycans, the relative proportion of these components can vary greatly between tissues, e.g. the dense matrix of type I collagen in the cornea, as opposed to the elastin-rich aorta and the disorganized matrix surrounding carcinomas (Benedek, 1971; Hynes, 2009; Meek and Knupp, 2015; Mouw et al., 2014; Overall and Blobel, 2007; Perumal et al., 2008). Regardless of tissue composition, cell transit is restricted by matrix pore size relative to the size and rigidity of the nucleus, the least deformable organelle in the cell body (Dahl, 2004; Davidson et al., 2014; Gerlitz and Bustin, 2011; Wolf et al., 2013). As such, in order to traverse matrix pores whose dimensions are smaller than that of the nucleus, cells must mobilize proteolytic enzymes and exert mechanical force to create physically negotiable passageways (Rowe and Weiss, 2008, 2009; Sabeh et al., 2009a; Wolf et al., 2013). By contrast, when the pore size exceeds that of the nucleus, proteolysis is no longer necessary to transmigrate tissue barriers (Sabeh et al., 2009a; Wolf et al., 2013). Although various macrophage-extracellular matrix interactions have been described, the impact of interstitial matrix remodeling on macrophage nuclear and cellular shape as well as invasion has not been previously characterized.

Efforts to characterize macrophage-interstitial matrix interactions have been largely restricted to substrates lacking the covalent cross-links that distinguish native ECM barriers *in vivo* (Demou et al., 2005; Sabeh et al., 2009a; Wiesner et al., 2014). Hence, despite the fact that stimulated macrophages can upregulate MT1-MMP expression, the contribution of the proteinase to type I collagen invasive activity and associated changes in nuclear shape remain undefined. To this end, we have characterized the nuclear and cytoskeletal organization of primary human macrophages as they traverse native mesenteric tissue as well as type I collagen gels of varying densities that retain their *in vivo* crosslinks. Here, we define a key role for macrophage MT1-MMP in supporting matrix transmigration across size-restrictive collagen barriers by generating ECM "tunnels" whose diameter can accommodate the rigid cell nucleus.

Results

Human macrophage morphology in the 3D interstitial matrix

The acellular mesenteric interstitial matrix is characterized by a ~50 μm thick 3-dimensional (3D) web-like network of ECM macromolecules (Figure 3.1A). Merged confocal image stacks through the entire interstitium reveal gaps between intertwining elastin and collagen I fibers upwards of 20 μm in diameter (Figure 3.1B). Earlier reports have demonstrated that fibroblasts or tumor cells embedded in dense 3D matrices in the presence of MMP inhibitors display a compacted, "rounded" morphology as a consequence of an inability to remodel the pericellular ECM and spread (Sabeh et al., 2009a; Wolf et al., 2013). However, 3D reconstructions of primary human macrophages that have crossed into the interstitium reveal no defects in overall cell morphology or nuclear shape in the presence of the pan-MMP inhibitor, BB-94 (Figure 3.1C-D), a finding consistent with the fact that cells infiltrating a large pore matrix whose diameter exceeds that of the nucleus need not proteolyze the surrounding matrix to establish an optimal cell shape (Wolf et al., 2013).

Human macrophage-elastin interactions

Upon infiltrating the mesentery, human macrophages are found in association with elastin fibrils (Figure 2.7C). Confocal immunofluorescence images reveal a highly fragmented elastin network (Figure 3.2A), wherein the ends of broken elastin fibers are found in association with adherent macrophages (Figure 3.2B). By reconstructing confocal images through the tissue, orthogonal views demonstrate that these broken elastin ends are engulfed by macrophage protrusions, consistent with proteolytic

remodeling (Figure 3.2C, arrowheads). While earlier studies have suggested that MMPs can participate in elastin remodeling, macrophages cultured in the presence of the blocking MT1-MMP antibody, DX-2400, continue to fragment the underlying elastin fiber network (Mecham et al., 1997; Xiong et al., 2009). (Figure 3.2D-F). Alternatively, members of the cysteine proteinase family, particularly cathepsins L and S, have been implicated in macrophage-mediated degradation of isolated elastin fibers (Punturieri et al., 2000; Reddy et al., 1995), but further work is required to verify their activity in our more physiologic tissue model.

Macrophages traverse increasingly dense type I collagen gels

While the *ex vivo* mesentery is characterized by a low-density type I collagen network, type I collagen in other tissues can reach significantly higher densities that potentially necessitate the mobilization of macrophage MT1-MMP (Wolf et al., 2013). In order to begin characterizing the effects of collagen density on macrophage infiltration, an easily manipulatable *in vitro* type I collagen model was adopted wherein 3D type I collagen hydrogels of varying density are assembled that contain physiologic levels of Schiff base covalent crosslinks (Sabeh et al., 2009b). To first test the barrier function of collagen gels that resemble low-density interstitial matrix, type I collagen gels (1.1 mg/ml) were fluorescently-labeled (red) and cultured in the presence of LPS-polarized human macrophages (green) for 6 days (Figure 3.3). At the end of this culture period, low-magnification confocal images of the collagen gels reveal that macrophages have displaced large areas of collagen that appear as dark “holes”, a finding that is usually defined as collagen “degradation” given the apparent disappearance of labelled collagen (Cougoule et al., 2012; Van Goethem et al., 2010) (Figure 3.3A). However, as shown by

high magnification, maximum intensity projections and orthogonal reconstructions, LPS-polarized macrophages transmigrate the thin collagen gel and adhere to the underlying glass surface (Figure 3.3B). Interestingly, however, macrophages that have adhered to the glass surface are not surrounded by areas of degraded collagen, but instead remain "draped" by the collagen gel, a finding consistent with collagen displacement rather than matrix degradation. Indeed, similar, if not identical, results are seen in the presence of BB-94 (Figure 3.3C-D). In a fashion similar to that observed when macrophages invade the mesenteric interstitium, equivalent cell morphology and nuclear shape suggest that proteolytic activity is not required during macrophage invasion across low density collagen I barriers.

In vivo tissues are often modeled with higher density collagen gels with matrix pore sizes (1-2 μm diameter) that restrict cell transit (Wolf et al., 2013). As such, LPS-stimulated macrophages were next cultured for 6 days atop collagen gels whose density was increased 2-fold (i.e. from 1.1 to 2.2 mg/ml with a pore size of ~2 μm). At the end of the 6-day culture period, confocal images reveal the surface of the collagen gel is decorated with macrophages in proximity to, but not adjoining, small ~4.5 μm diameter pores (Figure 3.4A arrowheads). Remarkably, with orthogonal reconstruction, we observe pores that have widened into large, ~40 μm diameter "caverns" enveloping macrophages that potentially formed the pore as a conduit to traverse the collagen gel (Figure 3.4A). To next determine the relative contribution of collagen proteolysis to this process, LPS-polarized macrophages were cultured in the presence of BB-94. In contrast to control macrophages, however, high magnification images of the surface of the collagen gel reveal that MMP-inhibited macrophages generate significantly smaller pores at the gel

surface (~1.5 μm diameter) despite retaining the ability to displace large zones of collagen, ~40 μm in diameter, from the glass surface (Figure 3.4C, arrowheads). Strikingly, following DAPI imaging, we find that the nuclei of MMP-inhibited macrophages are unable to follow the cell body and its associated cytoplasm to the glass interface, and are instead trapped at the surface of the collagen gel juxtaposed above the smaller pores generated within the underlying collagen gel (Figure 3.4C, orthogonal view). Furthermore, in the presence of BB-94, nuclei juxtaposing smaller pores are markedly deformed (Figure 3.4C).

MT1-MMP is required for nuclei to traverse dense collagen gels

Given that MT1-MMP is highly expressed in LPS-stimulated macrophages (Figure 2.6) and is a powerful type I collagenase (Rowe and Weiss, 2009; Sabeh et al., 2009a), macrophages were next cultured atop the high-density collagen gels in the presence of the MT1-MMP blocking antibody, DX-2400. As shown, in a fashion similar to that observed with macrophages cultured in the presence of BB-94, high-magnification confocal images of MT1-MMP-inhibited macrophages reveal nuclei trapped at the collagen surface in association with ~1.5 μm diameter pores (Figure 3.5A). Indeed, quantification of pore diameter in the presence of BB-94 or MT1-MMP blocking antibody reveal a significant decrease in average pore size relative to control (3.2 ± 0.4 μm vs 1.5 ± 0.14 μm) (Figure 3.5B). In addition, the presence of MMP inhibitors increased the number of nuclei unable to accompany the cell body across high-density type I collagen gels to the glass interface from 0% to ~20% (Figure 3.5C). Remarkably, on rare occasion, MMP-inhibited macrophages with obstructed nuclei were observed transiting type I collagen pores by markedly distorting the nuclear body (Figure 3.6A,B). 3D

reconstructions reveal dumbbell-shape nuclear distortions that appear as the nucleus is forced through the narrow collagen pore, illustrating the limited ability of macrophages to traverse size-restrictive matrix (Figure 3.6B,D). Together, these data demonstrate that MT1-MMP is required for successful macrophage transmigration of pore size-restrictive type I collagen barriers.

Discussion

Macrophages infiltrate a wide range of interstitial matrix barriers to mount effective immune responses (Mouw et al., 2014; Noy and Pollard, 2014; Wynn and Vannella, 2016). While movement through host tissues by other cell types is affected by matrix porosity relative to the deformability of the nucleus and protease expression (Wolf et al., 2013), the importance of these factors in regulating macrophage invasion have not been previously defined. Evidence from *in vitro* studies support a model wherein macrophages degrade and invade collagen-rich barriers by mobilizing the membrane anchored matrix metalloprotease, MT1-MMP (Matías-Román et al., 2005; Wiesner et al., 2014). However, insights into macrophage-interstitial matrix interactions have been limited by reliance on non-physiologic ECM models that largely rely on the use of tissue barriers with limited physiological relevance (Cougoule et al., 2012; Jevnikar et al., 2012; Van Goethem et al., 2011). For example, 3D models of invasion frequently employ Matrigel, a mouse carcinoma basement membrane extract largely composed of a non-covalently cross-linked composite of type IV collagen and laminin that neither recapitulates the mechanical properties of authentic basement membranes nor models the structural characteristics of the interstitial matrix (Halfter et al., 2013; Kleinman and Martin, 2005; Rowe and Weiss, 2009; Sodek et al., 2008). Alternative substrates, such as purified type I collagen, can be readily engineered to form low- and high-density gels as a simple model of the interstitial matrix variances encountered *in vivo* (Sabeh et al., 2009a; Wolf et al., 2013). However, this model has its own pitfalls, as only hydrogels constructed from acid-extracted collagen can re-assemble the covalent Schiff base crosslinks that define type I collagen-rich tissues (Demou et al., 2005; Sabeh et al., 2009a). By contrast, pepsin-extracted type I

collagen, a commonly used commercial product, forms non-covalent crosslinked hydrogels whose mechanical properties are distinct from native type I collagen barriers (Demou et al., 2005; Sabeh et al., 2009a). Given these limitations, we adopted both a native mesentery tissue model and covalently crosslinked low- and high-density acid-extracted collagen gels to evaluate macrophage-interstitial matrix interactions.

Current evidence suggests that fibroblast and cancer cell populations alter overall cell body and nuclear shape in response to changes in the architecture and pore size of the ECM (Rowe and Weiss, 2009; Sabeh et al., 2009a; Wolf et al., 2013). When confronted with pore sizes that exceed the dimensions of the nucleus, migrating cells traverse interstitial tissues by "simply" altering cell shape (Hung et al., 2013; Wolf et al., 2013). However, if the pore size of the matrix is significantly less than that of nuclear dimensions, migrating cells must either deform their nuclear shape or mobilize proteolytic enzymes to enlarge matrix pores (Thiam et al., 2016; Wolf et al., 2013). Consequently, in the absence of proteolytic activity, most cell types will display marked changes in nuclear shape as they confront diminishing pore sizes until such time that motile responses come to a halt when nuclear deformation reaches a limit that undermines nuclear integrity. In delineating the tissue-invasive potential of macrophages, we find that these cells do not require proteases, including MT1-MMP, to traverse the peritoneal interstitial matrix. Presumably, the loose weave existing between the elastin and collagen networks allows macrophages to negotiate this tissue without mobilizing proteolytic activity or perturbing nuclear shape to a significant degree. Interestingly, this tissue afforded us a remarkably high-resolution model of native elastin networks where we find that macrophages were not randomly arrayed within the interstitium, but instead were closely associated with the

underlying network of elastin fibrils. Of note, macrophages infiltrating inflamed adipose tissues were recently reported to similarly adhere to the elastin network, suggesting macrophage-elastin interactions may be a general paradigm of macrophage trafficking through interstitial tissues (Martinez-Santibanez et al., 2015). To our surprise, we also observed that macrophage-associated elastin fibrils were frequently fragmented within macrophage protrusions (Figure 3.2). As elastin networks were disrupted in the absence or presence of MT1-MMP, alternate proteolytic systems, such as cysteine proteinases (Punturieri et al., 2000; Reddy et al., 1995), are likely at play in the mesentery. The identity of these MMP-independent proteolytic systems remains to be determined as well as their potential role in supporting tissue invasion.

The ability of macrophages to negotiate low-density mesenteric interstitial matrix independent of MT1-MMP and without affecting cell or nuclear shape was similarly observed with human macrophages cultured on low-density type I collagen gels. Indeed, at this density, macrophages likewise displayed no MMP requirement in order to traverse the gel and undermine large areas of collagen from the glass surface. Interestingly, rather than mediate the bulk degradation of the collagen gel in fashion similar to fibroblasts and cancer cells (Hotary et al., 2000; Sabeh et al., 2004), macrophages penetrated the matrix and displaced the surrounding matrix upward, leaving the cell enveloped in a collagen "blanket". Similarly, macrophages traversed high-density gels and form "cleared" collagen zones as they displaced the surrounding collagen hydrogel upwards. However, under these conditions, macrophages generate distinct "tunnels" in the collagen matrix as they transmigrate the gel. In the presence of MMP inhibitors or an MT1-MMP-specific blocking antibody, collagen was again "cleared" or "lifted" from the glass surface, while the

diameter of the collagen tunnels decreased three-fold. Under these conditions, the macrophage nucleus was unable to track with the advancing cell body. Taken together, these data indicate that macrophages require MT1-MMP to enlarge collagen passageways to a degree that accommodates the cell nucleus, in stark contrast to bulk ECM degradation mediated by fibroblasts or cancer cells (Hotary et al., 2000; Sabeh et al., 2004). In the absence of MT1-MMP activity, the macrophage nucleus is trapped above the restrictive collagen pore, where the trailing nucleus likely encounters significant cytoskeletal forces that distort, and potentially rupture, the nuclear body (Denais et al., 2016; Raab et al., 2016). Indeed, in our MT1-MMP inhibited macrophage cultures, nuclear distortions ranged from a single bleb to an elongated “dumbbell” shape.

We find that while macrophages traverse low-density tissue in the absence of proteolytic activity, in order to traverse the restrictive pore size of high-density type I collagen, macrophages must mobilize MT1-MMP. However, in contrast to tumor cells that mount a bulk ECM remodeling program as they invade, macrophages only generate passageways through the collagen gel that are a fraction of the size of a single cell. Instead, and in accordance with recent investigations of cell migration across restrictive barriers (Wolf et al., 2013), the nominal expansion of collagen pores by macrophage-MT1-MMP appears to be the minimum necessary for macrophage-nuclear transit. Together, these data demonstrate that macrophages mobilize MT1-MMP to generate traversable passageways through the pore size-restrictive type I collagen barriers that they confront during macrophage immune responses.

Materials and Methods

Isolation of primary macrophages

Human peripheral blood monocytes (PBMCs) were isolated from whole blood of volunteers in accordance with institutional review board (IRB) approval and the patient's informed consent. PBMCs were separated in Lymphocyte Separation Medium (Corning) by density centrifugation, purified by CD14 selection (Miltenyi Biotec), and cultured at 2 x 10^6 in 6-well plates containing RPMI 1640 without serum. After 2 h, media was replaced with RPMI 1640 with 1% penicillin-streptomycin solution and 20% autologous serum for 5-7 days. Autologous serum was prepared by incubating non-heparinized whole blood at 37 °C for 1 h followed by centrifugation at 2,850 x g for 15 minutes, and sterile filtration of the serum fraction.

Ex vivo mesentery ECM preparation

Mesentery tissue were prepared as previously described (Witz et al., 2001; Hotary et al., 2006). Briefly, rat mesentery was mounted on 6.5-mm diameter Transwells (Sigma) with sterile surgical thread and decellularized with 0.1 N ammonium hydroxide. 1 x 10^5 human macrophages were cultured atop the tissue for six days with media changes every 48 hours. All experiments were performed in complete medium supplemented with 1 µg/mL LPS from *Escherichia coli* O111:B4 (Sigma) and in the absence or presence of 5 µM BB-94 (Tocris Bioscience). Human macrophages were also cultured with 75 µg/mL human isotype control IgG antibody or anti-MT1-MMP antibody DX-2400 (Ager et al., 2015) in medium with 20% heat-inactivated autologous human serum and 1% penicillin-streptomycin in the presence of 5 µL F_c-receptor blocking antibody TruStain FcX

(Biolegend). DX-2400 was provided by the Kadmon Corporation. After six days of culture, tissue constructs were washed with PBS, fixed with 4% PFA, and stained as described.

Collagen gel culture conditions

Neutralized solutions of acid-extracted rat-tail type I collagen were labeled with Alexa Fluor-594 (Invitrogen, Carlsbad, CA) and deposited on 4-well Lab-Tek II chambered glass slides (Thermo Fisher) at 1.1 or 2.2 mg/ml final concentration for low- or high-density gels, respectively. Mature macrophages were cultured atop labeled gels for 6 days in the presence of LPS and in the absence or presence of BB-94 or DX-2400 before PFA fixation and counter-staining as described.

Confocal fluorescence microscopy and analysis

PFA-fixed mesentery tissues were incubated with polyclonal antibodies targeting elastin (EMD Millipore cat #: 2039), at 1:150 dilution in a blocking solution of 1% bovine serum albumin-PBS for 1 h at room temperature then incubated with secondary fluorescent antibodies at 1:250 dilution. Macrophages cultured with mesentery or purified collagen were labeled with Alexa Fluor 488 phalloidin and DAPI (Sigma) for 1 h in blocking solution. Image acquisition was performed using a spinning disc confocal CSU-WI (Yokogawa) on a Nikon Eclipse TI inverted microscope with a 60x oil-immersion objective and the Micro-Manager software (Open Imaging). Fluorescent images were processed with ImageJ (National Institutes of Health) with 3D viewer plugin for orthogonal and 3D reconstructions. Confocal imaging of the mesenteric collagen I network was captured by second harmonic generation on a Leica SP5 inverted confocal microscope with a 60x oil-immersion objective.

Statistical Analysis

The area of collagen clearing from glass surfaces was calculated using ImageJ as follows; image intensity was enhanced and background subtracted using default settings, the images converted to black and white via binary function, inverted, and particles larger than a 1 μm^2 minimum cut off analyzed. The diameter of collagen surface pores was calculated with the line tool and ROI manager and graphed with GraphPad Prism. Nuclei were categorized based on localizing to the collagen surface or glass surface. Nuclei localized to the collagen surface but with the cytoskeleton spread on the glass surface were additionally counted as “Glass w/out nucleus” and graphed accordingly. Pore diameters are expressed as a box-and-whisker plot with mean ± SEM and comparisons were made with one-way ANOVA.

Notes

A version of Chapter 3 is under preparation for submission as a manuscript titled “MT1-MMP-Dependent Human Macrophage Transmigration Across Interstitial Matrix Barriers” by the following authors: Julian C. Bahr, Xiao-Yan Li, and Stephen J. Weiss.

Figure 3.1

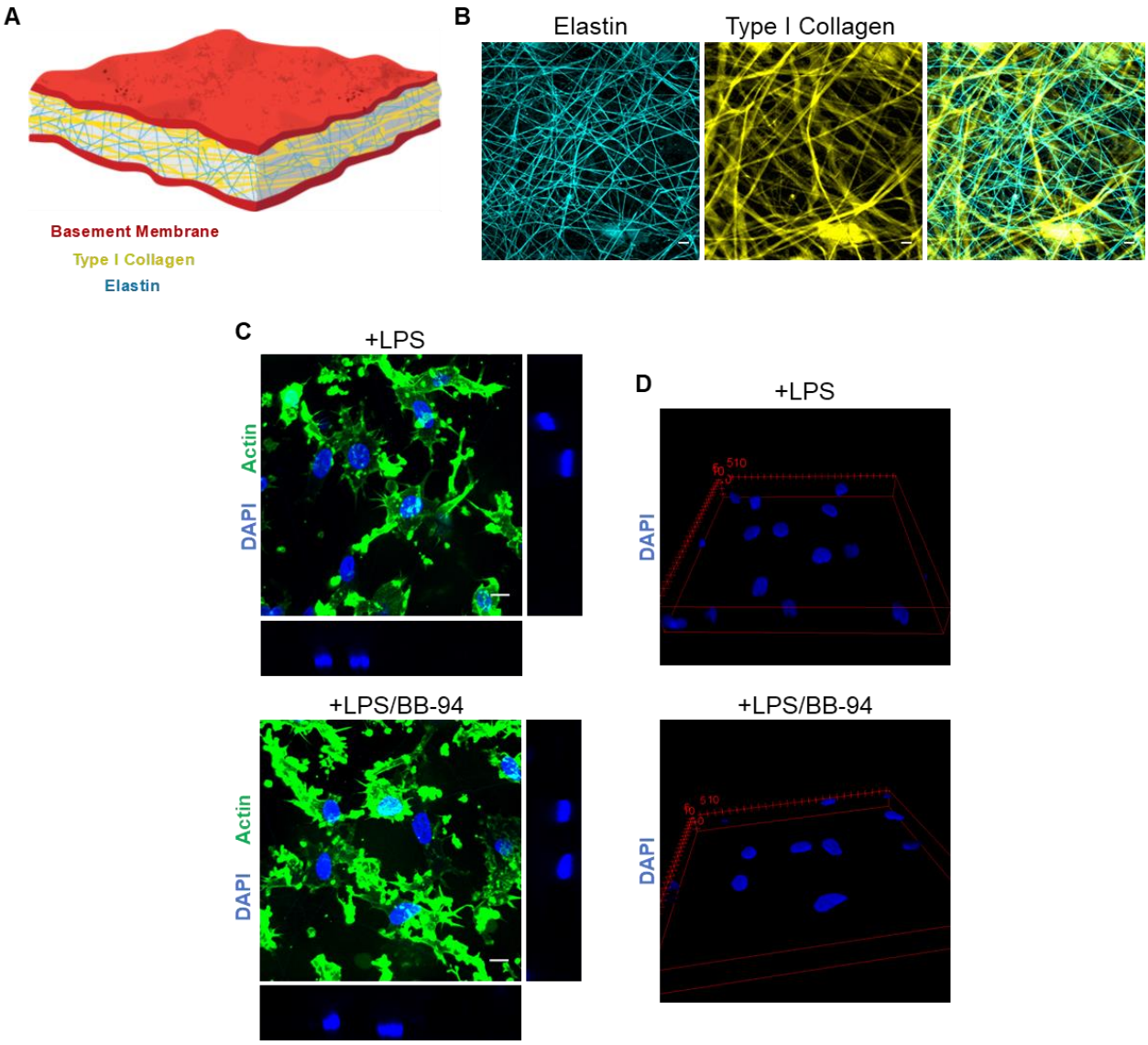

Figure 3.1 Polarized human macrophage morphology in native interstitial matrix
(A) Schematic illustration of the mesentery extracellular matrix. **(B)** 3D confocal reconstructions of elastin (blue, left panel), second harmonic generation of type I collagen (yellow, middle panel), and both in combination (right panel) in rat mesentery constructs. **(C)** Maximum intensity projection of human macrophages polarized with LPS (1 µg/mL) and in the absence or presence of a pan-matrix metalloproteinase inhibitor (5 µM BB-94). **(D)** 3D confocal reconstructions of interstitium-localized nuclei from human macrophages polarized with LPS (1 µg/mL) and in the absence or presence of a pan-matrix metalloproteinase inhibitor (5 µM BB-94). Images shown in (B-D) are representative of three replicates. Scale bars: 20 µm (B,); 10 µm (D).

Figure 3.2

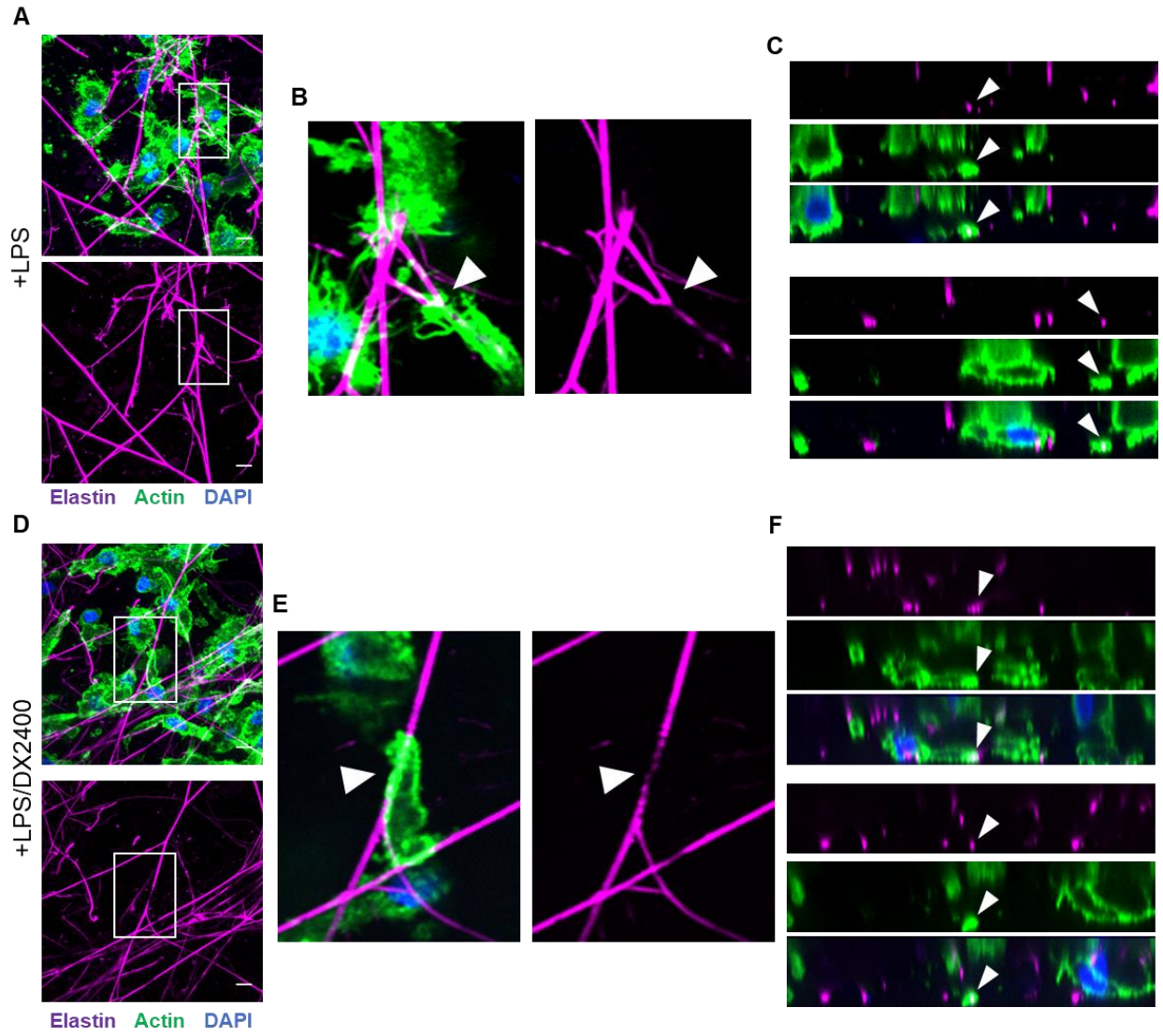

Figure 3.2 Polarized human macrophage remodeling of native elastin matrix
(A, D) Confocal immunofluorescence of human macrophages polarized with LPS (1 µg/mL) and in the absence or presence of the MT1-MMP blocking antibody DX-2400 (75 µg/mL), interacting with the native mesentery elastin network. **(B, E)** Magnified area (Boxes from panel A and D, respectively) of macrophage extensions overlapping with disrupted elastin strands (arrowheads). **(C, F)** xz and yz orthogonal reconstructions of panel (A, D) revealing that macrophages completely engulf broken elastin strands (arrowheads). Images shown are representative of three replicates. Scale bars: 10 µm.

Figure 3.3

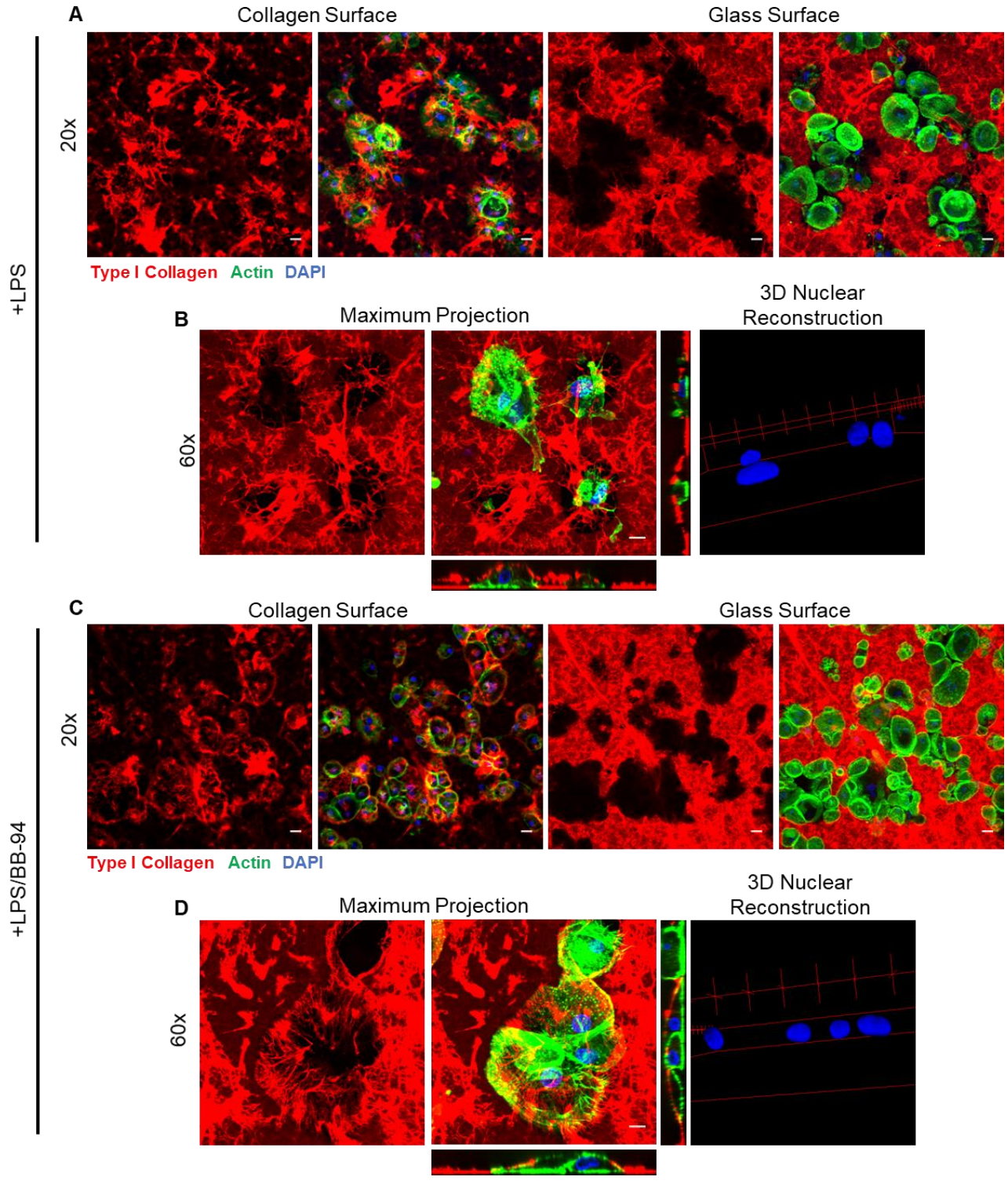
A
Collagen Surface
Glass Surface
20x
+LPS
Type I Collagen Actin DAPI
B
Maximum Projection
3D Nuclear Reconstruction
60x
C
Collagen Surface
Glass Surface
20x
+LPS/BB-94
Type I Collagen Actin DAPI
D
Maximum Projection
3D Nuclear Reconstruction
60x

Figure 3.3 MMPs are dispensable for macrophage infiltration of low-density collagen gels

(A, C) Low-magnification confocal immunofluorescence of human macrophages polarized with LPS (1 µg/mL) and in the absence or presence of a pan-matrix metalloproteinase inhibitor (5 µM BB-94) at the collagen surface (left panels) or at the glass surface (right panels) of 1.1 mg/mL type I collagen gels. **(B, D)** High-magnification maximum intensity projections, orthogonal views, and 3D nuclear reconstructions of human macrophages polarized with LPS (1 µg/mL) and in the absence or presence of a pan-matrix metalloproteinase inhibitor (5 µM BB-94). Images shown are representative of three replicates. Scale bars: (A, C) 20 µm, (B, D) 10 µm.

Figure 3.4

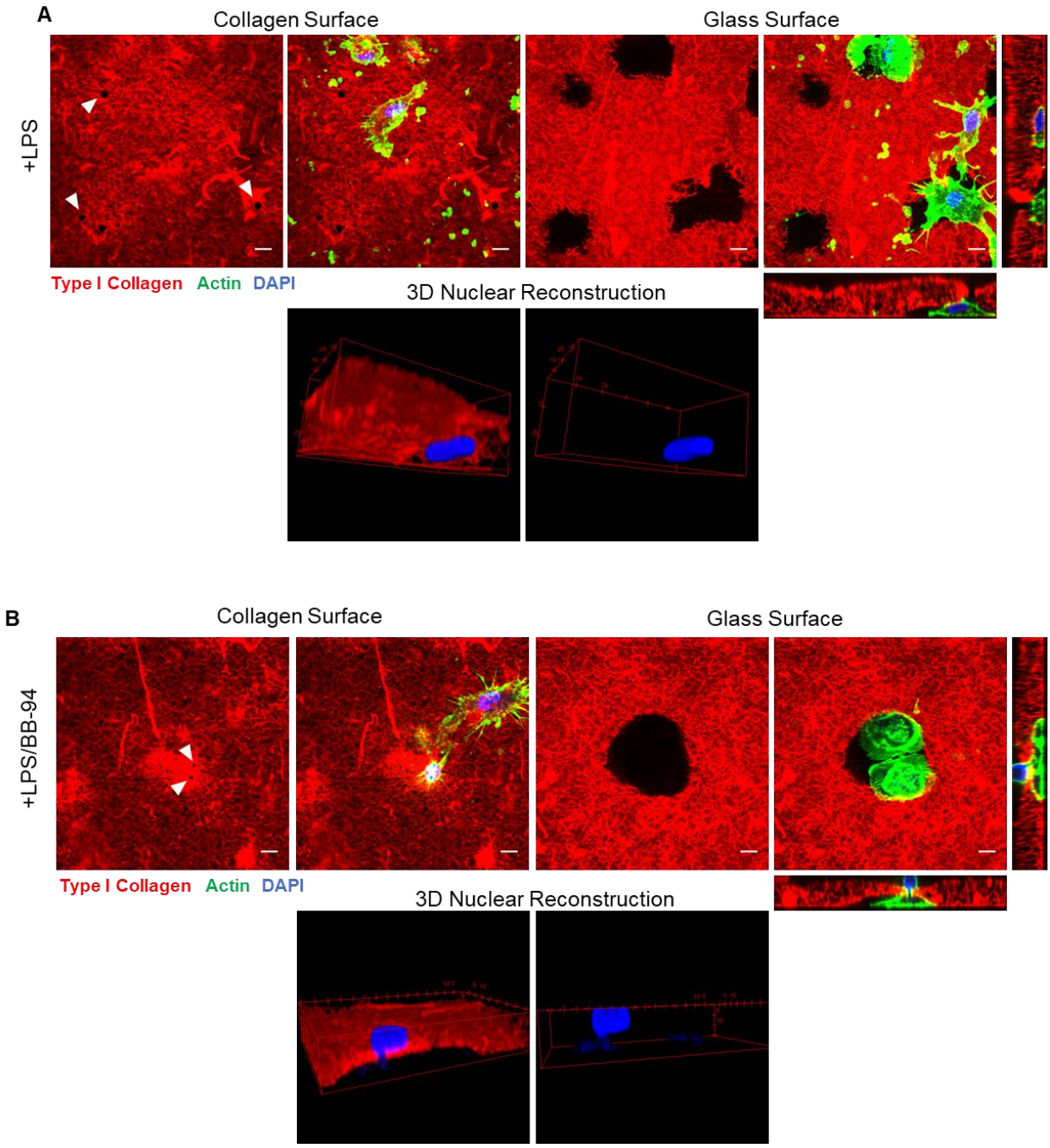

Figure 3.4 Human macrophage infiltration of high-density collagen gels
(A, B) High-magnification confocal immunofluorescence of human macrophages polarized with LPS (1 µg/mL) and in the absence or presence of a pan-matrix metalloproteinase inhibitor (5 µM BB-94) at the collagen surface (left panels) or at the glass surface (right panels) of 2.2 mg/mL type I collagen gels. Pores in the surface are marked with arrowheads. Confocal stacks of the nuclei were isolated and reconstructed

in 3D (lower panels). Images shown are representative of three replicates. Scale bars: (A, B) 10 µm.

Figure 3.5

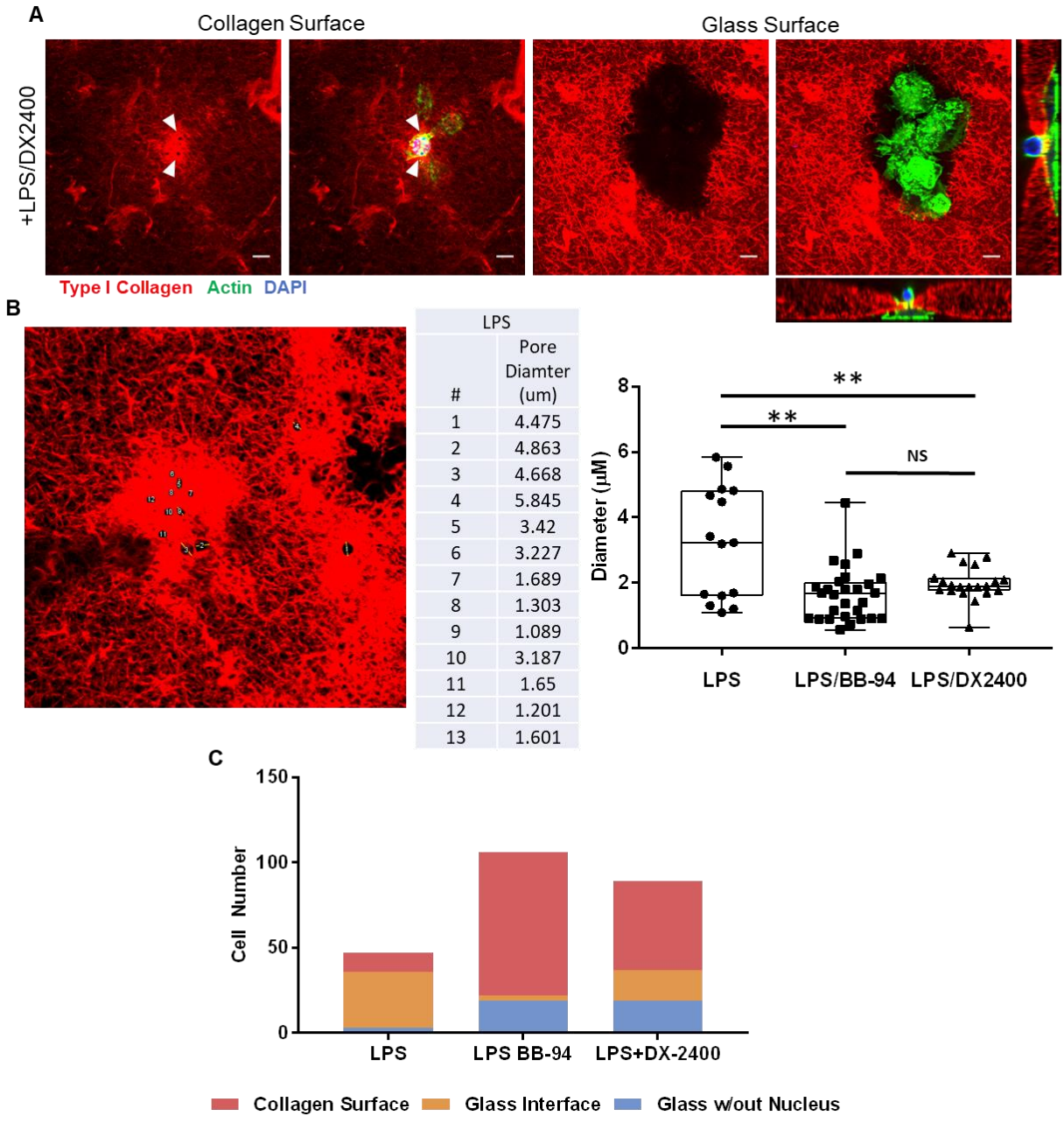

Figure 3.5 MT1-MMP-dependent transit of macrophage nuclei across high-density collagen gels

(A) High-magnification confocal immunofluorescence of human macrophages polarized with LPS (1 µg/mL) and in the presence of 75 µg/mL of MT1-MMP blocking antibody, DX-2400, at the collagen surface (left panels) or at the glass surface (right panels) of 2.2 mg/mL type I collagen gels. Pores in the surface are marked with arrowheads. **(B)** Quantification of collagen pore diameters in each condition (from Figure 3.4, 3.5) as analyzed by the ImageJ line tool and ROI manager. Results are expressed as box-and-

whisker plots with every measurement shown. **(C)** Quantification of the number of cell bodies localizing to the collagen surface, glass surface, and glass surface with nucleus trapped atop the collagen surface. (**) $P < .001$; ns, not significant; $n = 3$ biological replicates, >10 random fields/replicate. Images shown in (A) are representative of three replicates. Scale bars: (A)10 µm.

Figure 3.6

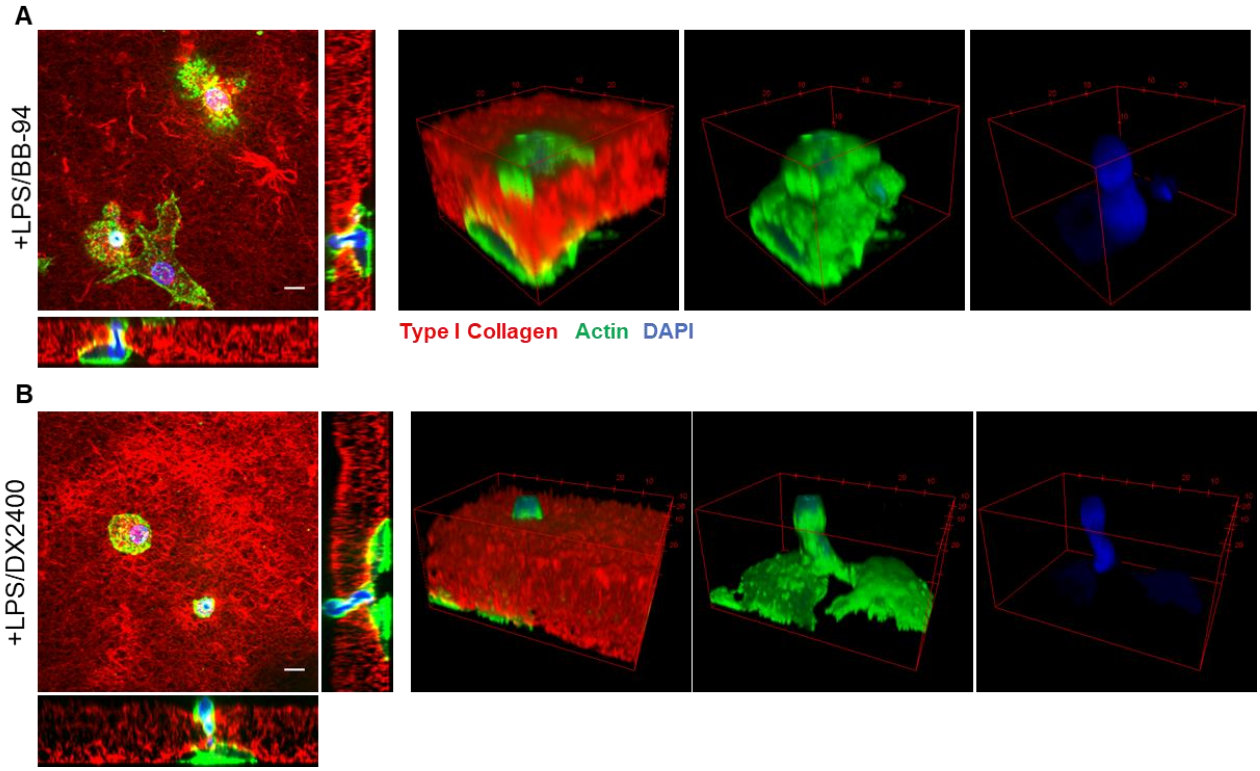

Figure 3.6 Nuclear deformation in high-density collagen gels
(A, B) *En face*, orthogonal, and 3D reconstructed high-magnification confocal immunofluorescence of human macrophages polarized with LPS (1 µg/mL) and in the presence of a pan-matrix metalloproteinase inhibitor (5 µM BB-94) or 75 µg/mL of MT1-MMP blocking antibody, DX-2400, on 2.2 mg/mL type I collagen gels. Images shown (A, B) are representative of three replicates. Scale bars: (A, B) 10 µm.

References

Ager, E. I., Kozin, S. V, Kirkpatrick, N. D., Seano, G., Kodack, D. P., Askoxylakis, V., … Jain, R. K. (2015). Blockade of MMP14 activity in murine breast carcinomas: Implications for macrophages, vessels, and radiotherapy. *Journal of the National Cancer Institute*, *107*(4).

Benedek, G. B. (1971). Theory of Transparency of the Eye. *Applied Optics*, *10*(3), 459.

Cougoule, C., Van Goethem, E., Le Cabec, V., Lafouresse, F., Dupré, L., Mehraj, V., … Maridonneau-Parini, I. (2012). Blood leukocytes and macrophages of various phenotypes have distinct abilities to form podosomes and to migrate in 3D environments. *European Journal of Cell Biology*, *91*(11–12), 938–949.

Dahl, K. N. (2004). The nuclear envelope lamina network has elasticity and a compressibility limit suggestive of a molecular shock absorber. *Journal of Cell Science*, *117*(20), 4779–4786.

Davidson, P. M., Denais, C., Bakshi, M. C., & Lammerding, J. (2014). Nuclear deformability constitutes a rate-limiting step during cell migration in 3-D environments. *Cellular and Molecular Bioengineering*, *7*(3), 293–306.

Demou, Z. N., Awad, M., McKee, T., Perentes, J. Y., Wang, X., Munn, L. L., … Boucher, Y. (2005). Lack of Telopeptides in Fibrillar Collagen I Promotes the Invasion of a Metastatic Breast Tumor Cell Line. *Cancer Research*, *65*(13), 5674–5682.

Denais, C. M., Gilbert, R. M., Isermann, P., McGregor, A. L., Te Lindert, M., Weigelin, B., … Lammerding, J. (2016). Nuclear envelope rupture and repair during cancer cell migration. *Science*, *352*(6283), 353–358.

Eming, S. A., Wynn, T. A., & Martin, P. (2017). Inflammation and metabolism in tissue repair and regeneration. *Science*.

Gerlitz, G., & Bustin, M. (2011, January). The role of chromatin structure in cell migration. *Trends in Cell Biology*.

Halfter, W., Candiello, J., Hu, H., Zhang, P., Schreiber, E., & Balasubramani, M. (2013). Protein composition and biomechanical properties of in vivo-derived basement membranes. *Cell Adhesion & Migration*, *7*(1), 64–71.

Hotary, K., Allen, E., Punturieri, A., Yana, I., & Weiss, S. J. (2000). Regulation of cell invasion and morphogenesis in a three-dimensional type I collagen matrix by membrane-type matrix metalloproteinases 1, 2, and 3. *The Journal of Cell Biology*, *149*(6), 1309–1323.

Hung, W.-C., Chen, S.-H., Paul, C. D., Stroka, K. M., Lo, Y.-C., Yang, J. T., & Konstantopoulos, K. (2013). Distinct signaling mechanisms regulate migration in unconfined versus confined spaces. *The Journal of Cell Biology*, *202*(5), 807–824.

Hynes, R. O. (2009, November 27). The extracellular matrix: Not just pretty fibrils. *Science*.

Jevnikar, Z., Mirković, B., Fonović, U. P., Zidar, N., Švajger, U., Kos, J., … Kos, J. (2012). Three-dimensional invasion of macrophages is mediated by cysteine cathepsins in protrusive podosomes. *European Journal of Immunology*, *42*(12), 3429–3441.

Kleinman, H. K., & Martin, G. R. (2005). Matrigel: Basement membrane matrix with biological activity. *Seminars in Cancer Biology*, *15*, 378–386.

Lin, E. Y., Nguyen, A. V, Russell, R. G., & Pollard, J. W. (2001). Colony-stimulating factor 1 promotes progression of mammary tumors to malignancy. *The Journal of Experimental Medicine*, *193*(6), 727–740.

Martinez-Santibanez, G., Singer, K., Cho, K. W., DelProposto, J. L., Mergian, T., & Lumeng, C. N. (2015). Obesity-induced remodeling of the adipose tissue elastin network is independent of the metalloelastase MMP-12. *Adipocyte*, *4*(4), 264–272.

Matías-Román, S., Gálvez, B. G., Genís, L., Yáñez-Mó, M., De La Rosa, G., Sánchez-Mateos, P., … Arroyo, A. G. (2005). Membrane type 1-matrix metalloproteinase is involved in migration of human monocytes and is regulated through their interaction with fibronectin or endothelium. *Blood*, *105*(10), 3956–3964.

Mecham, R. P., Broekelmann, T. J., Fliszar ¶, C. J., Shapiro, S. D., Welgus, H. G., & Senior, R. M. (1997). *Elastin Degradation by Matrix Metalloproteinases CLEAVAGE SITE SPECIFICITY AND MECHANISMS OF ELASTOLYSIS**. Retrieved from http://www.jbc.org/

Meek, K. M., & Knupp, C. (2015, November 1). Corneal structure and transparency. *Progress in Retinal and Eye Research*. Pergamon.

Mouw, J. K., Ou, G., & Weaver, V. M. (2014). Extracellular matrix assembly: A multiscale deconstruction. *Nature Reviews Molecular Cell Biology*.

Murray, M. Y., Birkland, T. P., Howe, J. D., Rowan, A. D., Fidock, M., Parks, W. C., & Gavrilovic, J. (2013). Macrophage migration and invasion is regulated by MMP10 expression. *PloS One*, *8*(5), e63555.

Noy, R., & Pollard, J. W. (2014). Tumor-Associated Macrophages: From Mechanisms to Therapy. *Immunity*, *41*(1), 49–61.

Ojalvo, L. S., King, W., Cox, D., & Pollard, J. W. (2009). High-density gene expression analysis of tumor-associated macrophages from mouse mammary tumors. *The American Journal of Pathology*, *174*(3), 1048–1064.

Overall, C. M., & Blobel, C. P. (2007). In search of partners: Linking extracellular proteases to substrates. *Nature Reviews Molecular Cell Biology*.

Perumal, S., Antipova, O., & Orgel, J. P. R. O. (2008). Collagen fibril architecture, domain organization, and triple-helical conformation govern its proteolysis. *Proceedings of the National Academy of Sciences*, *105*(8), 2824–2829.

Punturieri, A., Filippov, S., Allen, E., Caras, I., Murray, R., Reddy, V., & Weiss, S. J. (2000). Regulation of elastinolytic cysteine proteinase activity in normal and

cathepsin K-deficient human macrophages. *The Journal of Experimental Medicine*, *192*(6), 789–799.

Raab, M., Gentili, M., De Belly, H., Thiam, H. R., Vargas, P., Jimenez, A. J., … Piel, M. (2016). ESCRT III repairs nuclear envelope ruptures during cell migration to limit DNA damage and cell death. *Science*, *352*(6283), 359–362.

Reddy, V. Y., Zhang, Q. Y., & Weiss, S. J. (1995). Pericellular mobilization of the tissue-destructive cysteine proteinases, cathepsins B, L, and S, by human monocyte-derived macrophages. *Proceedings of the National Academy of Sciences of the United States of America*, *92*(9), 3849–3853.

Rowe, R. G., & Weiss, S. J. (2008). Breaching the basement membrane: who, when and how? *Trends in Cell Biology*, *18*(11), 560–574.

Rowe, R. G., & Weiss, S. J. (2009). Navigating ECM barriers at the invasive front: the cancer cell-stroma interface. *Annual Review of Cell and Developmental Biology*, *25*(1), 567–595.

Sabeh, F., Ota, I., Holmbeck, K., Birkedal-Hansen, H., Soloway, P., Balbin, M., … Weiss, S. J. (2004). Tumor cell traffic through the extracellular matrix is controlled by the membrane-anchored collagenase MT1-MMP. *The Journal of Cell Biology*, *167*(4), 769–781.

Sabeh, F., Shimizu-Hirota, R., & Weiss, S. J. (2009a). Protease-dependent versus-independent cancer cell invasion programs: Three-dimensional amoeboid movement revisited. *Journal of Cell Biology*, *185*(1), 11–19.

Sabeh, F., Shimizu-Hirota, R., & Weiss, S. J. (2009b). Protease-dependent versus - independent cancer cell invasion programs: three-dimensional amoeboid movement revisited. *The Journal of Cell Biology*, *185*(1), 11–19.

Sodek, K. L., Brown, T. J., & Ringuette, M. J. (2008). Collagen I but not Matrigel matrices provide an MMP-dependent barrier to ovarian cancer cell penetration. *BMC Cancer*, *8*(1), 223.

Thiam, H. R., Vargas, P., Carpi, N., Crespo, C. L., Raab, M., Terriac, E., … Piel, M. (2016). Perinuclear Arp2/3-driven actin polymerization enables nuclear deformation to facilitate cell migration through complex environments. *Nature Communications*, *7*, 10997.

Van Goethem, E., Guiet, R., Balor, S., Charrière, G. M., Poincloux, R., Labrousse, A., … Le Cabec, V. (2011). Macrophage podosomes go 3D. *European Journal of Cell Biology*, *90*(2–3), 224–236.

Van Goethem, E., Poincloux, R., Gauffre, F., Maridonneau-Parini, I., & Le Cabec, V. (2010). Matrix architecture dictates three-dimensional migration modes of human macrophages: differential involvement of proteases and podosome-like structures. *Journal of Immunology (Baltimore, Md. : 1950)*, *184*(2), 1049–1061.

Wiesner, C., Le-Cabec, V., El Azzouzi, K., Maridonneau-Parini, I., & Linder, S. (2014). Podosomes in space: Macrophage migration and matrix degradation in 2D and 3D

settings. *Cell Adhesion and Migration*. Taylor & Francis.

Wolf, K., te Lindert, M., Krause, M., Alexander, S., te Riet, J., Willis, A. L., … Friedl, P. (2013). Physical limits of cell migration: Control by ECM space and nuclear deformation and tuning by proteolysis and traction force. *Journal of Cell Biology*, *201*(7), 1069–1084.

Wynn, T. A., & Vannella, K. M. Macrophages in Tissue Repair, Regeneration, and Fibrosis, 44 Immunity § (2016). Cell Press.

Xiong, W., Knispel, R., MacTaggart, J., Greiner, T. C., Weiss, S. J., & Baxter, B. T. (2009). Membrane-type 1 matrix metalloproteinase regulates macrophage-dependent elastolytic activity and aneurysm formation in vivo. *The Journal of Biological Chemistry*, *284*(3), 1765–1771.

Chapter 4: Discussion

Macrophages infiltrate and remodel the ECM that serve as cellular scaffolding templates in all multicellular animals with ramifications that range from the beneficial (wound repair) to the injurious (chronic inflammation and metastasis) (Lewis et al., 2016; Wynn et al., 2013; Wynn and Vannella, 2016). Despite the ~500-million-year co-existence of ECM and phagocytic immune cells, efforts to gain mechanistic insights into macrophage-ECM interactions have only been made possible with the recent advent of more sophisticated *in vitro, ex vivo,* and *in vivo* model systems (Buchmann, 2014; Fidler et al., 2017; Kadler et al., 1996; Wolf et al., 2013). Confounding efforts to define these molecular mechanisms is a growing appreciation for macrophage heterogeneity, illustrated by recent studies describing the gamut of macrophage ontogeny and subsequent responses to microenvironmental cues that determine macrophage-ECM interactions (Ginhoux and Guilliams, 2016; Murray et al., 2014; Wynn et al., 2013). Potential mechanisms gleaned from unbiased macrophage gene expression arrays reveal the potential for dozens of distinct proteolytic and non-proteolytic responses to stimuli (Afik et al., 2016; Murray et al., 2013; Ojalvo et al., 2009; Wiesner et al., 2014). Therefore, it has been necessary to adopt *in vitro* and *ex vivo* systems to model the spectrum of macrophage-ECM interactions that permit mechanistic analysis of tissue remodeling or transmigration programs. Nevertheless, studies using ECM constructs

have, often in contradiction with each other, proposed distinct requirements for multiple proteases in macrophage trafficking and remodeling of the ECM (Cougoule et al., 2012; Jevnikar et al., 2012; Starnes et al., 2014; Van Goethem et al., 2010; Wiesner et al., 2014). However, to date, the model systems employed in these studies largely fail to recapitulate the fundamental structural or mechanical properties of native ECM barriers (Halfter et al., 2015; Randles et al., 2017; Rowe and Weiss, 2008, 2009). Thus, macrophage-ECM interactions during homeostasis or disease have remained almost completely undefined.

Herein, we have characterized macrophage-ECM interactions with an *ex vivo* model of the basement membrane/interstitial matrix interface. With these physiologic constructs in hand, we provide the first demonstration of macrophage-dependent proteolytic remodeling of the basement membrane. Furthermore, we have extended these observations by defining the MT1-MMP-dependent and independent mechanisms that allow macrophages to transmigrate basement membrane barriers. Further characterization of macrophage migration across 3D type I collagen matrices demonstrate that macrophages are able to traverse low- and high-density constructs in a quantitatively equivalent fashion. However, upon blockade of MT1-MMP catalytic activity, macrophages are unable to expand conduits through high-density collagen matrix to a size that is permissive for transiting the rigid nuclear body. As such, the macrophage cell body, but not the nucleus, transmigrate the collagen barrier. Together, these data provide novel insights into the molecular mechanisms by which macrophages traffic and remodel basement membrane and interstitial matrix barriers.

Based on macrophage cultures on commercial substrates such as Matrigel or pepsin-extracted type I collagen, a wide range of cysteine, serine, and metalloproteinase family members have previously been proposed to play critical roles in macrophage migration and ECM remodeling (Cougoule et al., 2012; Fleetwood et al., 2014; Starnes et al., 2014; Van Goethem et al., 2010; Wiesner et al., 2014). However, we now demonstrate that MT1-MMP alone is the dominant protease mobilized by macrophages during basement membrane transmigration and that it actively participates in proteolyzing type IV collagen and laminin. While MT1-MMP can activate a number of downstream proteinases, including MMP-2, MMP-8 and MMP-13, each of these MMP family members are sensitive to inhibition by TIMP-1, an antiproteinase that proved incapable of blocking MT1-MMP-dependent degradation.

A conclusion that MT1-MMP is the key effector of basement membrane remodeling is based on the use of a model of decellularized ex vivo mesentery ECM that allows for the interrogation of autonomous macrophage behavior in real-time and three dimensions. Critically, the mesentery model retains type IV collagen covalent crosslinks that define basement membrane integrity *in vivo,* but are not recapitulated by *in vitro* basement membrane constructs such as Matrigel (McCall et al., 2014). We then applied a validated model of macrophage activation wherein primary mouse or human macrophages were cultured in the presence of polarizing molecules that resemble the initiation (LPS) or resolution (IL-4) of inflammation (Murray et al., 2014). Under these conditions. LPS-polarized macrophages degraded cross-linked basement membrane to a greater extent relative to unstimulated or IL-4 stimulated macrophages. Systematic inhibition of each cysteine, serine, and metalloprotease family (all proposed by *in vitro* studies to be

required for macrophage-mediated ECM remodeling (Akkari et al., 2014; Jevnikar et al., 2012; Murray et al., 2013; Newby, 2016; Vérollet et al., 2011)) demonstrated a singular requirement for metalloproteases. Only specific ablation of MT1-MMP activity abrogated macrophage-mediated basement membrane degradation. Consistent with these findings, MT1-MMP is highly expressed in mouse and human macrophages and localizes to actin-rich macrophage protrusions *in vitro* (El Azzouzi et al., 2016; Wiesner et al., 2013). Interestingly, while MMP-mediated basement membrane remodeling by carcinoma cells is a prerequisite for their invasion into the interstitial matrix (Hotary et al., 2006; Rowe and Weiss, 2008, 2009), MT1-MMP-inhibited macrophages retained 3D migratory behavior by alternatively utilizing a non-proteolytic mechanism to access small preformed portals in the basement membrane. These data are the first descriptions of a unique hybrid ability utilized by macrophages to alternatively degrade the basement membrane during transmigration or non-proteolytically invading this barrier by transmigrating preformed passageways.

Following the degradation of the basement membrane, macrophages subsequently establish contact with the interstitial matrix where they are confronted with interlacing networks of type I collagen and elastin. In this regard, human tissues reveal remarkable variability in the relative density of interstitial matrix components (Cuddapah et al., 2014; Kadler et al., 1996; Randles et al., 2017; Rozario and DeSimone, 2010; Sherratt, 2009; Ushiki, 2002; Wolf et al., 2013). To dissect the molecular mechanisms involved in cell migration, investigators can recapitulate tissue variability with low- and high-density matrix models *in vitro* (Sabeh et al., 2009a; Wiesner et al., 2014; Wolf et al., 2013). Based on the observed size and rigidity of the nucleus, successful transmigration

of ECM barriers has been postulated to depend on the relative porosity of the intervening matrix relative to nuclear size (Wolf et al., 2013). Hence, we analyzed the relative ability of macrophages to traverse low-density and high-density acid-extracted type I collagen matrix that retain intact covalent crosslinks. Indeed, in our studies macrophages were able to negotiate the low-density matrix absent MMP activity yet required MT1-MMP to proteolytically expand collagen pores in high-density gels to a minimum size that allowed macrophage-nuclear transit. In the absence of MT1-MMP, nuclei that failed to transit restrictive collagen pores display marked distortions in nuclear shape. Therefore, without mobilizing the necessary proteolytic machinery (i.e. MT1-MMP), macrophages launch a futile attempt to traverse interstitial matrix barriers. Macrophages are critical regulators of pathological fibrosis that occur in response to chronic or dysregulated wound-healing (Wynn and Vannella, 2016). Given that fibrotic tissue is characterized by increased ECM density, crosslinking, and stiffness modeled in part by dense type I collagen matrix *in vitro*, we expect macrophages mobilize MT1-MMP to proteolytically traverse restrictive fibrotic ECM (Wynn and Vannella, 2016). However, further studies, particularly in the in vivo setting, will be needed to address these issues.

Together, these studies identify MT1-MMP as a requirement for macrophage-mediated remodeling of two distinct extracellular matrix barriers, i.e. the basement membrane and interstitial matrix. Macrophages display an intrinsic MT1-MMP-dependent ability to degrade the basement membrane in diverse microenvironments, most strikingly in response to pro-inflammatory stimuli, but not as a prerequisite to traversing the basement membrane-interstitial matrix interface. In addition, MT1-MMP is mobilized to expand passageways in dense type I collagen to permit nuclear transit. Hence, from the

perspective of basement membrane and high collagen density interstitial matrix barriers, our data identify macrophage MT1-MMP as a critical mediator of ECM remodeling.

Future Directions

Macrophage influx into developing tumors correlates with negative patient outcome, in part by promoting carcinoma cell invasion and metastasis (Afik et al., 2016; Noy and Pollard, 2014; Ries et al., 2014; Wyckoff et al., 2007; Wynn and Vannella, 2016). At the tumor site, macrophages upregulate the expression of powerful proteolytic enzymes, including the MT1-MMP, that are capable of remodeling the ECM barriers that confront invading tumor cells (Afik et al., 2016; Ojalvo et al., 2009, 2010; Rowe and Weiss, 2009; Sabeh et al., 2009a). In our studies, we have demonstrated that macrophages mobilize MT1-MMP to degrade physiologic ECM barriers *ex vivo*, however, the contribution of macrophage MT1-MMP to *in vivo* tumor progression has not been defined. Therefore, we propose that the mobilization of MT1-MMP by tumor-associated macrophages (TAMs) promotes ECM remodeling and subsequent carcinoma cell invasion.

Studies are underway to use transgenic models of breast cancer, i.e., *MMTV-PyVT* (PyMT), to analyze the specific role of macrophage MT1-MMP *in vivo* (Wagner et al., 2001). In this system, female mice develop carcinomas that display disorganized basement membranes in tandem with the appearance of cancer-infiltrating macrophages (Lin et al., 2001; Wagner et al., 2001). In the PyMT system, the monocyte lineage can be permanently labeled using a *Csf1r-Cre*$^{-}$*Rosa26R-tdTomato* transgenic line (Deng et al., 2010; Madisen et al., 2010). In this system, all cells expressing the CSF-1 receptor, i.e., a growth factor essential for macrophage differentiation and survival, excise a floxed stop

codon preceding a tdTomato fluorescent reporter (Deng et al., 2010; Madisen et al., 2010). Therefore, all cells that express *Csf1r* constitutively, including macrophages, express the red fluorescent signal. To begin characterizing macrophage-basement membrane interactions, PyMT animals were bred with *Csf1r-Cre*$^{-}$*Rosa26R-tdTomato* mice. Interestingly, in preliminary studies, tumor sections co-labeled with antibodies targeting type IV collagen reveal that macrophages localize to basement membrane structures, consistent with a potential role for TAM remodeling of ECM (Figure 4.1) (Wagner et al., 2001). To next determine if TAMs express MT1-MMP in vivo, we utilized an MT1-MMP^{LacZ} mouse, wherein β-galactosidase activity readily identifies MT1-MMP expressing cells (Soriano, 1999). MT1-MMP^{LacZ} animals were crossed with PyMT mice and β-galactosidase expression examined in tissue sections where macrophages were immunolocalized with anti-F4/80 antibodies, a macrophage-specific marker. Indeed, in preliminary experiments, β-galactosidase expression co-localizes with F4/80 immunofluorescence, demonstrating that TAMs actively express MT1-MMP *in vivo* (Figure 4.2). Given that TAMs associate with basement membranes and express MT1-MMP *in vivo*, studies are ongoing to generate macrophage MT1-MMP-deficient animals in the PyMT background using *Csf1r-Cre*$^{+/-}$*Mt1-mmp*$^{fl/fl}$ mice (Deng et al., 2010; Soriano, 1999; Tang et al., 2013; Wagner et al., 2001). These experiments should provide the first insights into the specific contribution of macrophage MT1-MMP to PyMT tumor progression *in vivo*.

In a similar fashion to breast cancer TAMs, brain-specific macrophages (I.e, microglia) associated with malignant brain tumors have been reported to upregulate MT1-MMP expression (Hambardzumyan et al., 2015; Markovic et al., 2009; Vinnakota et al.,

2013). Although the brain has a minimal interstitial matrix and is instead dominated by proteoglycan-rich ECM rather than fibrillar collagen (Zimmermann and Dours-Zimmermann, 2008), glioma cells are known to track along the abluminal surface of vascular basement membrane as a means to traffic through brain tissues – a process that may require MT1-MMP (Cuddapah et al., 2014; Kienast et al., 2010; Thomsen et al., 2017). Of note, recent studies have reported that microglial MT1-MMP expression promotes glioma expansion in an *ex vivo* brain slice model (Markovic et al., 2009; Vinnakota et al., 2013). Presumably, microglial cells may promote invasion by remodeling the vascular basement membrane in a manner that accelerates glioma invasion. In these studies, glioma cells were implanted in wildtype vs MT1-MMP global knockout brain slices where glioma invasion was promoted in control, but not knockout, tissue. However, as a consequence of using brain explant tissue harvested from MT1-MMP-null mice, where all cell types are targeted, it is impossible to identify the relative contribution of microglial cells alone. Furthermore, the studies were confined to an *ex vivo* model and the role of microglial MT1-MMP in regulating glioma progression *in vivo* has not yet been determined. Hence, we hypothesize that microglial MT1-MMP promotes glioma expansion in a basement membrane remodeling-dependent fashion. Thus, we have initiated studies utilizing a rapidly progressing mouse model of brain cancer, wherein GFP-labeled glioma cells were stereotactically injected into the brain of wild-type versus *Csf1r-Cre*$^{+/-}$*Mt1-mmp*$^{fl/fl}$ mice (Figure 4.3A). In this model, tumor progression proceeds in a manner resembling human glioblastoma (Candolfi et al., 2007). In preliminary studies, when glioma expansion in situ was determined by GFP expression, microglial MT1-MMP knockout mice were found to generate smaller tumors (Figure 4.3B). In addition, tumor

sections from microglial MT1-MMP knockout mice reveal markedly fewer cells expressing nestin, a specific marker of glioma stem cells, relative to control tumors. Interestingly, tumor sections from knockout mice reveal a significant increase in cells expressing Iba1, i.e., a specific marker of microglial cells, relative to control tumors (Figure 4.3C,D), suggesting that in brain tissue, MT1-MMP does not play a required role in supporting invasion. While the mechanism(s) that underlie the *increase* in microglial trafficking (or even, proliferation) remain to be defined, these data support the hypothesis that microglia MT1-MMP promotes tumor growth. Further studies are underway to establish the relative contribution of microglial MT1-MMP to glioma progression.

Summary

Macrophage trafficking and remodeling of ECM barriers has critical, albeit paradoxical, roles in host defense and tumor progression. During such events, macrophages respond to microenvironmental cues to appropriately (or inappropriately) mount a broad ECM remodeling program that potentially targets basement membrane and interstitial matrix structures. In our *ex vivo* model of native ECM barriers, primary mouse and human macrophages mobilize MT1-MMP to degrade the basement membrane. Inflammatory cues mimicking the initiation of an inflammatory response intensify the basement membrane remodeling program in an MT1-MMP-dependent fashion. Yet MT1-MMP-deficient macrophages retain the ability to traverse tissue barriers by non-proteolytic mechanisms alone. In a dense type I collagen model of the interstitial matrix we identify an MT1-MMP-dependent migration program wherein macrophages expand passageways through type I collagen to a minimum size that permits nuclear transit. These findings will soon be extended to *in vivo* tumor models in conjunction with

macrophage-specific MT1-MMP depletion to delineate the role of macrophage MT1-MMP in pathologic settings, including breast cancer and glioblastoma. Given the recent development of novel anti-MT1-MMP therapeutics (Ager et al., 2015; Devy et al., 2009), these studies should provide key information regarding the potential utility of targeting macrophage-mediated MT1-MMP remodeling programs in disease settings.

Figure 4.1

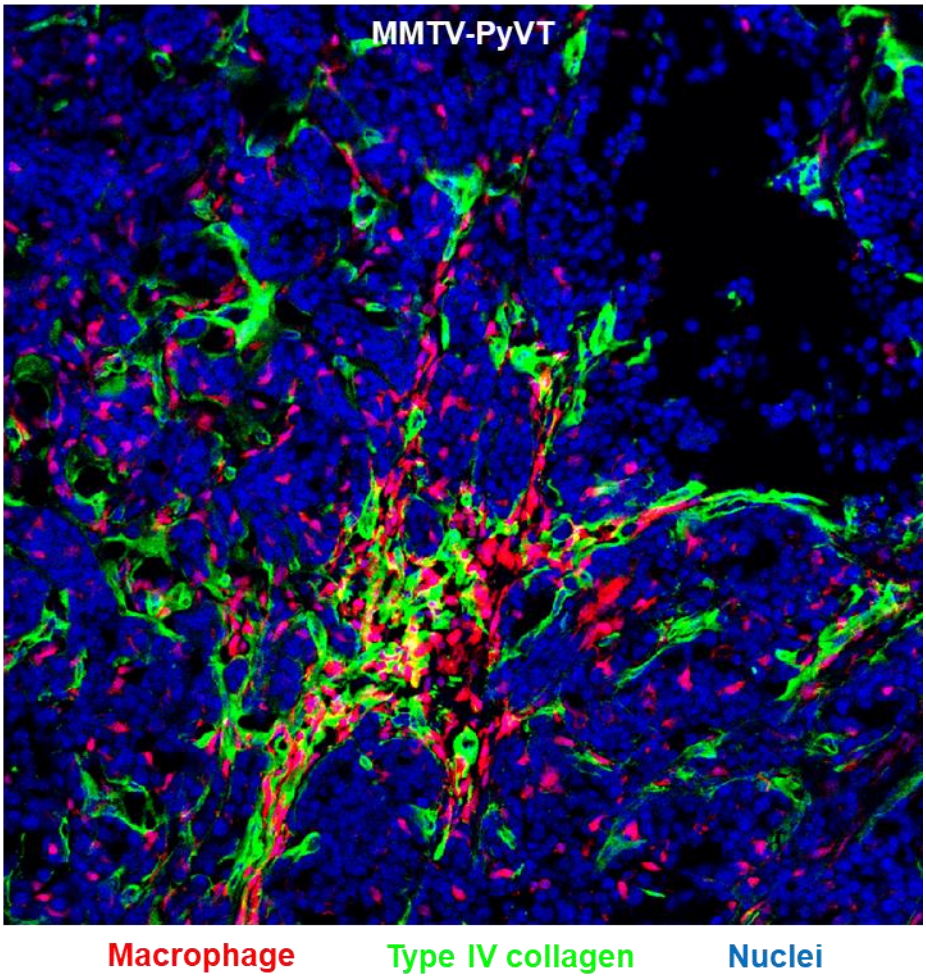

Figure 4.1: TAM-basement membrane co-localization *in vivo*
(A) In an advanced carcinomatous lesion of the mouse mammary gland (*PyMT-Csf1r-Rosa26-tdTomato*), macrophages (red) localize to basement membranes (green).

Figure 4.2

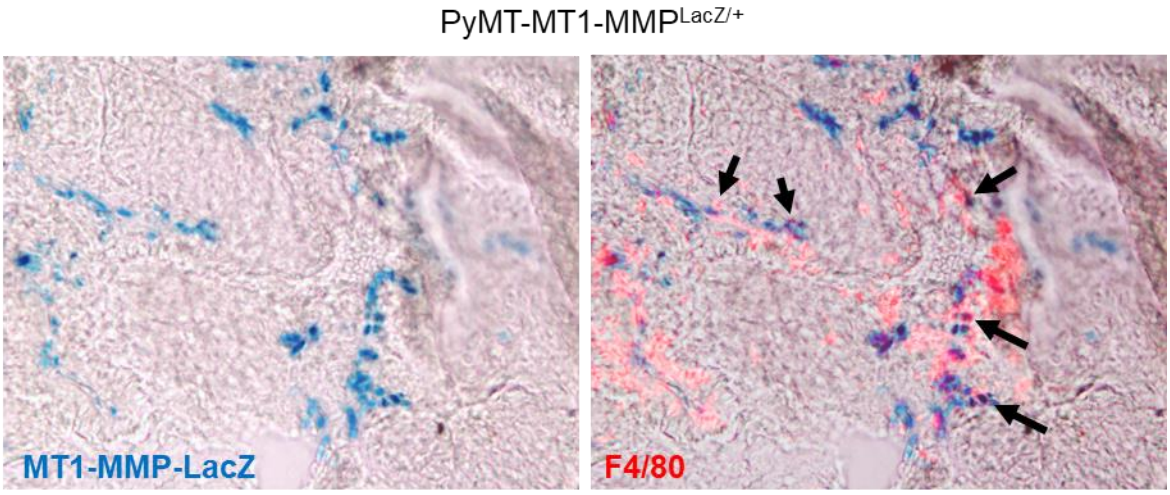

Figure 4.2: TAMs express MT1-MMP *in vivo*
LacZ staining of sectioned mammary gland tumors from PyMT-MT1-MMP^{LacZ} mice with immunofluorescent F4/80 counterstaining. Arrows denote co-localization of nuclear LacZ signal and surface F4/80 staining.

Figure 4.3

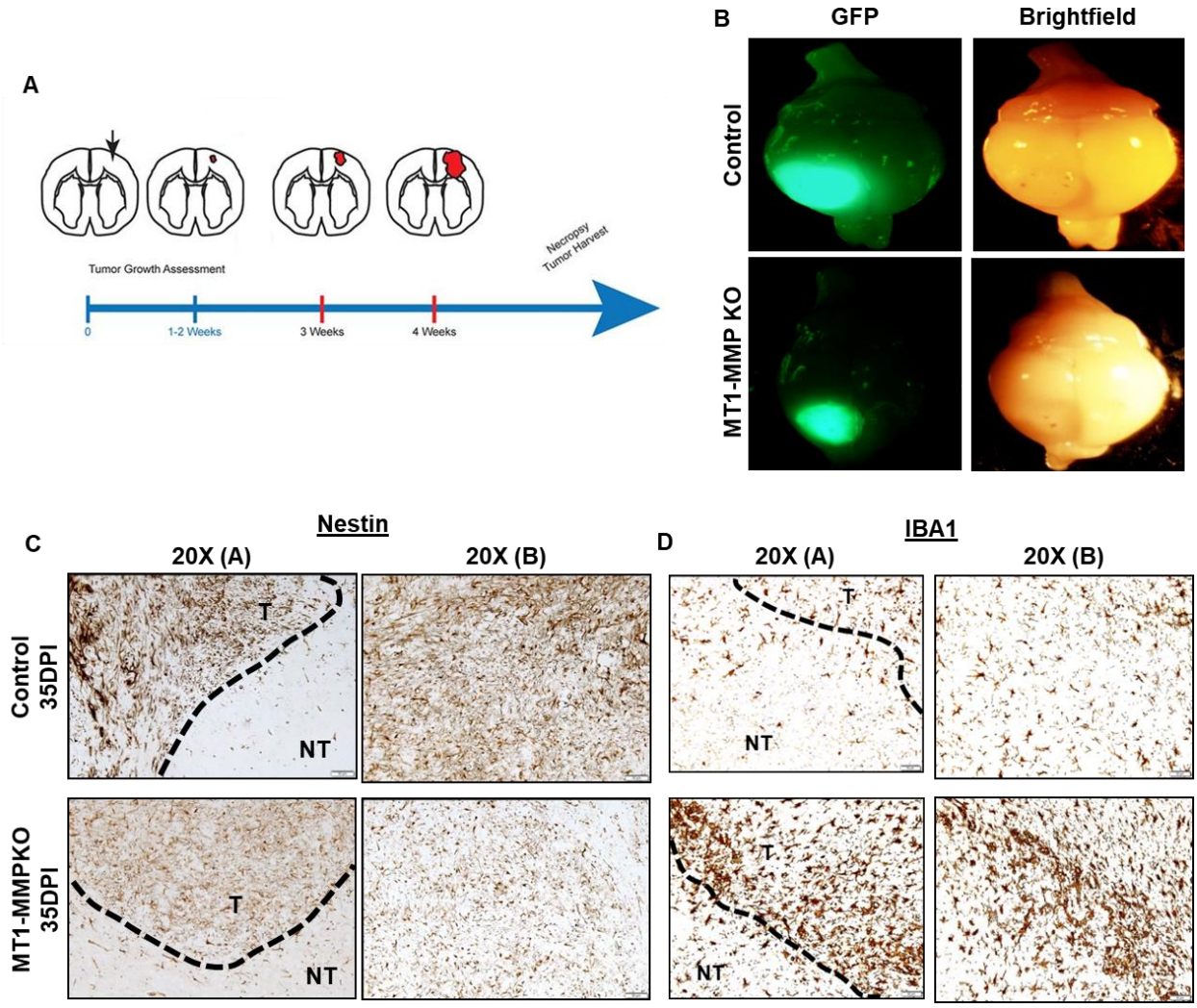

Figure 4.3. Microglia MT1-MMP-deletion in an *in vivo* glioblastoma model
(A) Schematic of the intracranial tumor xenograft (El Meskini et al., 2015) **(B)** Fluorescent and brightfield images of whole mount glioma-implanted brains. **(C)** Immunohistochemistry of nestin-positive glioma stem cell staining of the tumor (T) and adjacent non-tumor area (NT). **(D)** Immunohistochemistry of Iba1-positive microglia in the tumor (T) and adjacent non-tumor area (NT). Tumor boundary demarcated with a dotted line. 20x (B) images are of the tumor center. area (NT).

References

Afik, R., Zigmond, E., Vugman, M., Klepfish, M., Shimshoni, E., Pasmanik-Chor, M., … Varol, C. (2016). Tumor macrophages are pivotal constructors of tumor collagenous matrix. *The Journal of Experimental Medicine*, *213*(11), 2315–2331.

Ager, E. I., Kozin, S. V, Kirkpatrick, N. D., Seano, G., Kodack, D. P., Askoxylakis, V., … Jain, R. K. (2015). Blockade of MMP14 activity in murine breast carcinomas: Implications for macrophages, vessels, and radiotherapy. *Journal of the National Cancer Institute*, *107*(4).

Akkari, L., Gocheva, V., Kester, J. C., Hunter, K. E., Quick, M. L., Sevenich, L., … Joyce, J. A. (2014). Distinct functions of macrophage-derived and cancer cell-derived cathepsin Z combine to promote tumor malignancy via interactions with the extracellular matrix. *Genes and Development*, *28*(19), 2134–2150.

Buchmann, K. (2014). Evolution of Innate Immunity: Clues from Invertebrates via Fish to Mammals. *Frontiers in Immunology*, *5*, 459.

Candolfi, M., Curtin, J. F., Nichols, W. S., Muhammad, A. K. M. G., King, G. D., Pluhar, G. E., … Castro, M. G. (2007). Intracranial glioblastoma models in preclinical neuro-oncology: Neuropathological characterization and tumor progression. *Journal of Neuro-Oncology*, *85*(2), 133–148.

Cougoule, C., Van Goethem, E., Le Cabec, V., Lafouresse, F., Dupré, L., Mehraj, V., … Maridonneau-Parini, I. (2012). Blood leukocytes and macrophages of various phenotypes have distinct abilities to form podosomes and to migrate in 3D environments. *European Journal of Cell Biology*, *91*(11–12), 938–949.

Cuddapah, V. A., Robel, S., Watkins, S., & Sontheimer, H. (2014, July). A neurocentric perspective on glioma invasion. *Nature Reviews Neuroscience*. NIH Public Access.

Deng, L., Zhou, J.-F., Sellers, R. S., Li, J.-F., Nguyen, A. V, Wang, Y., … Lin, E. Y. (2010). A novel mouse model of inflammatory bowel disease links mammalian target of rapamycin-dependent hyperproliferation of colonic epithelium to inflammation-associated tumorigenesis. *The American Journal of Pathology*, *176*(2), 952–967.

Devy, L., Huang, L., Naa, L., Yanamandra, N., Pieters, H., Frans, N., … Dransfield, D. T. (2009). Selective inhibition of matrix metalloproteinase-14 blocks tumor growth, invasion, and angiogenesis. *Cancer Research*, *69*(4), 1517–1526.

El Azzouzi, K., Wiesner, C., & Linder, S. (2016). Metalloproteinase MT1-MMP islets act as memory devices for podosome reemergence. *The Journal of Cell Biology*, *213*(1).

Fidler, A. L., Darris, C. E., Chetyrkin, S. V, Pedchenko, V. K., Boudko, S. P., Brown, K. L., … Hudson, B. G. (2017). Collagen iv and basement membrane at the evolutionary dawn of metazoan tissues. *ELife*, *6*.

Fleetwood, A. J., Achuthan, A., Schultz, H., Nansen, A., Almholt, K., Usher, P., & Hamilton, J. A. (2014). Urokinase plasminogen activator is a central regulator of

macrophage three-dimensional invasion, matrix degradation, and adhesion. *Journal of Immunology (Baltimore, Md. : 1950)*, *192*(8), 3540–3547.

Ginhoux, F., & Guilliams, M. (2016, March 15). Tissue-Resident Macrophage Ontogeny and Homeostasis. *Immunity*. Elsevier.

Halfter, W., Oertle, P., Monnier, C. A., Camenzind, L., Reyes-Lua, M., Hu, H., … Plodinec, M. (2015). New concepts in basement membrane biology. *FEBS Journal*, *282*(23), 4466–4479.

Hambardzumyan, D., Gutmann, D. H., & Kettenmann, H. (2015, January). The role of microglia and macrophages in glioma maintenance and progression. *Nature Neuroscience*. NIH Public Access.

Hotary, K., Li, X.-Y., Allen, E., Stevens, S. L., & Weiss, S. J. (2006). A cancer cell metalloprotease triad regulates the basement membrane transmigration program. *Genes & Development*, *20*(19), 2673–2686.

Jevnikar, Z., Mirković, B., Fonović, U. P., Zidar, N., Švajger, U., Kos, J., … Kos, J. (2012). Three-dimensional invasion of macrophages is mediated by cysteine cathepsins in protrusive podosomes. *European Journal of Immunology*, *42*(12), 3429–3441.

Kadler, K. E., Holmes, D. F., Trotter, J. A., & Chapman, J. A. (1996). *Collagen fibril formation*. *Biochem. J* (Vol. 316). Retrieved from https://www.ncbi.nlm.nih.gov/pmc/articles/PMC1217307/pdf/8645190.pdf

Kienast, Y., Von Baumgarten, L., Fuhrmann, M., Klinkert, W. E. F., Goldbrunner, R., Herms, J., & Winkler, F. (2010). Real-time imaging reveals the single steps of brain metastasis formation. *Nature Medicine*, *16*(1), 116–122.

Lewis, C. E., Harney, A. S., Pollard, J. W., Shi, H. S., Zeng, Y. H., Wang, X. Z., … Jones, J. G. (2016). The Multifaceted Role of Perivascular Macrophages in Tumors. *Cancer Cell*, *30*(1), 18–25.

Lin, E. Y., Nguyen, A. V, Russell, R. G., & Pollard, J. W. (2001). Colony-stimulating factor 1 promotes progression of mammary tumors to malignancy. *The Journal of Experimental Medicine*, *193*(6), 727–740.

Madisen, L., Zwingman, T. A., Sunkin, S. M., Oh, S. W., Zariwala, H. A., Gu, H., … Zeng, H. (2010). A robust and high-throughput Cre reporting and characterization system for the whole mouse brain. *Nature Neuroscience*, *13*(1), 133–140.

Markovic, D. S., Vinnakota, K., Chirasani, S., Synowitz, M., Raguet, H., Stock, K., … Kettenmann, H. (2009). Gliomas induce and exploit microglial MT1-MMP expression for tumor expansion. *Proceedings of the National Academy of Sciences of the United States of America*, *106*(30), 12530–12535.

McCall, A. S., Cummings, C. F., Bhave, G., Vanacore, R., Page-Mccaw, A., & Hudson, B. G. (2014). Bromine is an essential trace element for assembly of collagen IV scaffolds in tissue development and architecture. *Cell*, *157*(6), 1380–1392.

Murray, M. Y., Birkland, T. P., Howe, J. D., Rowan, A. D., Fidock, M., Parks, W. C., & Gavrilovic, J. (2013). Macrophage migration and invasion is regulated by MMP10 expression. *PloS One*, *8*(5), e63555.

Murray, P. J., Allen, J. E., Biswas, S. K., Fisher, E. A., Gilroy, D. W., Goerdt, S., … Zhai, Y. (2014). Macrophage activation and polarization: nomenclature and experimental guidelines. *Immunity*, *41*(1), 14–20.

Newby, A. C. (2016). Metalloproteinase production from macrophages - a perfect storm leading to atherosclerotic plaque rupture and myocardial infarction. *Experimental Physiology*, *101*(11), 1327–1337.

Noy, R., & Pollard, J. W. (2014). Tumor-Associated Macrophages: From Mechanisms to Therapy. *Immunity*, *41*(1), 49–61.

Ojalvo, L. S., King, W., Cox, D., & Pollard, J. W. (2009). High-density gene expression analysis of tumor-associated macrophages from mouse mammary tumors. *The American Journal of Pathology*, *174*(3), 1048–1064.

Ojalvo, L. S., Whittaker, C. A., Condeelis, J. S., & Pollard, J. W. (2010). Gene expression analysis of macrophages that facilitate tumor invasion supports a role for Wnt-signaling in mediating their activity in primary mammary tumors. *Journal of Immunology (Baltimore, Md. : 1950)*, *184*(2), 702–712.

Randles, M. J., Humphries, M. J., & Lennon, R. (2017). Proteomic definitions of basement membrane composition in health and disease. *Matrix Biology*, *57*, 12–28.

Ries, C. H., Cannarile, M. A., Hoves, S., Benz, J., Wartha, K., Runza, V., … Rüttinger, D. (2014). Targeting Tumor-Associated Macrophages with Anti-CSF-1R Antibody Reveals a Strategy for Cancer Therapy. *Cancer Cell*, *25*(6), 846–859.

Rowe, R. G., & Weiss, S. J. (2008). Breaching the basement membrane: who, when and how? *Trends in Cell Biology*, *18*(11), 560–574.

Rowe, R. G., & Weiss, S. J. (2009). Navigating ECM barriers at the invasive front: the cancer cell-stroma interface. *Annual Review of Cell and Developmental Biology*, *25*(1), 567–595.

Rozario, T., & DeSimone, D. W. (2010, May). The extracellular matrix in development and morphogenesis: A dynamic view. *Developmental Biology*.

Sabeh, F., Shimizu-Hirota, R., & Weiss, S. J. (2009). Protease-dependent versus-independent cancer cell invasion programs: Three-dimensional amoeboid movement revisited. *Journal of Cell Biology*, *185*(1), 11–19.

Sherratt, M. J. (2009). Tissue elasticity and the ageing elastic fibre. *Age (Dordrecht, Netherlands)*, *31*(4), 305–325.

Soriano, P. (1999, January 1). Generalized lacZ expression with the ROSA26 Cre reporter strain [1]. *Nature Genetics*.

Starnes, T. W., Bennin, D. A., Bing, X., Eickhoff, J. C., Grahf, D. C., Bellak, J. M., …

Huttenlocher, A. (2014). The F-BAR protein PSTPIP1 controls extracellular matrix degradation and filopodia formation in macrophages. *Blood*, *123*(17), 2703–2714.

Tang, Y., Rowe, R. G., Botvinick, E. L., Kurup, A., Putnam, A. J., Seiki, M., … Weiss, S. J. (2013). MT1-MMP-Dependent Control of Skeletal Stem Cell Commitment via a β1-Integrin/YAP/TAZ Signaling Axis. *Developmental Cell*, *25*(4), 402–416.

Thomsen, M. S., Routhe, L. J., & Moos, T. (2017, October 28). The vascular basement membrane in the healthy and pathological brain. *Journal of Cerebral Blood Flow and Metabolism*. SAGE PublicationsSage UK: London, England.

Ushiki, T. (2002). Collagen Fibers, Reticular Fibers and Elastic Fibers. A Comprehensive Understanding from a Morphological Viewpoint. *Archives of Histology and Cytology*, *65*(2), 109–126.

Van Goethem, E., Poincloux, R., Gauffre, F., Maridonneau-Parini, I., & Le Cabec, V. (2010). Matrix architecture dictates three-dimensional migration modes of human macrophages: differential involvement of proteases and podosome-like structures. *Journal of Immunology (Baltimore, Md. : 1950)*, *184*(2), 1049–1061.

Vérollet, C., Charrière, G. M., Labrousse, A., Cougoule, C., Le Cabec, V., & Maridonneau-Parini, I. (2011). Extracellular proteolysis in macrophage migration: losing grip for a breakthrough. *European Journal of Immunology*, *41*(10), 2805–2813.

Vinnakota, K., Hu, F., Ku, M.-C., Georgieva, P. B., Szulzewsky, F., Pohlmann, A., … Kettenmann, H. (2013). Toll-like receptor 2 mediates microglia/brain macrophage MT1-MMP expression and glioma expansion. *Neuro-Oncology*, *15*(11), 1457–1468.

Wagner, K. U., Ward, T., Davis, B., Wiseman, R., & Hennighausen, L. (2001). Spatial and temporal expression of the Cre gene under the control of the MMTV-LTR in different lines of transgenic mice. *Transgenic Research*, *10*(6), 545–553.

Wiesner, C., El Azzouzi, K., Linder, S., Lütcke, A., Zerial, M., Simons, K., & Olkkonen, V. M. (2013). A specific subset of RabGTPases controls cell surface exposure of MT1-MMP, extracellular matrix degradation and three-dimensional invasion of macrophages. *Journal of Cell Science*, *126*(Pt 13), 2820–2833.

Wiesner, C., Le-Cabec, V., El Azzouzi, K., Maridonneau-Parini, I., & Linder, S. (2014). Podosomes in space: Macrophage migration and matrix degradation in 2D and 3D settings. *Cell Adhesion and Migration*. Taylor & Francis.

Wolf, K., te Lindert, M., Krause, M., Alexander, S., te Riet, J., Willis, A. L., … Friedl, P. (2013). Physical limits of cell migration: Control by ECM space and nuclear deformation and tuning by proteolysis and traction force. *Journal of Cell Biology*, *201*(7), 1069–1084.

Wyckoff, J. B., Wang, Y., Lin, E. Y., Li, J., Goswami, S., Stanley, E. R., … Condeelis, J. (2007). Direct visualization of macrophage-assisted tumor cell intravasation in mammary tumors. *Cancer Research*, *67*(6), 2649–2656.

Wynn, T. A., Chawla, A., & Pollard, J. W. (2013). Macrophage biology in development,

homeostasis and disease. *Nature*, *496*(7446), 445–455.

Wynn, T. A., & Vannella, K. M. Macrophages in Tissue Repair, Regeneration, and Fibrosis, 44 Immunity § (2016). Cell Press.

Zimmermann, D. R., & Dours-Zimmermann, M. T. (2008, October 12). Extracellular matrix of the central nervous system: From neglect to challenge. *Histochemistry and Cell Biology*.